Flood Assessment and Improving Flood Forecasting for a monsoon dominated River Basin: With Emphasis on Black-box Models and GIS

Kumulative Dissertationsschrift zur Erlangung des akademischen Grades

Doktor der Naturwissenschaften (Dr. rer. nat.)

Angefertigt am Institut für Ökologie, Fakultät Nachhaltigkeit

Leuphana Universität Lüneburg

Vorgelegte Dissertation von

Zaw Zaw Latt

Geb. Dezember 25. 1973 in Mandalay, Myanmar

Eingereicht am: 06.10.2014
Erstbetreuer und Gutachter : Prof. Dr. Ing- Hartmut Wittenberg
Zweitbetreuerin und Gutachterin : Prof. Dr. Brigitte Urban
Drittgutachter: Prof. Dr. Konrad Miegel

Tag der Disputation: 11.02.2015

Flood Assessment and Improving Flood Forecasting for a monsoon dominated River Basin: With Emphasis on Black-box Models and GIS

A cumulative dissertation submitted to the Leuphana University of Lüneburg for the academic degree

Doctor of Natural Science (Dr. rer. nat.)

Carried out at the Institute of Ecology, Faculty of Sustainability,
Leuphana University of Lüneburg

Dissertation submitted by

Zaw Zaw Latt

Born on December 25 1973 in Mandalay, Myanmar

Submitted on: 06.10.2014

Doctoral supervisor and reviewer:	Prof. Dr. Ing- Hartmut Wittenberg
Co-supervisor and reviewer:	Prof. Dr. Brigitte Urban
Reviewer:	Prof. Dr. Konrad Miegel

Date of Disputation: 11.02.2015

Acknowledgements

It is obvious that this research would not have been possible without motivation, help, input, suggestion, encouragement and collaboration of a great number of people. Although it is almost impossible to list all of them, I would like to acknowledge those who played a key role in materialization of this work.

I am deeply indebted to my reverend research-supervisor, Prof. Dr. Hartmut Wittenberg, without his continuous guidance I would not have been able to complete this work. I had the privilege to get his unconditional help in the research work, in discussing my ideas and results. He also spared his valuable time to accompany me during the field visit. A word of thanks is clearly not sufficient to express my gratitude for his contributions to this study.

I am cordially thankful to my honorable co-supervisor, Prof. Dr. Brigitte Urban. It was her,who provided me the valuable guidance and offered the opportunity to carry out my research in this prestigious Institute of Ecology, under the Faculty of Sustainability. Despite her busy hours, she always spared time for me in order to provide the required supports.

I am grateful to all members of my doctoral supervisory committee, for reviewing my dissertation and gave their valuable comments to improve it.

I am really grateful to Prof. Dr. Ullrich Günther for teaching me logical problems in the application of scientific theories in order to apply them to practical questions in the research, and to Prof. Andreas Reindl for sharing knowledge on how the research is to be framed and ethical principles to be followed in the course of the research.

I would like to express my deepest gratitude to Mr. Kyaw Myint Hlaing, director general of the Irrigation Department in Myanmar, without his kind supports and permission I would not be able to carry out my field research at the irrigation operation offices in Myanmar.

My sincere thanks are due to Dr. Win Win Zin, associate professor of the Civil Engineering Department, Yangon Technological University, Myanmar, who provided me basic GIS data and technical comments during my research stay in Myanmar.

I reserve my special thanks for my colleagues in the institute of ecology, Leuphana University of Lüneburg, without their encouragement it was not possible to complete this work. The accomplishment of this study would not have been possible in this limited time without the technical co-operation of my dear colleague, Tobias Drükler from WASY GmbH, Germany.

I also owe special words of thanks for Dr. Isabell May, who shared her valuable time in proofreading and correcting the submitted manuscripts for publication. I would like to thank Mrs. Dzairski, the secretary of the Institute of Ecology, without her necessary arrangement I could not work well in the office.

This study would not have materialized without the financial support available to me through the scholarship scheme of DAAD.

The special thanks go to the Irrigation Department and the Department of Meteorology and Hydrology in Myanmar, which not only made their data available in order to conduct this study, but also provided me the working place and their personal coordination during my research visit in Myanmar.

Last but not the least; I would like to express my gratefulness to each and every member of my family, especially my wife Sandar Soe Khin and my son Kaung Tayzar Latt who have provided me the constant and unconditional moral support during my study.

Dedication

I dedicate this work to my parents who always encourage me to pursue the doctoral degree, especially to my father who passed away before my doctoral study has started.

TABLE OF CONTENTS

List of Acronyms

AI	Artificial Intelligence
AM	Annual Maxima
ANN	Artificial Neural Network
ACF	Auto Correlation Function
AR	Autoregressive
ASEAN DRMI	Association of Southeast Asian Nations Disaster Risk Management Initiative
BFI	Baseflow Index
BFGS	Broyden-Fletcher-Goldfarb-Shanno
BP	Back Propagation
CCF	Cross Correlation Function
CE	Coefficient of Efficiency
CWC	Central Water Commission
CV	Coefficient Variation
DDM	Data Driven Model
DEM	Digital Elevation Model
DFP	Davidon-Fletcher-Powell
DMH	Department of Meteorological and Hydrology
DMSG	Disaster Management Support Group
DWIR	Directorate of Water Resources and Improvement of River Systems
EDA	Exploratory Data Analysis
EQp	Error of Peak Discharge
ETp	Error of Time to Peak
FAO	Food and Agricultural Organization
FFA	Flood Frequency Analysis
FFMI	Flash Flood Magnitude Index
FI	Flood Indicies
FIS	Fuzzy Inference System
FMLP	Feedforwaerd Multilayer Perceptron
GA	Genetic Algorithm
GIS	Geographic Information System

HJ	Hooke-Jeeves
HS	Harmony Search
ICSA	Immune Clonal Selection Algorithm
IF	Index Flood
LP	Log Pearson
MAPE	Mean Absolute Percent Error
MLP	Multilayer Perceptron
MLR	Multiple Linear Regression
MRC	Mekong River Commission
MRCS	Mekong River Commission Secretariat
MRE	Mean Relative Percent Error
NMS	Nelder-Mead Simplex
PACF	Partial Auto Correlation Function
PCA	Principal Component Analysis
R^2	Coefficient of Determination
RFFA	Regional Flood Frequency Analysis
RMSE	Root Mean-Square Error
SMLR	StepwiseMultiple Linear Regression
SSQ	Sum of squared deviation
TP	Time Period
UH	Unit Hydrograph
USDA	United States Department of Agriculture
USGS	United States Geological Survey
WMO	World Meteorological Organization

List of Symbols

A	Basin Area
E	Mean Basin Elevation
D	Euclidean Distance
f	Observed value in the Kriging method
F	Prediction of variable in the Kriging method
I	Inflow
L	Basin Length
O	Outflow
S	Basin Slope
SF	Shape Factor
K	Storage coefficient in Muskingum Routing
x	Weighting factor in Muskingum Routing
C_0, C_1, C_2	Muskingum routing coefficient
n, m	Routing parameter in nonlinear Muskingum model
η	Learning rate in ANN
CN	Soil Conservation Curve Number
Δw	Weight interconnections between nodes in ANN
w	Weight in ANN structure
W	Weighting coefficient in the Kriging method
b	Bias in ANN structure
ε	Error (disturbance) term in regression model
p	Probability Value
Q_e	Hypothetical Flood
Q_m	Mean Annual Maximum(Index) Flood
Tc	Time of Concentration
R	Mean Annual Rainfall

List of Figures

List of Tables

Summary

When flood disaster is considered country or region wise, South and Southeast Asia regions are the worst sufferers due to complex topography and high rainfall intensity during the southwest monsoon. In order to protect human lives and possessions against severe floods, understanding potential flood hazard as well as an early warning of the upcoming flood with a sufficient lead time is necessary. Therefore, special attention must be paid to significant research and development activity for upgrading the existing models as well as for developing new ones in order to meet the regional and local requirements. In this thesis, limited data availability in the region has been addressed to further develop tools and techniques for river flood prediction.

As the third largest river of Myanmar, the Chindwin River with 113800 km^2 was considered as the study area because it has great importance as a water resource and a transport artery of Myanmar. Prior to the investigation of black-box forecasting approaches, hydrologic aspects of monsoon floods were analyzed using statistical and frequency analysis with the data covering the period 1966 to 2011. To analyze the change in flood values, the relative differences of flood quantiles for return periods of 2 to 1000 years in two time phases, 1966-1990 and 1991-2011, with respect to the entire observation period were compared. The expected floods of the latter period are found to be the highest. Overall, flood probability and time series analyses show that the upper and middle parts of the basin have particularly high flood risks. One-dimensional hydraulic (MIKE 11) simulations also agree with that the upper half of the basin is likely to suffer frequent floods. Flood risks in Myanmar, particularly the Chindwin River, continue to rise in the last two decades as evidenced by the interannual structure of regional climate, suggesting that robust approaches for estimating and characterizing floods would be valued by society.

Since the flood warning or forecasting system does not aim at providing explicit knowledge of the rainfall–runoff process, applications of black-box approaches have been extensively researched in case of data deficiency. In this context, data driven models and hydrologic routing method were investigated for flood prediction at gauged sites. For developing forecasting models, the Mawlaik station of the Chindwin River is considered as the forecasting station, which has been defined as the flood prone site.

As a tool for multi-step forecasting at gauged sites, performances of stepwise multiple regression (SMLR) and artificial neural network (ANN) techniques were investigated. Future river stages are modeled using past water levels and rainfall from the forecasting station as well

as from the hydrologically connected upstream station. The input vector selection of both approaches involved auto-, partial- and cross-correlation of the data series. The developed models were calibrated with flood data from 1990 to 2007 and validated with data from 2008 to 2011. Model performances were compared for one- to five-day ahead forecasts. With a high accuracy, both candidate models perform well for forecasting the full range of flood levels. The ANN models show a clear-cut superiority to the SMLR models, particularly in predicting the extreme floods. The contribution of upstream data to both types of models improve the forecasting performance with higher R^2 values and lower errors. Considering the commonly available data in the region as primary predictors, the results would be useful for real time flood forecasting, avoiding the complexity of physical processes.

In case of deficiency in meteorological data, the Muskingum routing model is a widely used technique with known hydrographs, despite the limitations in its linear form. However, this method, even in its nonlinear forms with more parameters, is not often adequate for flood routing in natural rivers with multiple peaks. Therefore, as an alternative approach for flood forecasting at gauged sites, the feedforward multilayer perceptron (FMLP) model was developed according to the Muskingum formula in a black-box manner. The results are compared to that of other reported methods, that have tackled the parameter estimation of the nonlinear Muskingum model for the Wilson's benchmark data with a single-peak hydrograph. Evaluating performance statistics, the FMLP model outperforms other methods in flood routing of the well-known benchmark data. Further, the FMLP routing model was also proven to be a promising model for routing real flood hydrographs with multiple peaks of the Chindwin River. Unlike other parameter estimation methods, the ANN models directly capture the routing relationship, based on the Muskingum equation and perform well in dealing with complex systems of a natural river.

On the other hand, understanding potential flood response and possible flood estimation in ungauged catchments can assist the water resources practitioners in management decision. Therefore, in the context of ungauged sites, principal components and clustering techniques were applied for detecting homogeneous regions with similar flood response, and the neural network-based regional models were developed. Based on catchment physiographic and climatic attributes, the principal component analysis yields three component solutions with 79.2% cumulative variance. The Ward's method was used to search initial cluster numbers prior to *k*-means clustering, which then objectively classifies the entire catchment into four homogeneous

groups. For each homogeneous region clustered by the leading principal components, the regional index flood models are developed via the ANN and regression method using the longest flow path, basin elevation, basin slope, soil conservation curve number and mean annual rainfall, which are less correlated each other. At the stage of developing regional models, main concern is not only to establish regional IF models via two approaches, but also to reveal the inconsistency in the performances of the conventional power form model (regression method) under the conditions of using the log domain as well as real domain. To address this shortcoming, ANN approach was investigated in the regional models. In the real domain, the ANN models capture the nonlinear relationships between the index floods and the catchment descriptors for each cluster, showing its superiority towards the conventional regression method. Overall, the robustness of the black box approaches will satisfy the requirement of the flood forecasting system in a developing country, where physical and hydro-metric data are scarce. The feasibility of such models to the natural river basin is successfully validated with real data. In all cases, relationships between input and output with a given concept of the approaches are established as per the existing hydro-meteorological conditions and data availability. Better understanding the regional characteristics of flood risks and improving forecasting practices for a monsoon river represents reliable contributions of black-box forecasting approach that will be a key feature in the future.

Zusammenfassung

Betrachtet man Flutkatastrophen national oder regional, so sind Süd- und Südostasien auf Grund komplexer Topographie und intensiver Niederschläge während des Südwest-Monsuns besonders gefährdet. Zum Schutz humanen und wirtschaftlichen Kapitals vor schweren Überflutungen sind neben dem Verständnis potentieller Überflutungsgefahren vor allem Frühwarnsysteme mit ausreichenden Vorlaufzeiten wichtig. Deshalb gilt der Forschung und Entwicklung bestehender Vorhersagemodelle besondere Aufmerksamkeit, ebenso wie der Neuentwicklung von Modellen, die regionale und lokale Gegebenheiten berücksichtigen. Auf Grund limitierter Datenverfügbarkeit in diesen Regionen werden in dieser Arbeit Werkzeuge und Techniken zur Hochwasservorhersage untersucht und weiter entwickelt.

Als drittgrößter Fluss Myanmars wurde der Chindwin Fluss mit einem Einzugsgebiet von 113.800 km² als Untersuchungsgebiet ausgewählt, da er sowohl zur Wassernutzung als auch als Wasserstraße bedeutend für Myanmar ist. Vor der Betrachtung von Black-Box Prognosen wurden hydrologische Aspekte von Monsoon-Überschwemmungen auf Grundlage statistischer und frequenter Analysen mit Daten von 1966 bis 2011 untersucht. Um Veränderungen in den Mengenabflüssen berücksichtigen zu können, wurde die relative Abweichung der Quantile für die Wiederkehrzeit zwischen 2 und 1.000 Jahren in zwei Abschnitten, 1966-1990 und 1991-2011, unter Berücksichtigung des gesamten Zeitraums, miteinander verglichen. Dabei zeigte sich, dass die prognostizierten Hochwasserabflüsse der zweiten Periode am höchsten sind. Insgesamt ergab die Analyse der Überflutungswahrscheinlichkeiten und Zeitserien, dass das obere und mittlere Einzugsgebiet höhere Überflutungswahrscheinlichkeiten aufweisen. Auch die eindimensionale Simulation (MIKE 11) weist auf häufigere Hochwasserereignisse in der oberen Hälfte des betrachteten Flussgebiets hin. In den letzten beiden Dekaden stieg in Myanmar, insbesondere am Chindwin Fluß, die Zahl der Hochwasserereignsse nachweislich an. Dies ist auf die unterjährige Struktur des Regionalklimas zurückzuführen. Diese Situation lässt vermuten, dass robuste Ansätze zur Abschätzung und Charakterisierung von Hochwasser von der Gesellschaft bewertet werden.

Da Flutwarn- und Vorhersagesysteme oftmals nicht die genaue Kenntnis der Niederschlag-Abfluss-Prozesse vorraussetzen können, ist die Anwendung von Black-Box-Modellen bei mangelnder Datengrundlage ausführlich erforscht worden. In diesem Zusammenhang wurden auch datenbasierte Modelle und hydrologische Routing-Modelle zur Flutvorhersage an Messpegeln untersucht. Am Chindwin Fluss wurde die Mawlaik Station zur Entwicklung von Vorhersagemodellen als Mess- und Vorhersagestation gewählt, da diese als überflutungsanfällig

eingestuft wurde.

Als Techniken für multi-step Vorhersagen an Messstandorten wurden die Schrittweise multiple lineare Regression (SMLR) und Künstliche Neuronale Netze (ANN) untersucht. Zukünftige Flusspegelstände wurden mit Hilfe von vorhandenen Pegelständen und Regenreihen aus der Messstation ebenso wie von einer hydrologisch vernetzten Station flussaufwärts modelliert. Die Input-Vektor-Auswahl beider Methoden beinhaltet auto-, teil- und Kreuzkorrelationen der Datenserien. Die entwickelten Modelle wurden mittels Überflutungsdatenreihen von 1990 bis 2007 kalibriert und mit Daten von 2008 und 2011 validiert. Die Ergebnisse wurden mit ein- bis fünftägigen Vorhersagen verglichen. Mit hoher Genauigkeit lieferten beide untersuchten Modelle genaue Vorhersagen über die gesamte Bandbreite der Pegelstände. Die ANN Modelle zeigten im Vergleich zu den SMLR Modellen dabei eine klare Überlegenheit insbesondere in der Vorhersage von Extremfluten. Die Einbeziehung der Daten von flussoberhalb verbesserte in beiden Modelltypen die Vorhersagegenauigkeit mit höheren R^2-Werten und geringeren Fehlern. In Anbetracht der allgemein verfügbaren Daten für das Untersuchungsgebiet als primären Einflusswert, können die Ergebnisse nützlich sein für eine Echtzeitflutvorhersage unter Vermeidung der komplexen physikalischen Prozesse.

Bei fehlender meteorologischer Datengrundlage und bekannter Abflussganglinie ist das Muskingum Routing Verfahren eine weit verbreitete Methode, trotz der Beschränkungen in seiner linearen Form. Dennoch ist diese Methode, auch in nonlinearer Art mit mehr Parametern, oft nicht passend für Flood Routing Berechnungen in natürlichen Gewässern mit vielen Abflussspitzen. Als Alternative wurde deshalb das Feedforward Multilayer Perceptron Modell (FMLP) in Anlehnung an das Muskingum Verfahren gemäß eines Black-Box-Modells entwickelt. Die Ergebnisse wurden mit denen der anderen angeführten Modelle verglichen, welche die Parameterschätzung des nonlinearen Muskingum Models für Wilson's Vergleichsdaten mit einer einzigen Abflussganglinie angegangen sind. Bei höheren Leistungsstatistiken ist die FMLP Modell besser als andere Methoden für Flood Routing vom dem bekannten Wilson's Vergleichsdaten. Darüber hinaus wurde die FMLP Modell auch bewiesen, ein zuverlässiges Modell für das Routing mit mehreren Abflussganglinien sein. Anders als andere Parameterabschätz-Methoden erfassen ANN Modelle, basierend auf dem Muskingum Equation, direkt die Abflussbeziehung, und funtkionieren gut mit den komplexen Systemen natürlicher Flussläufe.

Andererseits kann das Verstehen von möglichen Hochwasserereignissen und deren Vorhersage in datenlosen Einzugsgebieten wasserwirtschaftliche Fachleute in Managemententscheidungen helfen. Deshalb wurden Einzugsgebiete ohne vorhandene Messdaten nach Haupteinflussgrößen gruppiert um homogene Regionen mit ähnlichen Hochwasserereignissen festzulegen. Auf dieser

Grundlage wurden neutrale netzwerkbasierte Regionalmodelle entwickelt. Basierend auf den physiografischen und klimatischen Attributen der Einzugsgebiete ergaben sich mittels Hauptkomponentenanalyse drei Komponentenlösungen mit 79,2 % kumulativer Varianz. Die Ward-Methode wurde verwendet, um erste Clusternummer zu suchen vor der K-Means Clustering, womit dann das gesamte Einzugsgebiet objektiv in vier Gruppen klassifiziert wurde.
Für jede dieser nach den Hauptmerkmalen geordneten Gruppen wurde mittels ANN und Regressionsmethode unter Benutzung des längsten Fließweges, Einzugsgebietshöhen und -neigungen sowie Bodenkennwerten und jährlichen Niederschlagsmengen, ein regionales Index-Hochwasssermodell entwickelt. Bei der Entwicklung eines regionalen Modells liegt das Hauptaugenmerk nicht nur darauf ein IF Modell mittels zweier Methoden zu entwickeln, sondern auch darauf die Unstimmigkeiten der Leistung des herkömmlichen Kraftform-Modell (Regressionsmethode) bei Nutzung der Log Domain als Real Domain aufzudecken. Um sich diesem Fehler zu widmen, wurde die Anwendung von ANN in regionalen Modellen untersucht. In der Real Domain erfasste das ANN-Verfahren die nonlineare Beziehung zwischen Index-Hochwasser und den Einzugsgebietsdeskriptoren für jede Gruppierung und zeigte damit seine Überlegenheit gegenüber den konventionellen Regressionsmethoden.
Insgesamt genügt die Zuverlässigkeit des Black-Box-Ansatzes den Anforderungen des Hochwasservorhersagesystem in einem Entwicklungsland, insbesondere mit Blick auf die knappe, vorhandene Grundlage physikalischer und hydrometrischer Daten. Die Übertragbarkeit solcher Modelle auf natürliche Flussgebiete wurde erfolgreich mit vorhandenen Datenreihen validiert. In allen Fällen konnten die Beziehungen zwischen In- und Output mit den bewährten Methoden gemäß den existierenden meteorologischen Gegebenheiten und verfügbaren Grundlagendaten nachvollzogen werden.
Ein besseres Verständnis der regionalen Charakteristika von Hochwassergefahren sowie die Verbesserung von Vorhersageanwendungen unter Anwendung von Black-Box-Vorhersage-Modellen werden die Hauptmerkmale für zukünftige Hochwasservorhersagen von Fließgewässern in Monsun-Gebieten sein.

I. FRAMEWORK PAPER

CHAPTER 1
BACKGROUND

Floods rank highly among the most devastating natural disasters in the world, leading to higher significant economic and social damages than any other natural phenomenon (DMSG 2001). Flood risk arises because people use river flood plains which conflicts with the natural function of the water conveyance (Stancalie et al, 2006; Marchi et al. 2010). Therefore, understanding the hydro-meteorological processes that control flooding is extremely important from both scientific and societal perspectives. For reducing vulnerability against flood risks, strategies of living with flood deal with non-structural measures, out of which a flood assessment tool helps water resources engineers characterize the watershed behaviors during floods (Gendreau and Gilard 1998). In case of application oriented in flood forecasts, time to peak and flow volume are important, while in case of object oriented, the purpose of design models is to predict hypothetical floods with statistical return periods (Shahzad 2011).

Although the processes which generate river floods could be understood, their spatial and temporal complexity are normally incorporated into flood forecasting procedures only in a generalized and largely empirical manner. Since hydrological and hydraulic situations change with time, flood forecasting models should be capable not only of using the current output of continuous monitoring systems, but also of continuously updating model inputs. Even where such system exit, they are still far from perfect. In many countries, significant research and development activity is being concentrated for upgrading the existing models as well as for developing new ones in order to meet the regional and local requirements.

1.1 River Flood Forecasting System

Flood forecasting models can help with translating what is observed into estimates of flooding extents and are increasingly used to improve lead time and accuracy of warnings (Sene 2008). River flood prediction generally requires the forecast of flood hydrograph at the gauging stations and calculation of water levels or discharge at critical locations in a river reach. A typical flood forecasting system may consist of a number of subsystems that include precipitation forecasts, unit hydrograph (UH), rainfall-runoff models, flood routing and inundation models (Shrestha 2005). Das and Saikia (2010) pointed out that in practical application, some of the techniques have limitations. For example, rainfall-runoff relationship is very much dependent on storm frequency, initial soil moisture conditions and storm duration. Similarly, UH method may produce error due to its limitation of assumption of uniform rainfall distribution over the entire catchment. For the operational flood management, geographic information system (GIS) tools

facilitate the integration and spatial analysis of data, while the numerical models provide the tools to forecast the likely magnitudes, extent and duration of flood events. One extreme is techniques based on physical laws and theoretical concepts that govern hydrological processes: the so-called hydrodynamic models. Another extreme is the purely empirical, black-box techniques: those that make no attempt to model the internal structure, but only match the input and output of the catchment system (WMO 2009).

In fact, model selection depends on the amount of data available, the complexity of the hydrological processes to be modeled, reliability, accuracy and lead time required, and user requirements. From a practical point of view, WMO (2009) recommends that a flood forecasting model should satisfy the following criteria:

(a) Provide reliable forecasts with sufficient warning time;

(b) Have a reasonable degree of accuracy;

(c) Meet data requirements within available data and financial means

(d) Feature easy-to-understand functions;

(e) Be simple enough to be operated by operational staff with moderate training.

Despite several forecasting techniques, some are too complicated to calibrate and require robust optimization tools; and some need to know better understanding of physical processes in the catchments (Varoonchotikul 2003). Although comprehensive models may provide increased warning time and greater degree of accuracy, they may have very elaborate input data requirements. However, all input data for a specific model may not be available on a real-time basis in many regions. Therefore, significant research on developing forecasting models from data only has been a prime interest in water resources management in developing countries in order to address the specific hydrological problems, which make applied methods likely to be trapped in available data.

1.1.1 Black-box Approach

Black-box models can be considered of little significance in enhancing the understanding of hydrological and hydraulic processes; nevertheless in operational hydrology their usefulness can be paramount. A black-box system can be viewed in terms of its input, output and transfer characteristics (system model) without any knowledge of its internal workings (Fig. 1.1).

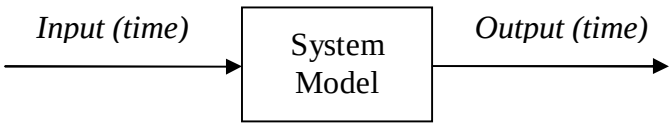

Fig. 1.1 A black-box system

Empirical black-box models belong to two main categories (He et al. 2014). The first is linear models, which use a linear time-invariant response function to model the relationship of rainfall to runoff, like Nash model and UH. The second category is the nonlinear models such as Fuzzy system and artificial neural network (ANN), which are based on a nonlinear response function and time-varying characteristics for describing the rainfall–runoff processes.

In the context of black-box approach, the application of data driven model in flood forecasting such as statistical approaches (regression and correlation methods) and data mining techniques (ANN, genetic programming, support vector machines etc.) are gaining in popularity. The data driven approaches are capable of simulating any variables that have been trained for and are relatively easy to set up and are advantageous because of their capability to handle highly nonlinear formation of data in dynamic systems.

1.2 Description of the Study

The trend of flood disaster is increasing with time and continent wise. Flood events in Asia, where the monsoon season is dominant, accounts over one third of the world's total number of flood events (Dutta and Herath 2004). This increasing trend in Asia has some relationship with the facts that many regions are under the highest influence of monsoon with high annual rainfall intensity and cyclones/typhoons. (Das and Saikia 2010). Having struck by the large amount of rainfall, South and Southeast Asian countries are the worst sufferer. The assessment of water resources in a region usually must cope with a general lack of data, both in time (short observed series) as well as in space (ungauged basins) (Sene 2008). With network density of 12000 km^2/station, Myanmar rivers are an example of a poorly gauged basin. Consequently improper spatio-temporal data monitoring, storage and transmission still lead to the lack of reliable flood management system for monsoon dominated river basins in these regions.

1.2.1 Myanmar, a typical monsoon Country

Characterized by tropical rain forest and monsoon climates with a high and constant seasonal rainfall, Myanmar, the second biggest country in Southeast Asia, is located in the northwestern part of the Indochina peninsula, between 9°32'N and 28°31'N latitudes (with most of the area between the Tropic of Cancer and the Equator) and between 92°10'E and 101°11'E longitudes (Fig. 1.2). Lying within the tropics and the great Asiatic continent to the north and the wide expanse of the Indian Ocean to the south, Myanmar furnishes one of the best examples of a monsoon country. Flood occurrence in Myanmar can be generally recognized as 6% in June, 23% in July, 49% in August, 14% in September and 8% in October respectively. Among four major rivers of Myanmar, the occurrence of extreme floods in the rivers of Ayeyarwaddy and

Chindwin is mostly associated with the pronounced monsoon trough and cyclone storm crossing Myanmar and Bangladesh coast during pre-monsoon and post-monsoon.

The topographically complex Chindwin catchment was selected for this research because the Chindwin River and its associated flood plain are considered to have high economic and ecological values, but receive relatively little attention. With 113,800 km^2, the river basin is the third largest river and one of the principal water resources of the country. However, streamflow is sparsely monitored in the catchment with there being only five gauges in 930 km river reach. The Chindwin River is the biggest tributary of the well-known Ayeyarwaddy River, which is one of the major principal rivers in the South East Asia region. Extreme floods, hit in the basin during the southwest monsoon, are hardly controlled and consequences are not properly forecasted.

1.2.2 Research Needs

What is needed in flood forecasting is a system that can be updated continuously without the costly and laborious resurveying. Since prolonging forecasting and warning times enables the affected people to safeguard their belongings as well as their lives, a lead time must be assured with a span that allows for an effective reaction to the forecast. In addition, the desired generalization of flood information requires a sound method of transferring available information to other sites because only a sample of natural streamflows is gauged in developing countries. The possible approaches analyzed in this research would help address the problem of data deficiency in flood forecasting and provides improved estimates of flood discharge. Further, they must fit to regional conditions and be workable with the database in the region. Indeed, the choice of models should never be restricted to how much physical meaning embedded in the models, but to meet the forecasting requirements. In this context, feasibility of black-box models to river flood forecasting needs to be extensively focused. In order to pay more attention to flood prone areas as well as to formulate efficient forecast models considering influencing flood generating factors, analytical flood assessment should also be emphasized in the region of interest prior to the development of the forecast models.

1.2.3 Objectives

The overall objective of the research is to improve flood assessment and forecasting, based on local conditions and available database, in a sustainable manner for a monsoon rain-fed basin, where observed data are scarce and flood hazard is critical.

The specific objectives are:

(1) To understand the currently applied flood forecasting system in Myanmar as well as in the similar climatic regions

(2) To assess the hydrologic behaviors and potential floods of a typical monsoon river basin

(3) To formulate flood forecasting models via black-box approaches in a cost-effective and sustainable manner

(4) To define the possible measures in parameter estimation for flood assessment and forecasting model

(5) To recommend a knowledge platform at the watershed level by facilitating a flood forecasting tool into integrated water resources management.

1.3 Structure of the Thesis

The dissertation comprises of a framework paper and appendices (published and submitted articles). The framework paper is structured into five chapters. A brief outline of the chapters is given below.

Chapter 1 provides the general background on the vital role of river flood forecasting. This chapter also gives the overview of the study, highlighting the research needs and objective of the study. Chapter 2 gives the general assessment of the current flood forecasting system in Myanmar and its neighboring countries in South and Southeast Asia. The chapter highlights on the weakness of the current flood forecasting practices in Myanmar. Chapter 3 presents the research methods, describing basic concepts, limitations and fundamental structures with respect to river flood forecasting. It includes data driven approaches (multiple linear regression and ANN) and Muskingum routing in flood forecasting for gauges sites. For flood forecasting at ungauged sites, neural network-based regional index flood modeling with GIS is presented. Chapter 4 describes an overview of the results of the major applications. Chapter 5 provides overall conclusions on the important findings, and the perspective of black-box models for further research in the area of river flood prediction.

CHAPTER 2
FLOOD FORECASTING SYSTEM IN SOUTH AND SOUTHEAST ASIA REGIONS

The need for reliability in flood forecasting has been stressed frequently. Improvement in river flood forecasting in developed countries has resulted partly from the global increase in stream gauging stations and partly from major and accelerating advances in both the technology of data collection (e.g. weather radar, satellite imagery) and processing, and telecommunication systems (Smith and Ward 1998). On the other hand, national flood forecasting systems in most developing countries are somewhat satisfactory for river stage forecasts whereas flash floods and overland flood assessments are still under development. This chapter provides a brief overview of current forecasting systems in monsoon countries in the South and Southeast Asia, where flood hazards and risks are the highest in Asia. A brief conclusion on the weakness of the current flood forecasting system in Myanmar is also given.

2.1 Flood Forecasting System in Myanmar

Flood forecasting deficiencies in Myanmar were dramatically exposed many decades ago. Despite water level forecasts with minimum lead times for major large-scale rivers, there was no forecast for ungauged rivers and ineffective forecasts for coastal areas, where only meteorological forecasts are available. In Myanmar, the Department of Meteorology and Hydrology (DMH) is solely responsible for the flood management in terms of hydrological aspects whereas the Irrigation Department takes especially physical measures against flooding. As shown in Fig. 2.1, forecasting stations are only at the major rivers; Ayeyarwaddy, Chindwin, Sittaung, Thanlwin, Dokhtawady, Bago and Shwegyin with the station number 12, 5, 2, 1, 2, 1 and 1 respectively. It can be seen that the density of hydro-metric monitoring stations is relatively low, and thus many flood prone regions across the country remain ungauged and unforecasted. For streamflow monitoring, this situation is beyond the minimum density of 1500km^2/station, recommended by the WMO (2008). There are 41

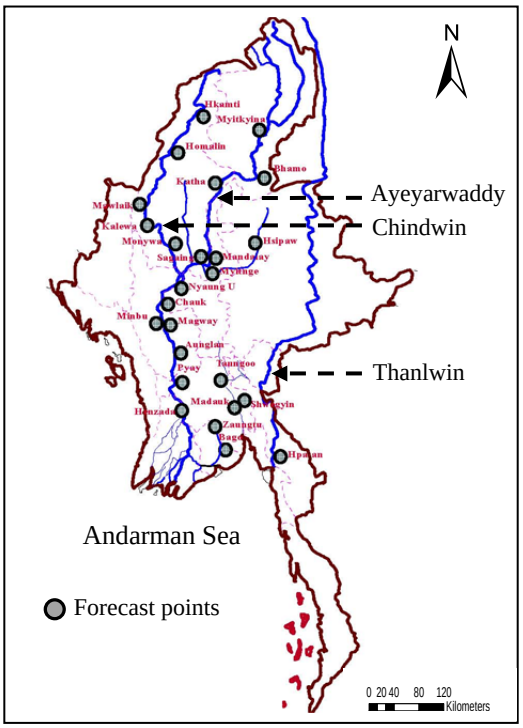

Fig. 2.1 Forecasting Stations in Myanmar

hydro-meteorological stations, 63 meteorological stations and 37 flow monitoring stations across the country. However, flood forecasts are available only for 24 stations of major rivers. River stages and rainfall are currently monitored on a daily basis at all observation stations. Rating curves for all gauging stations are used to transform observed water levels into discharges.

2.1.1 Flood Types and Vulnerable Area

Flood magnitudes and types in Myanmar vary due to the different physiographic regions across the country, and can generally be categorized as follows:(a) *Riverine floods* (b) *Flash floods* (c) *Localized floods* (d) *Flooding due to cyclone and storm surge.* Riverine floods are the most common to the country, and they occur when the monsoon troughs or low pressure waves superimpose on the general monsoon pattern resulting in intense rainfall over strategic areas of the river catchments.

The catchment areas of major rivers in the north and central zone are prone to riverine floods. The Southern Delta also faces riverine floods when there are flood tides and high streamflows at the same period. In the northern mountainous regions, at the confluences of the Ayeyarwady River, the snow in the higher altitude melts and flash floods occur quite frequently at the beginning of summer. Along the coastal regions, floods are a secondary hazard generated by cyclones.

2.1.2 River Flood Forecasting Techniques

Flood forecasting system may range from simple empirical methods to complex physical models, depending on data availability and forecast requirements. As shown in Table 2.1, it is clear that each type of system has its advantages and disadvantages. Although the simplest are often the cheapest to set up and operate, and tend to generate the most reliable forecast, their lead time is usually the shortest of all.

Category 3, 4 and 5 enable forecast systems to accommodate extensive data inputs. Such kind of forecasts, which require reliable quantitative data monitoring, could not be practiced for operational purposes in Myanmar yet, but for specific uses in academic research as well as for very specific areas in water resources planning. In the context of real-time practice in Myanmar, forecast category 1 and 2 are still widely practiced only for major rivers. Even though conventional, widely used techniques for flood forecasting in Myanmar are simple stage correlation method and multiple regression analysis for daily forecasts in flood seasons. Frequency analysis and conceptual models are also used in addressing specific problems.

Table 2.1 Flood Forecasting Categories (Adapted from Smith and Ward, 1998)

Category	System Description	Forecast lead time	Sophistication of forecast procedures	Expense	Potential uncertainty
1	Real-time measurement of **streamflow** with routing/correlation to key location	Shortest	Simplest	Least	Least
2	Same as 1 but including **precipitation** in correlation to key location	Short	Simple	Little	Little
3	Real-time measurement of precipitation, streamflow, temperature, etc. plus a **catchment runoff model**	Long	More complex to very complex	More to very	More
4	Same as 3 but including a **meteorological model**	Longer	Very complex	Very	More
5	Same as 4 including **weather forecasts** (precipitation, temperature, etc.)	Longest	Most complex	Most	Most

(a) Multiple Regression Models

Multiple regression technique (Table 2.2) is applied by using only observed water levels from the upper stations to predict the water levels at the lower stations of a basin.

Table 2.2 Regression-based forecasting models for selected rivers in Myanmar

Station/City	Water Level (H) Forecast Formula	River
$Homalin_{t+1}$	$= 0.95H_{HMt} + 0.02\ H_{HTt-1} + 0.35\ H_{HTt(Change)} + 114.57$	Chindwin
$Mawlaik_{t+1}$	$= 0.93H_{MLt} + 0.001\ H_{HMt-1} + 0.05\ H_{HTt-3} + 0.79\ H_{HMt-1(Change)} + 0.02\ H_{HTt-3(Change)} + 16.81$	Chindwin
$Nyaungoo_{t+1}$	$= 0.63H_{MYt} + 0.67\ H_{SGt-1)}-250$	Ayeyarwaddy
$Pyay_{t+1}$	$= 0.40H_{BMt} + 0.58\ H_{MLt-1} + 1628$	Ayeyarwaddy

(Station Name: HT=Hkamti, HM=Homalin, ML=Mawlaik, MY=Monywa, SG=Sagaing, BM=Bamaw)

It can be seen that the classical multiple regressions are applied only for large river basins with 1-day lead time. DMH has assessed itself that using regression method, water level forecast for the pre-monsoon period is excellent; poor for the peak monsoon period; and good for the late

monsoon period (DMH 2012). As a result, the current forecasts should be practiced with much cares, especially during high flood seasons.

(b) Frequency Analysis

Flood frequency analysis is normally used for probabilistic forecasts using annual maximum water levels. Commonly used frequency distribution functions by the DMH are Log Normal, Gumbel Extreme Value 1 and Log Pearson III, depending on annual maxima series produced by the different river systems. At present, probabilistic forecasts are available only for seven rivers: Ayeyarwaddy, Chindwin, Sittaung, Thanlwin, Bago, Shwegyin and Dokehtawady, as the availability of annual maxima series for other rivers are not consistent.

(c) Conceptual Models

A large proportion of flood forecasting relies upon the use of conceptual catchment models (category 3) which have either been developed initially or adapted subsequently to operate in a real time mode. In Myanmar, DMH reported that the conceptual models (Sacramento model, Tank model, Streamflow Synthesis and Reservoir Regulation (SSARR) model, HBV model, and Discrete Linear Cascades model) could be used for river forecasting in sub-systems, and the channel routing for operational use in some cases. However, these conceptual and routing methods are not consistently practiced for real-time forecasting during flood seasons, but used only for planning and management purposes in specific areas.

2.2 Flood Forecasting System in Mekong River Basin

The flood forecasting and river monitoring system of the Mekong River Commission (MRC) consists of three main components: data collection and transmission, forecast operation, and forecast dissemination (Manusthiparomet et al. 2005).

Table 2.3 Operational data for flood forecasting and river monitoring works by MRC

Item	Wet Season (Jun-Oct)	Dry Season (Nov-May)
Forecasting Activities	Flood Forecasting	River Monitoring
Data Delivery to MRCS	Daily	Weekly
Day-ahead Forecast	5-Day Forecast	7-Day Forecast
Water Level Data	44 Stations (including 2 Sta. from China)	19 Stations
Rainfall Data	44 Stations (including 2 Sta. from China)	19 Stations
Forecasting Points	21 Stations	19 Stations

For data and information exchange and sharing of the MRC, the hydro-meteorological data from 42 stations of the four MRC member countries (the Lao People's Democratic Republic, Cambodia, Vietnam and Thailand) in the Lower Mekong Basin as well as 2 stations data from China are sent to the Mekong River Commission Secretariat (see Table 2.3).

At present, the SSARR model is applied to the upper and middle reaches, while regression models are used for the lower reaches of the delta with overbank flow (see Fig 2.2). An ANN model is also applied to both, upper and lower reaches. The ANN technique is used not only as a forecasting tool, but also it importantly serves for increased forecast accuracy through the process of double checking with the forecasts produced by the SSARR and regression models. After flood water levels at key stations are forecasted, MIKE-11 (one dimensional fully hydrodynamic model) is employed to simulate flood water depth and flood extension over the Cambodian floodplain. The existing MRC Forecasting System was supposed to be adequate. However, rapid population growth in the region, intensification of agriculture, climate change, changes in land use and river morphology, and rapid technology development makes the system be upgraded.

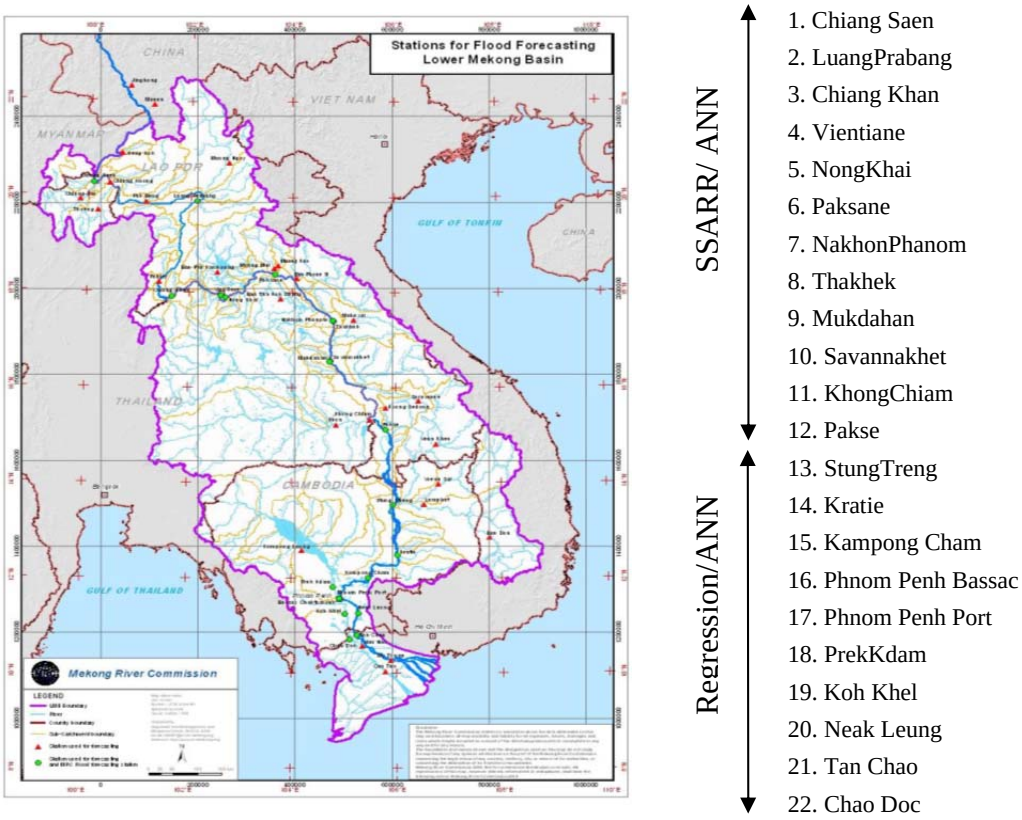

Fig. 2.2 Forecasting stations in the Mekong River basin (Adapted from Manusthiparomet et al. 2005)

2.3 Flood Forecasting System in Bangladesh

Flood forecasting systems in Bangladesh can be divided into three categories: (a) flood forecasting in the rivers caused by the upstream rise of river stage as well as rainfall in the catchment, (b) forecasting overland flows from upstream, and (c) flash flood forecasts in small basins due to localized heavy rainfalls.

Bangladesh Flood Forecasting and Warning Center collects measurements of water level, rainfall and satellite pictures. During the monsoon season, a numerical model of the Bangladeshi river network simulates the water levels during the previous 7 days (hind-cast simulations) and during the coming 3 days (forecast simulation). More precisely the forecasting starts during early monsoon when the water level of any measuring stations is 60 cm below danger level. Basically, MIKE 11 model is applied incorporating all major rivers and floodplains, comprising of 8, 2000 km^2. With 30 forecasting stations, the total length of the modeled rivers amounts to 7270 km. This is linked to a lumped conceptual rainfall-runoff model (MIKE11 RR) which generates inflows from catchments within the country.

The confidence level of forecasts has been defined on the basis of mean absolute errors as compared to observed levels at forecast stations. The present operational forecasting in Bangladesh is said to be satisfactory for river floods with a limited lead time, and not for overland flow assessment and flash floods. Flood forecasting model for 10-day lead time is under development.

2.4 Flood Forecasting System in India

Across India, there are 175 Forecasting sites, out of which, 28 are inflow forecast station and 147 are water level forecast stations. Forecasting methods in India depend upon availability of data at the time of the forecast, physiographic characteristics of the watershed, warning time available, infrastructure availability and purpose of the forecast.

Simple statistical correlations using a gauge to gauge/discharge are being used for some forecasting sites. MIKE-11 models are also in use for some sites in Damodar, Godavari, Mahanadi and Chambal basins. For major rivers, flood forecasts are issued once a day with 1- to 3-day lead time, while twice a day with lead time from 12 hours to 24 hours for medium rivers. For flashy river, forecasts are delivered multiple times (more than twice) a day with a warning time less than 2 hours. Under the bilateral flood forecasting and warning system for transboundary rivers, India has cooperated with Nepal, Bangladesh, Bhutan, Pakistan and China for exchange of data on real-time basis.

According to the present norms of CWC (2010), a forecast of a flood forecasting site is considered to be reasonably accurate if the difference between the forecast and the corresponding observed level of the river lies within +/-15cm. In case of inflow forecasts, a variation of inflow volume within +/-20% is considered acceptable.

2.5 Conclusion

Conventional regression methods as well as ANN models are still widely practiced for operational uses in flood forecasting for the Mekong River, while forecasting systems have been upgraded with complicated and distributed models. As seen the forecasting systems in neighboring regions like India and Bangladesh, they are trying to improve or have improved the existing system, which is formerly based on the regression models, by applying more physics in the system at least using 1-D hydraulic models. The forecast lead times for these regions are more than 3 days. The hydrometric stations in those countries are of a sufficient density at least to cover the flood prone regions.

With abundant water resources and numerous flood prone rivers, density of hydrometric networks in Myanmar is not inadequate and physical-based forecasting systems are still far behind the practice. The weakness of the current forecasting systems in Myanmar can be seen as follows:

- In using regression techniques, model inputs could not be used consistently and vary from station to station.
- While the forecast lead time is only for 1 day at most stations, the forecast accuracy is not satisfactory for extreme floods during monsoon.
- The current forecasts are intended only for the gauged sites in the major rivers, and thus flood forecasting for ungauged catchments are not available.
- Sufficient amount of quantitative rainfall are not available and inconsistent
- Data availability and monitoring is not the same for river systems, despite an operational flood forecasting is highly dependent upon reliable and timely data.
- Ground information (topography, soil and land use etc.), which affects on flood generating, are not available in a good resolution.

Under these circumstances, robust and sustainable flood forecasting approaches for a developing country are needed to answer the flood problems either in gauged or ungauged sites. Being able to provide more lead time, they must be adaptable to local conditions and workable with an available database in the region, without much effort in continuous updating such models.

CHAPTER 3
RESEARCH METHODS

In order to fulfill the research objectives, the major works on flood assessment and forecasting practices are addressed in four research articles (Fig. 3.1). Out of which, the first article focus on the flood hydrology and trend assessment to characterize the potential flood risks. The second and third articles focus on the development of flood forecasting tools for gauged sites in different aspects. The fourth article emphasizes the flood response assessment and regionalization for ungauged sites. In the context of a black box approach, data driven and routing methods to river flood modeling are mainly analyzed.

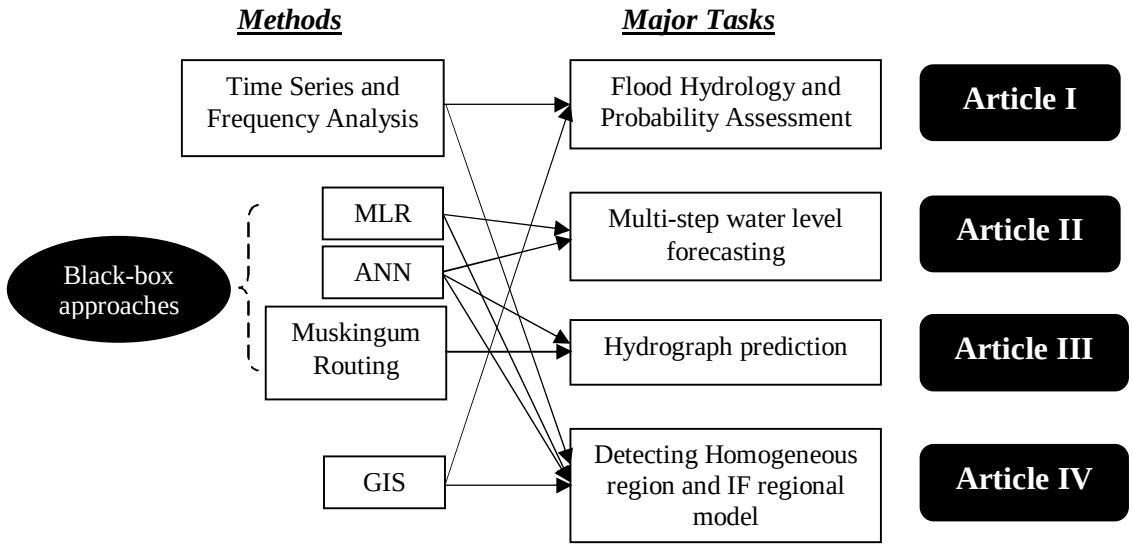

Fig. 3.1 Applied methods for major applications

3.1 Time Series and Frequency Analysis

As a preliminary study, time series and frequency analyses are used to assess the potential flood, and understand the hydrologic behavior of the monsoon river basin. Time series analysis was applied to detect the trends of annual maximum, Qmax (the largest magnitude that occurred in each year) series and their deviation at each gauging station. The significance of a linear trend for annual maxima series was assessed whether the slope value is significantly different from zero (i.e. no trend) or not. For the test of significance, the *P*-value was determined by referring to a *t*-distribution. The null hypothesis of no trend is rejected if the *p* value is smaller than the significance level. In this study, a trend was considered to be significant at 5% significance level. If the *p* value is less than or equal to 0.05, there is a significant trend. If not, there is not enough evidence of a meaningful trend in this significance level.

As a supplement, non-parametric Mann-Kendall test (Mann 1945; Kendall 1975) together with Sen's Slope estimator are also used to determine the temporal trend for Qmax, daily maximum rainfall (1-D Rmax), 3-Day maximum rainfall (3-D Rmax), 7-day maximum rainfall (7-D Rmax) and annual monsoon rainfall (total rainfall during June and October) at five stations.

A probabilistic approach is also required to incorporate the effects of the occurrence of many extreme events into flood risk management decisions (WMO 2008). The annual maximum series is applied in frequency analyses because there is a simple theoretical basis for extrapolating the frequency of annual series data beyond the range of observation. Among numerous probability distributions, the log-Pearson type III distribution (LP3) distribution is used to fit a sample of extreme hydrological data. The distribution describes a variable x whose logarithm $y = log\ x$ is Pearson III distributed. Using LP3, the hypothetical floods with different return periods (2 to 1000 years) are estimated for gauged stations, and the regional frequency curve can also be produced. Computed hypothetical floods at each gauging station are analyzed with respect to different time spans, in order to detect the changes in flood quantiles. The computed index floods (flood with return period of 2.33 years) will also be used for index flood regionalization for ungauged basins (Section 3.4).

3.2 Flood Forecasting using Data Driven Models

Data-driven modeling (DDM) constitutes a universal approximation of input and output signals, without explicitly taking into account the physical processes in a system (Fig. 3.2). Shrestha (2005) stated that these models are able to make abstraction and generalization of the processes, and provide a fast and relatively easy means of model development for highly complex, non-linear and dynamic systems.

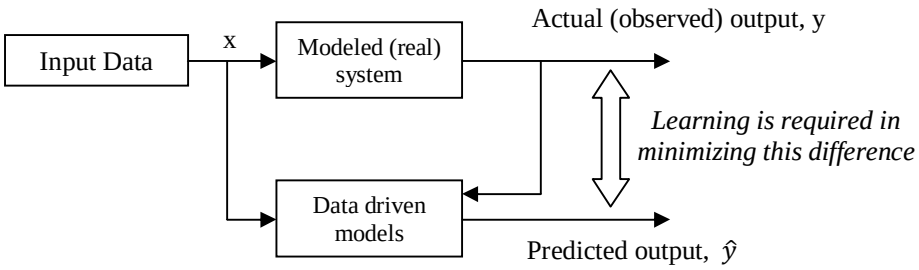

Fig. 3.2 Process of learning in DDM (Adapted from Solomatine and Ostfeld 2008)

Examples of the most popular DDM methods are statistical methods, artificial neural networks and fuzzy rule-based systems. As an attempt to improve the current forecasting practices in Myanmar, multiple linear regression and ANN methods are applied for multi-step ahead

forecasting models. For both approaches, the input vector (x_i) includes water level and rainfall, and the output (y) is forecasted water levels for 1- to 5-day lead times.

3.2.1 Multiple Linear Regression

In the case of multiple explanatory variables, multiple linear regression (MLR) is to explain as much as possible of the variation observed in the response variable, leaving as little variation as possible to unexplained "noise". The general form of a regression model for k independent variable is given by

$$Y = \beta_0 + \beta_1 X_1 + \beta_2 X_2 + \ldots\ldots\ldots + \beta_k X_k + \varepsilon \quad (3.1)$$

where, y is the response variable. β_0 is the intercept. $\beta_1, \beta_2, \ldots, \beta_k$ are the slope coefficients for the explanatory variables. ε is the remaining unexplained noise in the data (the error). The independent variables $X_1, X_2, \ldots, X_k$ may all be separate basic variables, or some may be functions of a few basic variables. The least-squares method is used to choose the best-fitting model, which is the one that minimizes the sum of squares of the distance between the observed responses and those predicted by the fitted model. Since MLR is one of the statistical techniques, attention should be paid to the conditions of multicollinearity, heteroscedasticy and autocorrelation in model development.

Stepwise multiple linear regression (SMLR) method is applied as an alternative way of approaching the problem of multicollinearity. Moreover, instead of selecting the most important variables a priori, SMLR method is a way of choosing predictors of a particular dependent variable by an iterative procedure on the basis of a partial F test (Kleinbaum et al. 1998, Merz 2011). Input vector selection is based on partial-, auto-, and cross-correlation of water level and rainfall data. The antecedent data, which are within the significant limit, are incorporated into the SMLR models.

3.2.2 Artificial Neural Network

As an alternative approach to flow forecasting, ANN technique is applied as a competitor to the conventional regression method, which has been applied as a benchmark forecast model in Myanmar, as well as in many developing countries. ANNs are bottom-up approaches for not making any prior assumptions about the model structure (Khatibi et al. 2011). ANNs are inspired by the capability of human brains to learn from highly complex nonlinear information in a parallel distributed network. Among the many fields of artificial intelligence, ANN is gaining a prime status, owing to its interesting properties such as "learning" from the examples, the ability to represent non-linearity by means of a smaller number of parameters and the least

required information regarding the process to be modeled (Yegnanarayana 1994; Pal and Srimani 1996).

The black-box type flood forecasting can be classified under the category of pattern mapping (Sajikumar and Thandaveswara 1999). Feed-forward multilayer perceptron (MLP) network (Rumelhart et at. 1986) is usually used for pattern mapping problems. In a feed-forward network, information passes only in one direction, i.e. from the neurons of a layer to the succeeding layer. Thus, all input to a neuron in a particular layer is from the preceding layer and the unidirectional connection strengths are known as weights. The presence of a nonlinear activation function is an important characteristic; otherwise the MLP reduces to a linear model (Haykin 1994, Shrestha 2005). An MLP network (Fig. 3.3), which has been used in this study, consists of a set of sensory units that constitute the input layer, one or more hidden layers of computational nodes (neurons) and an output layer of computational nodes. A typical neuron of the ANN consists of the following features:

- *Input:* Propagates input signal to neuron.
- *Synaptic weights:* Interneuron connections that weighs their respective input signals.
- *Bias:* Threshold that has an effect of either increasing or decreasing the net input.
- *Output:* Provides the output signal of the neuron.

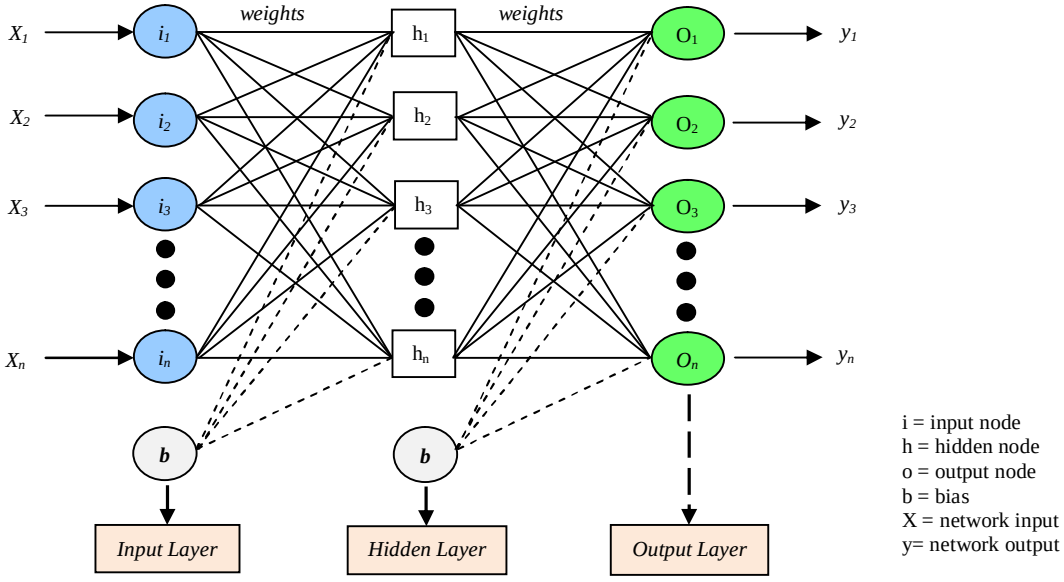

Fig. 3.3 Configuration of feed forward ANN (multi layer perceptron) network

A neuron consists of multiple inputs and a single output. The sum of the product of inputs and their weights minus bias (b) leads to a net as follows:

$$net = \sum x_i \, . \, w_i - b \qquad (3.2)$$

Then the output of a neuron, f(net) is decided by an activation function that determines a response of the node to the input signal it receives (see Fig. 3.4).

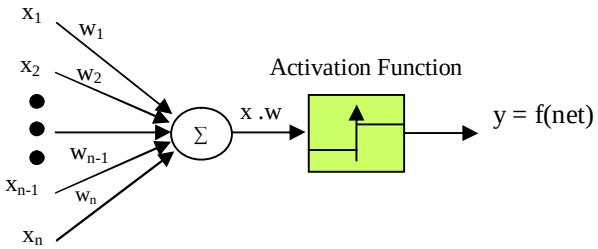

Fig. 3.4 A processing element with an activation function

The commonly used activation functions, which were also used in this study, are as follows:

(i) ***Linear Function****:* Defined as f(x) = x, making the network takes any values as predicted outputs may be distorted by non-linear activation functions.

(ii) ***Sigmoid function****:* Given as f(x) = $\frac{1}{1+ e^{-x}}$ **,** which produces an output in the range of 0 to +1.

(iii) ***Hyperbolic tangent function****:* Given as *f(x) = tan (x)* = $\frac{e^{x}-e^{-x}}{e^{x}+ e^{-x}}$, which produces an output in the range of -1 to +1.

The limiting amplitude range of the asymptotes of the sigmoid and hyperbolic tangent functions produces a 'squashing effect' to the input signal, which is useful in keeping the output of a neuron within a reasonable dynamic range (Tsoukalas and Uhrig 1997). The sigmoid and hyperbolic tangent functions are used in the hidden layers. A linear function is applied at the output layer, making it possible for the network to take any value.

The design of an ANN model consists of the selection of appropriate network architecture and the training algorithm. An optimum ANN model can be considered as the one with the best performance while retaining simple and compact network architecture. Until now, no general theory has existed for determining the optimal network geometry and three layered feed forward network ensures the required network performances in the flood forecasting context (Cullmann and Schmitz 2011). In this thesis, ANN structures with one hidden layer are considered in all cases of forecast model development.

3.2.2.1 Neural Network Training

The training process of ANN involves the presentation of inputs and target to the network, and the adjustment of the weights and bias until the specified performance criteria is met. This is similar to the idea of model calibration, which is an integral part of hydrological or

hydrodynamic modeling. In order to generate an output vector Y = (y_1, y_2,……,y_n), a training (learning) process is employed to find optimal weight matrices and bias vectors that minimize a predetermined error function given as follows.

$$E = \sum_{p=1}^{p} \sum_{i=1}^{N} (y_i - t_i)^2 \quad (3.3)$$

In flood forecasting, t_i and y_i represent the observed flood magnitudes and the computed ones by ANN model of the i^{th} node respectively; N is the number of output nodes and p denotes the number of training patterns. In supervised learning, which is mostly used in forecasting problems of water resources systems, the network performance is judged by comparing the desired outputs corresponding to the target vector with the actual outputs. The most frequently used learning rule in many ANN applications is error back propagation, which belongs to supervised learning algorithm and is essentially a gradient-descent algorithm that minimizes the network error function (Minn and Halls, 1996). Based on Eq. (3.4) (ASCE 2000), the network weights and biases are adjusted by moving a small step in the direction of a negative gradient of the error function during each iteration (Thirumalaiah and Deo 1998). The iterations continue until a specified convergence or number of iterations is achieved.

$$\Delta w_{ij}(n) = -\eta * \frac{\partial E}{\partial w_{ij}} + \alpha * \Delta w_{ij}(n-1) \quad (3.4)$$

Where $\Delta w_{ij}(n)$ and $\Delta w_{ij}(n-1)$ are weight interconnections between node i and j during the n^{th} and $(n-1)^{th}$ pass or epoch. η and α denote learning rate and momentum, respectively. To perform a parallel comparison with regression method, ANN models are also trained using the same input vectors that have been identified by the SMLR models.

For the ANN model to be able to generalize the system, it is important that the set of data contains different conceivable events. A large number of unnecessary inputs will lead to a complex model, and drastically slow down the training process. In the model development, 80% of the data were used for calibration while 20% were used for validation. As Minns and Hall (1996) stated that ANNs are a prisoner of their training data, the extrapolation capability of ANN has been regarded as a main problem. However, it can be overcome by appropriate data scaling. As an important step in preprocessing, the calibration data sets were standardized in a linear scale subtracting the mean and divided by the standard deviation in order to overcome numerical difficulties during the training.

3.3 Flood Forecasting using Hydrologic (Muskingum) Routing

In case of no climatic and catchment parameters to be used in forecasting models, hydrologic routing would be an efficient alternative to predict outflow hydrograph with known inflow hydrographs. The Muskingum method (McCarthy 1938) is the most widely used method of

hydrologic flood routing, and has been extensively researched to find an ideal parameter estimation of its nonlinear forms, which require more parameters, and are not often adequate for flood routing in natural rivers with multiple peaks. To address this shortcoming, application of Muskingum routing coupling with ANN technique is investigated in this thesis.

The Muskingum method is referred to routing in a lumped system for handling a variable discharge-storage relationship, based on the continuity equation as

$$I - O = \frac{dS}{dt} \tag{3.5}$$

Where I = inflow to the reach, O = outflow from the reach, $\frac{dS}{dt}$ = rate of change in channel storage with respect to time. In its original concept, the linear storage function for the Muskingum method with two parameters is expressed as a function of both inflow and outflow given by

$$S = K [xI + (1-x)O] \tag{3.6}$$

In which S = storage volume; I = inflow; O = outflow; K = a time constant or storage coefficient; and x = a dimensionless weighting factor. K accounts for the translation (or concentration) portion of the routing, as being interpreted as the travel time of the flood wave from the upstream end of the downstream end of the channel reach. The parameter x accounts for the storage portion of the routing and is a function of the flow and channel characteristics that cause runoff diffusion. From continuity equation (Eq. 3.5) and storage equation (Eq. 3.6), the outflow yields in finite difference form

$$O_{t+\Delta t} = C_0 I_{t+\Delta t} + C_1 I_t + C_2 O_t \tag{3.7}$$

Where, C_0, C_1, and C_2 are function of K, x and Δt. Since $C_0+C_1+C_2 = 1$, and the routing coefficients can be interpreted as weighting coefficients, which are constant throughout the routing procedures. The parameters K and x are conventionally estimated using a graphical (i.e. trial and error) method. Despite the use of the trial and error method for many decades, it is time consuming and likely to be subjective (Chu 2009) as well as such estimates tend to be approximate (O′Donnell 1985). The graphical method is dependable unless a linear storage function is not duly violated in the channel reach. However, linear routing in a natural river becomes complicated by the fact that storage is not a function of outflow alone (Linsley et al. 1975).

3.3.1. Non-linear Muskingum Models

In natural river reaches, it is common to observe the nonlinear storage function and thus, significant errors may arise in downstream flood routing with the use of the conventional linear

Muskingum approach (Barati 2013). Frequently quoted nonlinear (NL) forms of Muskingum model in literature (Gill 1978; Kim et al. 2001; Barati 2013; Geem 2013) are

$$S = K[x\,I^n + (1-x)O^n] \quad (NL\text{-}1) \tag{3.8}$$

$$S = K[x\,I^n + (1-x)O^m] \quad (NL\text{-}2) \tag{3.9}$$

$$S = K[x\,I + (1-x)O]^m \quad (NL\text{-}3) \tag{3.10}$$

Following a similar derivation to that of NL-1, Easa (2013) proposed a four-parameter nonlinear Muskingum model as follows:

$$S = K[x\,I^n + (1-x)O^n]^m \quad (NL\text{-}4) \tag{3.11}$$

These nonlinear models have an exponential parameter *n* and *m*, which presumably makes the models closely search the nonlinear relation between accumulated storage and weighted flow (Kim et al. 2001). Among nonlinear models, three-parameter NL-3 model is the most commonly used in flood routing as it increases the accuracy of the routing (Orouji et al. 2013). Unlike in the linear model, *K* in the nonlinear model does not describe the travel time of the flood wave and *x* does not need to have the same preconditions (Barati 2011; Easa 2013). The parameters *x*, *K*, *n* and *m* in nonlinear models cannot be estimated through a simple graphical method. The calibration procedure becomes more complicated and use optimization algorithms in searching best routing parameters in order to minimize the objective function, defined as the sum of squared deviation (SSQ) (Eq. 3.12). This is minimized in terms of the routing parameters by applying the different optimization techniques.

$$\text{Min SSQ} = \sum_{t=1}^{n}\left(O_t - \hat{O}_t\right)^2 \tag{3.12}$$

Where O_t and $\hat{O}_t$ represent the observed outflow and the routed outflow.

Therefore, the optimization model for NL-3 and NL-4 may be expressed in Eqs. (3.13) and (3.14) respectively as

$$\text{SSQ} = \sum_{t=1}^{n}\left[O_t - \left\{\left(\frac{1}{1-X}\right)\left(\frac{S_t}{K}\right)^{1/m} - \left(\frac{x}{1-x}\right)I_t\right\}\right]^2 \tag{3.13}$$

$$\text{SSQ} = \sum_{t=1}^{n}\left[O_t - \left\{\left(\frac{1}{1-X}\right)\left(\frac{S_t}{K}\right)^{1/m} - \left(\frac{x}{1-x}\right)I_t{}^n\right\}^{1/n}\right]^2 \tag{3.14}$$

The value of parameter *x* may range theoretically -∞ to 0.5 (Strupczewski & Kundzewicz 1980) while other parameter *K*, *n* and *m* have no specific constraints.

3.3.2 Application of ANN in Muskingum Routing

Even nonlinear Muskingum models may not be applicable to every flood event is likely because the inflow-outflow relationship in natural rivers depends not only on the storage characteristics, but also on other external influences. Moreover, a natural monsoon river has high external

influences on the relationship between storages and inflow-outflow patterns that could not be fully captured by conventional flood routing procedures. Therefore, a novel black box approach, namely ANN method, helps a direct mapping of observed outflows and inflows according to the Muskingum formula (Eq. 3.7) and minimizes the discrepancy between observed and routed flows, (Fig. 3.5). ANN-based Muskingum models are trained (calibrated) according to the concepts described in the section (3.2.2.1). The proposed model is compared to eight optimization methods for the benchmark data. The hydrologic routing enhanced by ANN technique was proven to be promising alternative for predicting the benchmark hydrograph by minimizing SSQ as well as real flood hydrographs of the Chindwin River.

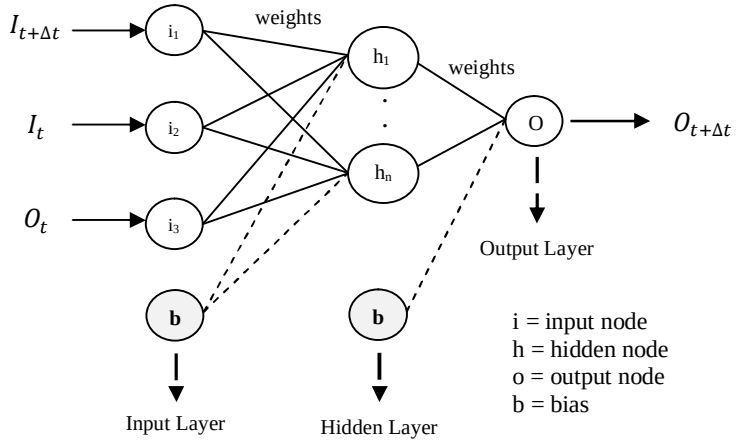

Fig. 3.5 Structure of the MLP model for Muskingum routing

3.4 Flood Response Assessment and Regionalization for ungauged Sites

Knowledge of the spatial distribution of flood response units is crucial to understanding the regional context and also essential for predicting floods at ungauged sites, which is still a challenge for practitioners in many regions. As a supporting tool for the flood management system, this section mainly explores the methods for detecting homogeneous regions with similar flood responses using GIS, and ANN-based regional index flood modeling.

3.4.1 Determination of Homogeneous Region

According to WMO (2009), homogeneous regions can be defined in three different ways (see Fig. 3.6): (a) as geographically contiguous regions; (b) as geographically non-contiguous regions; (c) as neighborhood, where each target station is associated with its own region. Using geographical proximity alone as surrogate for hydrological similarity might not be satisfactory since the regionalized areas may be hydrologically heterogeneous (Smith and Ward 1998). Given that sufficient flood data will seldom be available at the sites of interest, regionalization

with flood statistic is not possible, and it makes sense to use climatic and hydrologic data from nearby and similar locations (Maidment 1993).

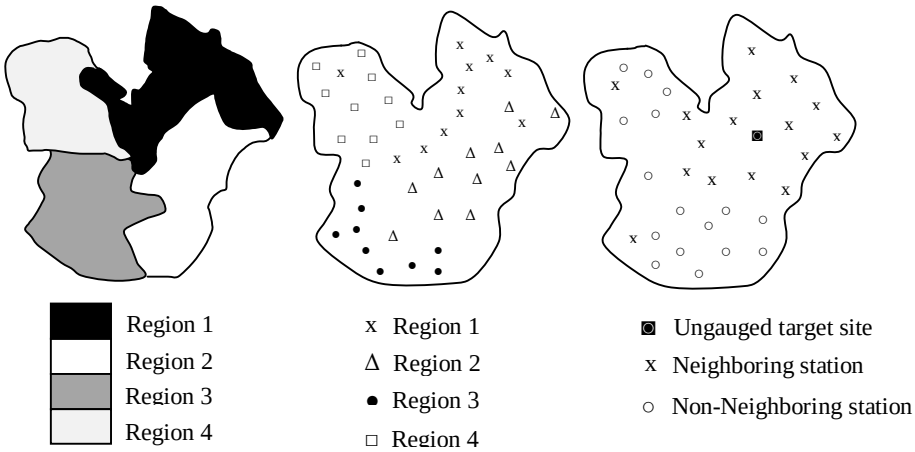

Fig. 3.6 (a) Geographically contiguous region, (b) Non-contiguous homogeneous regions, (c) Hydrologic neighborhoods (Adapted from WMO 2009)

Rao and Srinivas (2008) mentioned the approaches to the regionalization of the watershed include: (i) method of residuals (Thomas and Benson 1970); (ii) the canonical correlation analysis (Ouarda et al. 2000); (iii) region of influence (ROI) approach and its extensions (Cunderlik and Burn 2006); (iv) hierarchical approach and its extension to ROI framework (Zrinji and Burn 1996); (v) the cluster analysis (Hosking and Wallis 1997). In this thesis, approaches for forming non-contiguous homogeneous regions are considered based on catchment descriptors and climatic attributes by using multivariate analysis i.e. factor and cluster analyses.

3.4.1.1 Key Factors on Flood Generation

The choice of variables for pooling homogeneous regions and regional flood models depends on data availability and influences on flood generation (GREHYS 1996). Therefore, eight independent variables, including five physiographic properties (area, elevation, slope, length and shape factor), two response variables (time of concentration and soil conservation service curve number), and one climatic variable (mean annual rainfall) were considered as flood causative factors for pooling homogeneous regions.

(a) Soil Conservation Service Curve Number (CN)

In classifying homogeneous regions, terrestrial information such as land use and soil types are needed to be included (Hosking and Wallis 1997). A basin can be characterized by a single parameter called CN which is an empirical parameter determined by the land cover description

and hydrologic soil groups. It is a convenient representation of the potential maximum soil retention. Higher CN value represents higher runoff.

(b) Time of Concentration

Time of concentration (Tc) is a function of flow length and slope, and influences the shape and runoff peak (USDA 1986). The time for runoff measures the time that water travels from the most hydrological remote points of the watershed to points of interest within the watershed and thus can be considered a significant factor in runoff generation. Tc for main stream was decided using the classical formula by Kirpich (1940) as $T_C = 0.0078 \left(\frac{L}{\sqrt{S_0}}\right)^{0.77}$

Where, *Tc* is in hours, *L* is the maximum length of the main watercourse (km) and S_0 is its average channel slope.

(c) Mean Annual Rainfall

Climatic condition over the study area such as duration, intensity and distribution of rainfall plays a vital role in defining hydrologic response of the watershed. In flood regionalization, mean annual rainfall (MAR) was used a contributing factor. An ordinary Kriging method with GIS was applied for spatial interpolation to produce MAR value at each grid cell in the entire catchment

3.4.1.2 Multivariate Analysis

To select catchment descriptors from a large data set, an objective factor analysisis used to reduce the number of variables, and to detect the structure of in the relationships between variables, that is to classify variables. A principal component analysis (PCA) is one method of factor analysis, which looks at the total variance among the variables. The criterion for the rotation is to maximize the variance (variability) of the new variable (factor), while minimizing the variance around the new variable. The selected flood causative variables described in the section (3.4.1.1) are reduced to significant factors by PCA while retaining maximum variation of the original data set. Then, the factor scores determined by PCA have been subsequently used for the clustering homogeneous region using Ward and K-mean algorithms in order to produce similar flood response regions.

3.4.2 Regional Index Flood Models

For each homogeneous region clustered by leading principal components, regional Index Flood models have been developed via two approaches: conventional power form (regression model)

and ANN. The power form model is the most commonly used relation between flood statistics and a set of climatic and catchment characteristics within a region (Thomas and Benson 1970; Cunnane 1988). Independent variables for the regional IF model are considered based on the lower interrelation among the selected variables, which have been described in the section (3.4.1.1). Then, the relationship between IF and the independent catchment descriptors becomes

$$Q_m = \alpha_0 L^{\alpha_1} S^{\alpha_2} E^{\alpha_3} CN^{\alpha_4} R^{\alpha_5} \mathcal{E} \quad (3.15)$$

where Q_m is the IF of each ungauged site in the clustered region in $m^3 s^{-1}$. α_0, α_1, α_2, α_3, α_4 and α_5 are the regression coefficients. $\mathcal{E}$ is the multiplicative disturbance term. *L*, *S*, *E*, *CN* and *R* represent basin length, basin slope, mean basin elevation, soil conservation curve number and mean annual rainfall respectively. By a logarithmic transformation, the above equation was linearized to find the parameters. However, the estimates of flow statistics from the linearized models via log transformation may be biased in the real domain (Pandey and Nguyen 1999; Eng et al. 2007). In this thesis, this shortcoming is overcome by using a neural network in searching relationship between index flood magnitude and catchment descriptors in a real domain (Fig. 3.7). ANN-based regional IF models are trained (calibrated) according to the concepts described in the section (3.2.2.1).

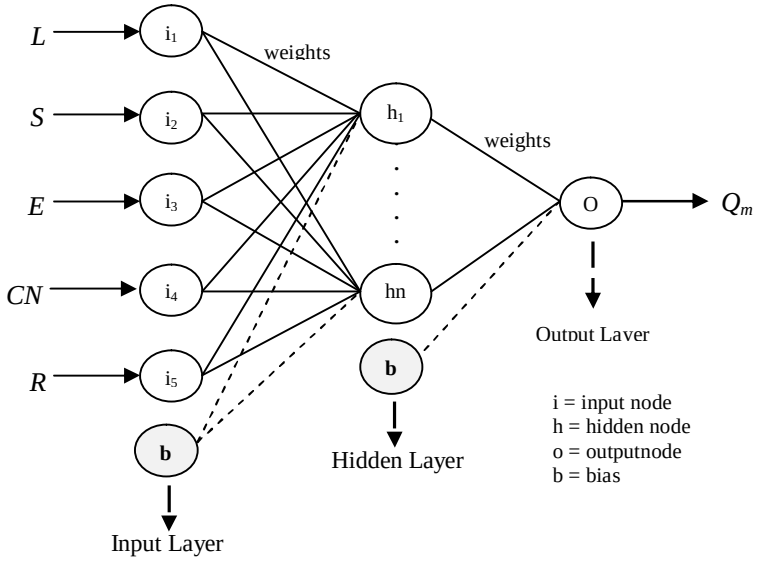

Fig. 3.7 Configuration of the feedforward ANN (multilayer perceptron) network for IF regional models

3.5 GIS Application for Catchment Parameterization

The central role of the GIS in the hydrological modeling process suggested by Maidment (1993) is (a) spatial representation in hydrological assessment; (b) hydrological parameter determination; (c) hydrological modeling within GIS; and (d) linking the GIS and hydrological

models to utilize the GIS as an input. In this thesis, spatial representation and catchment parameterization using GIS are extensively focussed.

Initially, raw digital elevation model (DEM) data of the study area are corrected to create a depressionless DEM by filling the sinks. Then watershed characterization was done by using the ArcHydrol Tools function in ArcGIS which processes and analyzes the corrected DEM data to characterize topography, measure basin parameters, identify surface drainage, subdivide watersheds, and quantify the drainage network. Catchment parameters with respect to the five gauging stations on the Chindwin River are used in the flood risk assessment (section 3.1).

Major clustering variables for regionalization are derived using spatial analysis and raster calculator functions in GIS in accordance with the associated hydrological concepts. For spatial interpolation in preparing a gridded map for each clustering variable, the geostatistical ordinary Kriging method is used. Afterwards, the spatial distribution of the catchment and climatic parameters was extracted for each subbasin and used for flood regionalization (section 3.4).

CHAPTER 4
OVERVIEW OF THE RESULTS

This thesis has focused on the assessment of flood risk in term of flood probability and the trend of annual maximum flows in a monsoon dominated basin, and further provided scientific messages on developing black-box models with different aspects in order to suit the forecasting requirement of developing countries where hydrometric data are scarce. All kinds of flood studies have been carried out in the Chindwin River basin in northern Myanmar, which was also treated as a case study in the development of the forecasting models. The major accomplishments in this thesis are summarized as follows:

- In article I, hydrologic aspects of monsoon floods in the Chindwin river basin are analyzed using statistical and frequency analyses, as high rainfall intensities with spatial and temporal variation during the southwest monsoon causing severe floods are threatening the region. It was found that flood responses vary due to the complex topography and rainfall distribution over the catchment. In the Chindwin basin, mean annual flood rises with the increase of the catchment areas, and coefficient of variation of annual maxima series is changing with increasing catchment size. At five gauging stations along the main river, time series of annual maxima showed no trend of the mean value. However, according to the linear regression statistics, the deviation of annual peaks from their means (regardless of positive or negative) showed increasing trends with positive slopes at all stations in the last decades (1991-2011). Deviation trends at Hkamti and Mawlaik stations are highly significant at the 5% level with the *p* value of 0.001 and 0.05 respectively. In addition, flood quantiles are determined for return periods of 2 to 1000 years using the data covering the period 1966 to 2011. Comparing the expected floods with the highest observed floods, suggests that these correspond in the upper mountainous catchment (Hkamti and Homalin) to about 100-year events. In the central flat terrain with medium elevations (Mawlaik) maximum observed flood has a statistical return interval of about 50 years, while in the lower part of the dry zone area (Kalewa and Monywa) it is about 15 years. Time series and flood probability analyses showed that the upper and middle parts of the basin have particularly high flood risks. To analyze the changes in flood values of different return periods, the relative differences of flood quantiles in two time phases, 1966-1990 (TP-1) and 1991-2011(TP-2), with respect

to the entire observation period are compared. Overall, the year 1990 was considered the trend change year for the Chindwin watershed because the deviations of annual maxima series of all stations are getting larger around this year. Beyond the 5-year return period, expected floods are 2.5% to 26% higher for the data of TP-2, compared to that of TP-1. In comparisons of relative differences in flood values of two series with respect to the entire series, flood values are increasing 3% to 15% at different stations in the TP-2, while the flood values of the TP-1 are decreasing up to 13% with the exception of Homalin station. The highest difference (either high or low values) was found at the Hkamti station, followed by Mawlaik, Monywa and Kalewa respectively. This significance shows that the change in flood quantiles of the Chindwin River is decreasing from upstream to downstream. Without having significant evidences of anthropogenic effects, the cause of the increasing variability in annual peaks is probably due to the interannual structure of regional climate and changes in monsoon intensity. The result gives a motivation for further analysis of flood forecasting approaches by paying more attention to the area with relatively high probability floods in this poorly gauged basin. **(Appendix 1)**

- Due to limited data sources, practical situations in most developing countries favor black-box models in real time operations. Therefore, in article II, performances of stepwise multiple regression (SMLR) and artificial neural network (ANN) models, as tools for multi-step forecasting Chindwin River floods, are investigated in a simple and robust approach. Future river stages are modeled using past water levels and rainfall at the forecasting station as well as at the hydrologically connected upstream station. The forecasting models are developed for the Mawlaik station, which has been defined as the flood prone station in the first article. The developed models are calibrated with flood data from 1990 to 2007 and validated with data from 2008 to 2011. Correlation analyses suggest antecedent water level and rainfall data up to 5 lags could be considered as the input vector. Since the dependent water level series is almost normally distributed and the autoregressive process is dominant, the most recent antecedent data have a greater impact on the regression models. With a high accuracy of R^2 values ranging from 0.8 to 0.99, both SMLR and ANN models provided satisfactory results in a forecasting water level up to five days ahead during the monsoon flood season. In a comparison of forecasting performances, the ANN models are superior to the SMLR models,

particularly in predicting the extreme floods. In the model development, at-site rainfall could not much contribute to the model performance in terms of R^2. Nonetheless, involvement of the rainfall reduced the prediction errors in the ANN models, which have the inherent ability of capturing nonlinearity. The contribution of upstream data to both models can improve the forecasting performance with higher R^2 values and lower errors. Overall, the ANN models can predict high floods with less than 1% error for one step ahead forecast. Considering the commonly available data in the region as primary predictors, the results would be useful for real time flood forecasting, avoiding the complexity of physical processes. **(Appendix 2)**

- The third article examines the application of ANN in the Muskingum flood routing as an alternative black-box approach in case of no climatic and catchment parameters. The feedforward multilayer perceptron (FMLP) models are developed according to the Muskingum equation and their performances are investigated in two case studies. The first case study is based on the well-known Wilson's benchmark data, which has only a single peak and is reported to present a nonlinear relationship between weighted discharge and storage. The performance of the proposed FMLP Muskingum model is compared to that of the previously reported methods, which have been used in the parameterization of nonlinear Muskingum routing. Using the sum of squared deviation (SSQ), coefficient of efficiency (CE), error of peak discharge and error of time to peak, the FMLP model shows a clear-cut superiority over other methods in flood routing of well-known benchmark data. The best SSQ values of previously reported methods for the three-parameter and four-parameter nonlinear Muskingum models were 36.77 m^3s^{-1} and 7.67 m^3s^{-1} respectively. The FMLP model in this research can reduce the SSQ value up to 4.05 m^3s^{-1}. In the second case study, the FMLP model is also proven to be a promising tool for routing real flood hydrographs with multiple peaks of the Chindwin River. The best structure of FMLP mode in this case is 3-3-1, which provides CE values of 0.99 in calibration and 0.98 in validation. This article presents a successful attempt to validate the prediction of real flood events in this natural river via hydrologic routing enhanced by ANN technique. Unlike other parameter estimation methods in Muskingum routing, the FMLP models directly capture the routing relationship based on the Muskingum equation, showing its robustness and predictability in real flood cases. **(Appendix 3)**

- In the second and third articles, the applications of data driven models are dedicated only to gauged sites. Therefore, through the example of the Chindwin River basin, article IV presents the application of principal components and clustering techniques for detecting hydrological homogeneous regions, and a neural network-based regionalization approach for estimating index floods (IF) at ungauged catchments. Based on catchment physiographic and climatic attributes, the principal component analysis yields three-component solutions with 79.2% cumulative variance. The Ward's method is used to search initial cluster numbers prior to *k*-means clustering, which then objectively classifies the entire catchment into four homogeneous groups. Mean annual rainfall, basin elevation and basin slope have the greatest contribution to classifying the hydrological similarities of the Chindwin watershed. Overall the entire Chindwin catchment is likely to have moderate to high flood potential. For each homogeneous region clustered by the leading principal components, the regional IF models are developed via the ANN and regression methods using the longest flow path, basin elevation, basin slope, soil conservation curve number and mean annual rainfall, which have lower inter-correlation with each other. The ANN based IF models for each region explore more consistency in all performance indices, providing CE value higher than 0.95 in both calibration and validation, whereas the regression model has the least efficiency in validation although it has a higher performance with a *CE* value of 0.9 in calibrating. The result shows that the ANN approach captures the nonlinear relationships between the IF and the catchment descriptors for each cluster, showing its superiority towards the conventional regression method, for which the bias of parameter estimation via log transformation is concerned. As a result, better understanding of similar flood response areas and knowing IF for the entire Chindwin river basin would ease the flood management in Myanmar. **(Appendix 4)**

Overall, this thesis explores a better understanding of flood causative factors and the trends of hypothetical floods in the monsoon dominated river. Furthermore, the main contribution of the thesis is to improve the current flood forecasting system of Myanmar by introducing the black-box methods whose versatility have been proven in flood prediction at gauged and ungauged sites using available data, and whose predictability is quite satisfactory and meets the regional requirements. In particular, the main advantages of ANN models to be explored in this thesis is less data requirement, suitability of any data type in the model development, avoiding physical

meaning of the model structure and free from any statistical prerequisites. The overall results would contribute to national water resources planning and management in Myanmar. The methodology can lend itself to other similar regions where catchment data are scarce.

CHAPTER 5
CONCLUSIONS AND PERSPECTIVES

5.1 Conclusions

To cope with the situation of data deficiency in developing countries, one must develop predictive models that may use one or few of the available hydrometric data to issue a reliable forecast of good quality, which are a decisive factor for a successful early warning. In this context, this thesis had been inspired by the robustness of black-box forecasting approaches that originates from data driven methods and hydrologic routing. For the scientific community to benefit more from thesis, it is important to convey a message about how their capabilities are effective in flood forecasting in general, and particularly how these approaches help the practitioners in flood assessment in case of data scarcity in Myanmar i.e. regional context. Driven by these situations, a number of studies have been undertaken with flood cases of the meso-scale Chindwin River in northern Myanmar.

In terms of probability, flood risks in the upper half of the basin are higher, especially in the recent decades. Strong trends in standard deviation and probability curves along the main stream suggest more extreme events are likely to happen in coming years. Despite a weak evidence of urbanization and substantial changes in land management in the catchment, the cause of the increasing variability in annual peaks is, however, probably due to the interannual structure of regional climate and changes in monsoon intensity. This finding also leads to a conclusion that compared to other factors, hydroclimate parameters likely influence more on the generation of floods in the region and become a key input to the flood forecasting model in the context of Myanmar rivers.

On the other hand, multiple flood characteristics (e.g. shape, volume and peaks of hydrograph) cannot be modeled by the probability of flood peaks, and the risk estimation for a flood event of a certain dimension depends strongly on hydrological forecasts. Therefore, the core of the research deals with the proper design of a river flood forecasting model for the flood prone region of the Chindwin River. The application of SMLR and ANN models in multi-step river stage prediction (Appendix 2), ANN application in Muskingum flood routing (Appendix 3) and neural network based regionalization for ungauged catchment (Appendix 4) demonstrate the robustness of such data models in the context of predicting any desired flood magnitude based on the existing hydro-meteorological conditions and data availability. This implies an

introduction of the simple and robust forecasting approach for a monsoon-dominated river basin in a sustainable manner.

As an improvement of current forecasting approaches, when developing multi-step ahead forecasting models under two conditions: (a) using at-site data only and (b) using upstream data, both regression and ANN models provide reliable forecasts up to 5-day lead time which is sufficient for flood warning and evacuation. The developed ANN models achieved by no means their best performances via a parallel comparison with SMLR models. Nonetheless, the neural network approach has shown consistently better performances than the conventional MLR technique in both conditions, especially for extreme flood prediction. The result not only shows the relevance of using ANN in flood forecasting with limited data types, but also reveals the clear-cut superiority of ANN models to regression models using the same input data, for the conditions under which the regression technique has the best performance. This study would be a remedy to the shortcoming of previous studies due to unfair comparison between these two approaches. For more lead times, performances of the models can be further improved by adding other prediction variables such as rainfall and temperature not only from hydrologically connected stations, but also nearby stations in the catchment. Although using more information is challenging for linear regression models, ANN models can incorporate different predictors and would provide better forecasts.

In case of no meteorological data, the outflow hydrograph from a stream channel can be predicted by routing methods. In chronological order, better solutions for parameter estimation of Muskingum routing were proposed in minimizing the SSQ value with respect to the benchmark Wilson's data. Very few studies reported the applicability and performance of the proposed method in real flood cases with a successful validation. The fact that even nonlinear Muskingum models may not be applicable to every flood event is likely because the inflow-outflow relationship in natural rivers depends not only on the storage characteristics, but also on other external influences. As a remedy for such a shortcoming, the FMLP network with error back propagation was applied for Muskingum flood routing, and its performance was assessed for the benchmark data in comparison with previous methods as well as for real flood cases of the Chindwin River. In both cases, the performance of the FMLP models was found to be quite satisfactory in terms of all performance indices. The ANN approach can disregard any external disturbances and successfully capture the inflow-outflow relationship of the real flood cases on the basis of the Muskingum formula which is sensitive to high disturbances by lateral inflows

into the system. With a set of inflow-outflow records for a river reach, the proposed approach has been further shown to be a promising tool for routing of real flood events in natural rivers.

Despite the spatial distribution of flood response units is essential for the effective flood management, gauging all streams is neither possible nor desirable especially in developing countries. In case of deficiency in flood statistics, different climatic and physiographic attributes across the Chindwin catchment suggested that it is possible to generalize the effects of climatic and catchment attributes on floods within the defined homogeneous regions. Mean annual rainfall, basin elevation and basin slope have the greatest contribution to classifying the hydrological similarities of the Chindwin watershed. In the development of regional IF models, the conventional power form (regression) models did not show reliable results in the validation stage although the calibration result was quite satisfactory. In a comparison using real data in the power form models, the model performance is slightly lower than that of the linearized models via log transformation. The regression based IF model has its statistical assumption and the log-transformed solution of the conventional power form (regression based) model for the parameter estimation could be biased in a real domain. The neural network approach, with the inherent ability of capturing nonlinearity, has shown better results in both calibration and validation.

In addition to the issue of model performance, the presented approaches are also found to be data efficient and worked well. The data-driven models, once trained correctly, yield the reliable results from the limited or desired input and output data, which can be either linear or non-linear. This quality is very useful to water resources management with limited resources. These models are flexible to use, and computationally fast and reliable. Further, the data models need only pruned input data from the stations, which have a higher correlation. Extrapolation capability of ANN, formerly regarded as its disadvantage, is no longer a problem and it can be overcome by using the appropriate data scaling in model training. Traditionally, simplified modeling techniques like statistical methods have been used to solve the problems posed by lack of data as long as the relationship between applied variables shows a strong linearity. However, real world situations never guarantee such conditions. Therefore, nonlinear data driven techniques like ANNs are particularly useful for application involving complicated nonlinear processes that are not easily modeled by traditional means. Although this study used for large data set (1990-2011) for five days ahead flood level prediction, these models can also be trained with little data. In IF regionalization, such a merit of requiring less data has also been confirmed

by ANN models. The proposed methodology is believed to be employed to emulate the role of simplified forecasting techniques in Myanmar and similar regions.

5.2 Perspectives for Further Research

In the flood assessment, interannual variation of streamflow should further be validated with the detail spatial precipitation data at the regional level. Attention should also be paid to human activities which alter regional hydrologic regimes, affecting long-term changes in streamflow at both seasonal and regional scales. Flood extents should be analyzed with finer spatial scale.

As this study has shown, estimating future floods of a river system is possible by the data driven models using commonly available data in the region, without any comprehensive data requirements. However, a number of potential areas of future research with regard to river flood prediction still remain in the context of data driven modeling. One of the most important aspects is to complete a detailed quantitative sensitivity analysis and uncertainty assessment of the models, in order to examine the relative contribution of the model parameters, initial conditions and input variables to the model's overall predictive uncertainty. Further investigations should be conducted to identify other significant predictors that are commonly available in the region, and build more accurate forecasting models using various relevant methods. In regionalization processes, spatial flood data must have a sufficient density to cover the entire catchment. Therefore, modifications of the regional IF models are required from time to time using more available flood data and catchment attributes. Even if the observed flood data will not be expected in the near future, it is recommended that synthetic annual maximum discharge series of ungauged basins would be generated using available climatic data. For further improvement of the models, relevant analysis and data from regional networks and adjacent territories as well as from international sources should be acquired. Further, the ANN approach could be adapted to the distributed modeling of watersheds, using multiple precipitations as inputs for a finer analysis.

There is no doubt that black-box modeling will be a key feature in the management of flooding over coming decades, especially in developing countries where catchment monitoring is extremely limited and flooding is the most critical issue in countries' socioeconomic development.

References

ASCE Task Committee on application of artificial neural networks in Hydrology (2000) Artificial neural networks in hydrology. I: Preliminary concepts. J. Hydrol. Eng. 5(2): 115-123.

Barati R (2013) Application of Excel solver for parameter estimation of the nonlinear Muskingum models. KSCE Journal of Civil Engineering, KSCE, Vol. 17, No. 5, pp. 1139-1148.

Chu HJ (2009) The Muskingum flood routing model using a Neuro-Fuzzy Approach. KSCE Journal of Civil Engineering, KSCE, Vol. 13, No. 5, pp. 371-376.

Cullmann J, Schmitz GH (2011) Design of artificial neural networks for flood forecasting. In: Flood risk assessment and management. How to specify hydrological loads, their consequences and uncertainties. [Schumann AH (ed.)]. Springer Science+Business Media B.V.

Cunderlik JM, Burn DH (2006) Switching the pooling similarity distances: Mahalanobis for Euclidean. Water Resources Research 42:W03404. doi: 10.1029/2005WR004245

Cunnane C (1988) Methods and merits of regional flood frequency analysis. Journal of Hydrology, 100: 269–290

CWC (Central Water Commission) (2010) Flood forecasting and warning network performance appraisal. Government of India, Central Water Commission, Flood forecasting monitoring directorate. New Delhi.

Das MM, Saikia MD (2010) Hydrology. Eastern Economy Edition. New Delhi.

DMH (Department of Meteorology and Hydrology) Myanamr (2012) Activity Report on the 9th Monsoon Forum.

DMSG (2001) The Use of Earth Observing Satellites for Hazard Support: Assessments and Scenarios. Final report of the CEOS Disaster Management Support Group, NOAA, Department of Commerce, USA.

Dutta D, Herath S (2004) Trends of floods in Asia and flood risk management with integrated river basin approach. Proceedings of the Second International Conference of Asian-Pacific Hydrology and Water Resources Association, Singapore. Volume **1**, 55-63.

Easa SM (2013) New and improved four-parameter non-linear Muskingum model. Water Management, Institute of Civil Engineers (ICE), doi:10.1680/wama.12.00113

Eng K, Milly PCD, Tasker GD (2007) Flood regionalization: a hybrid geographic and predictor-variable region-of-influence regression method. ASCE Journal of Hydrologic engineering 12: 585–591

Geem ZW (2006) Parameter estimation for the nonlinear Muskingum model using the BFGS techniques. Journal of Irrigation and Drainage Engineering. ASCE, Vol. 132, No. 5, pp. 474-478.

Gendreau N, Gilard O (1998) Structural and non-structural implementations – Choice's arguments provided by inondabilité method. In: RIBAMOD River basin modelling, management and flood mitigation Concerted action [Casale R, Pedroli GB, Samuels P (Eds.)]. Proceedings of the first workshop, Delft. EUR 18019 EN. 241-250.

Gill MA (1978) Flood routing by the Muskingum method. Journal of Hydrology, Vol. 36, pp. 353-363.

GREHYS (1996) Presentation and review of some methods for regional flood frequency analysis. Journal of Hydrology 186: 63–84

He Z, Zhao W, Liu H (2014) Comparing the performance of empirical black-box models for river flow forecasting in the Heihe River Basin, Northwestern China. Hydrological Processes 28. P: 1-7

Haykin S (1994) Neural Networks A comprehensive foundation. Macmillan College Publishing, New York.

Hosking JRM, Wallis JR (1997) Regional frequency analysis. UK, Cambridge University Press.

Kendall MG (1975) Rank Correlation Methods, 4th edition. Charles Griffin, London.

Khatibi R. Ghorbani MA, Kashani MH, Kisi O (2011) Comparison of three artificial intelligence techniques for discharge routing. Journal of Hydrology 403: 201-212. doi: 10.1016/j.jhydrol.2011.03.007

Kim JH, Geem ZW, Kim ES (2001) Parameter estimation of the non-linear Muskingum model using harmony search. Journal of the American Water Resources Association, Vol. 37, Issue 5, pp. 1131-1138.

Kirpich ZP (1940) Time of concentration of small agricultural watersheds. Civil engineering 10(6): p–362

Kleinbaum DG, Kupper LL, Muller KE, Nizan A (1998) Applied regression analysis and other multivariable methods. 3rd Edition. Duxbury Press, Pacific Grove, USA.

Linsley RK, Kohler MA, Paulhus JL (1975) Hydrology for Engineers. McGraw-Hill, New York, USA.

Maidment DR (1993) Handbook of Hydrology. McGraw-Hill.

Mann HB (1945) Non-parametric tests against trend. Econometrica 13:245-259

Manusthiparomet C, Apirumanekul C, Mahaxay M (2005) Flood Forecasting and River Monitoring System in Mekong River Basin. Second Southeast Asia Water Forum, Bali, Indonesia.

Marchi L, Borga M, Preciso E, Gaume E (2010) Characterization of selected extreme flash floods in Europe and implications for flood risk management. Journal of Hydrology **394**(1-2): 118-133.

McCarthy GT (1938) The unit hydrograph and flood routing. Proc., Conference of the North Atlantic Division, U.S Army Corps of Engineers, New London, C.T.

Merz R (2011) Advances in regionalizing flood probabilities. In: Flood risk assessment and management. How to specify hydrological loads, their consequences and uncertainties. [Schumann AH (ed.)]. Springer Science+Business Media B.V.

Minns AW, Hall MJ (1996) Artificial neural networks as rainfall-runoff models. Hydrological sciences, Vol. 41, Issue 3, pp. 399-417.

O′Donnell T (1985) A direct three-parameter Muskingum procedure incorporating lateral inflow. Hydrological Sciences, Vol. 30, Issue 4, pp. 479-496.

Orouji H, Haddad OB, Mehdipour EF, Mariño MA (2013) Estimation of Muskingum parameter by meta-heuristic algorithms. Water Management, Institute of Civil Engineers (ICE), Vol.166, Issue 6, pp. 315-324.

Ouarda TBMJ, Hache M, Bruneau P, Bobee B (2000) Regional flood peak and volume estimation in Northern Canadian Basin. Journal of Cold Region Engineering ASCE 14(4): 176-191.

Pal SK, Srimani PK (1996) Neurocomputing - Motivation, Models, and Hybridization. Computer 29(3): 24-28

Pandey GR, Nguyen V-T-V (1999)A comparative study of regression based methods in regional flood frequency analysis. Journal of Hydrology 225: 92–101

Rao AR, Srinivas VV (2008) Regionalization of watershed. An approach based on cluster analysis. Water Science and Technology Library Vol. 58. Springer Science+Business Media B.V.

Rumelhart DE, Hinton GE, Williams RJ (1986) Learning internal representations by error propagation. In: Parallel Distributed Processing, Vol.1, Cambridge, MIT press: 318-362.

Sajikumar N, Thandaveswara BS (1999) A non-linear rainfall-runoff model using an artificial neural network. Journal of Hydrology 216: 32-55.

Sene K (2008) Flood warning, forecasting and emergency response. Springer Science + Business Media B.V.

Shahzad MK (2011) A Data based flood forecasting model for the Mekong River. PhD Thesis.

Shrestha RR (2005) River Flood Prediction Systems: Towards complementary hydrodynamic, Hydrological and Data Driven Models with Uncertainty Analysis. PhD Dissertation. Universitat Karlsruhe (TH), Germany.

Smith K, Ward R (1998) Floods – Physical processes and human impacts. John Wiley, England.

Solomatine DP, Ostfeld A (2008) Data-driven modelling: some past experiences and new approaches. Journal of Hydroinformatics 10(1): 3-22. doi: 10.2166/hydro.2008.015

Stancalie G, Catana S, Irimescu A, Savin E, Diamandi A, Hofnar A, Oancea S (2006) Contribution of Earth Observation data supplied by the new satellite sensors to flood management. In: Transboundary floods: Reducing risks through flood management [Marsalek J, Stancalie G and Balint G (eds.)]. NATO Science Series IV. Earth and Environmental Sciences Vol. 72 , 287 - 304.

Strupczewski W, Kundzewicz Z (1980) Muskingum method revisited. Journal of Hydrology, Vol. 48, Issue 3-4, pp. 327-342.

Thirumalaiah K, Deo MC (1998) Real-Time Flood Forecasting Using Neural Networks. Computer Aided Civil and Infrastructure Engineering 13: 101-111.

Thomas DM, Benson MA (1970) Generalization of streamflow characteristics from drainage-basin characteristics. Geological survey water-supply paper 1975.

Tsoukalas LH, Uhrig RE (1997) Fuzzy and neural approaches in engineering. John Wiley and Sons, Inc., New York.

USDA (United States Department of Agriculture) (1986) Urban Hydrology for small watershed. Technical Release 55.

Varoonchotikul P (2003) Flood forecasting using Artificial Neural Network. Swetz and Zeitlinger B.V. Lisse, The Netherlands.

WMO (World Meteorological Organization) (2008) Guide to Hydrological Practices. Volume 1 Hydrology- From Measurements to Hydrological Information. WMO-No. 168. 6th Edition. Geneva.

WMO (World Meteorological Organization) (2009) Guide to Hydrological Practices. Vol. II Management of Water Resources and Application of Hydrological Practices. WMO-No. 168. Sixth Edition.

Yegnanarayana B (1994) Artificial neural networks for pattern recognition. Sãdhanã, Vol. 19: 189-238.

Zrinji Z, Burn DH (1996) Regional flood frequency with hierarchical region of influence. Journal of Water Resources Planning and Management 122(4): 245-252.

Unpublished Documents:

Chit K (2009) Innovative Strategies for Urban Flood Management considering Climate Change in Myanmar.

Thein HM, Tun S (2008) Floods, forecasting system and management in Myanmar. 6th Annual Mekong Flood Forum.

Yi T (2006) Water Management Activities in Myanmar. International Workshop for Earth Observation in Water Management Services. Thailand. 4th Annual Mekong Flood Forum, Siem Reap, Cambodia, 18-19 May 2006.

Online Resources:

http://www.mrcmekong.org/

http://www.ffwc.gov.bd/

http://india-water.gov.in/ffs/

http://india-wris.nrsc.gov.in/wrpinfo/index.php?title=Main_Page

Publication and Conference Contribution

Articles in international peer-reviewed journals

1. **Latt, Z. Z**., Wittenberg, H. 2014. Hydrology and Flood Probability of the Monsoon Dominated Chindwin River in Northern Myanmar. *Water and Climate Change*. doi: 10.2166/wcc.2014.075
2. **Latt, Z. Z**., Wittenberg, H. 2014. Improving flood forecasting in a developing country: A comparative study of stepwise multiple linear regression and artificial neural network. *Water resources Management 28(8)*: 2109-2128. doi: 10.1007/s11269-014-0600-8
3. **Latt, Z. Z**. 2014. Application of Feedforward Artificial Neural Network in Muskingum Flood Routing: A Black-box Forecasting Approach for a Natural River System. (submitted manuscript)
4. **Latt, Z. Z**., Wittenberg, H., Urban, B. 2014. Clustering hydrological homogeneous regions and neural network based index flood estimation for ungauged catchments: An example of the Chindwin River in Myanmar. *Water Resources Management 29(3)*. doi: 10.1007/s11269-014-0851-4

Conference Contribution

Latt, Z. Z. and Wittenberg, H. 2013. Flood severity and Trends in a Monsoon dominated country: An example from the Chindwin River in northern Myanmar. International Conference on Natural Sciences and Engineering. World Academy of Sciences. 26-27 September, Rome, Italy. WASET 8:1321-1322 (Oral presentation)

Declaration 1

This PhD dissertation entitled with "***Flood Assessment and Improving Flood Forecasting for a monsoon dominated River Basin: With Emphasis on Black-box Models and GIS***" consists of four articles mentioned in the authors' contribution table.

Three articles were written by me as the first author, and one as the single author. The first author also carried out the field work, data analysis, development of research methods and the interpretation and discussion of the results achieved. All tables and figures embedded in the thesis were solely prepared by the first author, except those which were given with legal citations in the text.

I avouch that all information given in the authors' contribution table is true in each instance and overall.

Zaw Zaw Latt

Lüneburg, 2nd October 2014

Authors' contributions to the articles and articles publication status

Article*	Title	Specific contributions of all authors	Author status	Weighting factor	Publication status**	Conference contributions
1	Hydrology and flood probability of the monsoon-dominated Chindwin River in northern Myanmar	Z. Z. Latt H. Wittenberg	Co-author with predominant contribution [Überwiegen der Anteil]	1.0	Journal of Water and Climate Change (2014) DOI:10.2166/wcc.2014.075 IF=1.044 (2013)	
2	Improving Flood Forecasting in a Developing Country: A Comparative Study of Stepwise Multiple Linear Regression and Artificial Neural Network	Z. Z. Latt H. Wittenberg	Co-author with predominant contribution [Überwiegen der Anteil]	1.0	Water Resources Management (2014) 28(8):2109 – 2128 DOI: 10.1007/s11269-014-0600-8 IF=2.463 (2013)	
3	Application of Feedforward Artificial Neural Network in Muskingum Flood Routing: A black-box Forecasting Approach for a Natural River System	Z. Z. Latt	Single author [Allein-Autorenschaft]	1.0	(Submitted manuscript under review)	
4	Clustering hydrological homogeneous regions and neural network based index flood estimation for ungauged catchments: An example of the Chindwin River in Myanmar	Z. Z. Latt H. Wittenberg B. Urban	Co-author with predominant contribution [Überwiegen der Anteil]	1.0	Water Resources Management (2015) 29(3): 913 – 928 DOI: 10.1007/s11269-014-0851-4 IF=2.463 (2013)	
			Sum:	**4.0**		

* Article order according to the sequence of attachment
**IF = Impact Factor

II. APPENDICES

Article I

Hydrology and Flood Probability of the Monsoon Dominated Chindwin River in Northern Myanmar

Zaw Zaw Latt, Hartmut Wittenberg

Reprinted from Journal of Water and Climate Change,
In Press doi:10.2166/wcc.2014.075, with permission from the copyright holders,
IWA Publishing

Hydrology and flood probability of the monsoon-dominated Chindwin River in northern Myanmar

Zaw Zaw Latt and Hartmut Wittenberg

ABSTRACT

As the third largest river of Myanmar, the Chindwin River has great importance as a water resource and transport artery. At 113,800 km^2 the basin is comparable in size to the Elbe basin in Europe, although with higher rainfall and runoff. During the southwest monsoon high rainfall intensities with spatial and temporal variation causing severe floods are threatening the region. The study aims to analyze the hydrologic aspects of monsoon floods using statistical and frequency analysis. Flood responses vary due to the complex topography and rainfall distribution over the catchment. Time series of annual maximum floods shows no trend of the mean value. The deviation of annual maxima from the respective mean values, however, has increased significantly in recent decades. Flood quantiles are determined for return periods of 2 to 1,000 years using the data covering the period 1966 to 2011. Flood probability analysis shows that the upper and middle parts of the basin have particularly high flood risks. To analyze the change in flood values, the relative differences of flood quantiles in two time phases, 1966–1990 and 1991–2011, with respect to the entire observation period are compared. The expected floods of the latter period are the highest.

Key words | catchment characteristics, flood characteristics, hydrologic aspects, probability, southwest monsoon, trends

Zaw Zaw Latt (corresponding author)
Hartmut Wittenberg
Faculty of Sustainability,
Institute of Ecology,
Leuphana University of Lueneburg,
Scharnhorststr. 1, C13.112,
Lueneburg 21335,
Germany
E-mail: *zawzawlatt@khalsa.com*

INTRODUCTION

Many regions of the world are experiencing an intensification of floods caused by changing land use and climate. Consequently, risks to human life and possessions are increasing, made worse by population growth, urbanization, settlement in flood plains and development (Huntington 2006; Marchi *et al.* 2010). Global warming has caused greater climatic volatility shown by changing precipitation patterns, increased frequency and intensity of extreme weather events including flooding and has led to a rise in global mean sea level (Parry *et al.* 2007; ADB 2009). Streamflow variability is not only highly dependent on anthropogenic activities, but also on seasons and climate (Daniel & Daniel 2006). With their dynamic nature, floods may develop at any space and time scales that conventional rainfall and discharge observation systems are not able to monitor (Marchi *et al.* 2010). Consequently the atmospheric and hydrological generating mechanisms of flash floods in many regions are poorly understood (Borga *et al.* 2011). Hence, understanding the hydro-meteorological processes of flash flooding is extremely important, from both scientific and societal perspectives.

Most Asian countries have suffered from flood disasters frequently. As stated by Dutta & Herath (2004), out of the total number of flood events in the world during the past 30 years, 40% occurred in Asia. The regional distribution shows that South Asia is the most affected region with 39%, followed by Southeast Asia with 30%, East Asia with 25% and with 6% the West Asia region is the least affected. Sharma (2012) observed that the flood events across Asia have increased threefold and sixfold between 2000 and 2009, in comparison with the events in the 1980s and 1970s, respectively. In humid tropical and subtropical climates, especially in the realms of the monsoon, river flooding is a recurrent natural phenomenon (Sanyal & Lu

doi: 10.2166/wcc.2014.075

2004). The southwest monsoon, the seasonal change of winds caused by the reversal of the land–ocean temperature gradient, brings high rainfall over large areas of Asia especially in the South and Southeast Asian countries. Hydrological processes related to land surface and water resources management are strongly affected by the regional characteristics (Kondoh *et al*. 2004). The Intergovernmental Panel on Climate Change (Parry *et al*. 2007) reported that the mean surface air temperature in Southeast Asia increased at the rate of 0.1–0.3 °C per decade between 1951 and 2000. Consequently, the frequencies of extreme weather events such as heavy precipitation and tropical cyclones have increased considerably in Southeast Asia along with an increase in the interannual variability of daily precipitation in the Asia summer monsoon. These climatic changes have brought massive flooding, landslides, and droughts in different regions and have caused extensive damage to property, assets and human life. Studies on the Bagmati watershed in Nepal by Sharma & Shakya (2005) and Dhital & Kayastha (2012) explained that the frequency and duration of monsoon floods have increased since 1991 while their magnitudes have already reached the statistical 100-year flood. Delgado *et al*. (2010) described that in the Mekong River, likelihood of extreme floods has increased during the last decades although the probability of an average flood decreased.

Over global land monsoon regions, monsoon rainfall intensity showed a downward trend during 1950–2004 (Zhou *et al*. 2008). However, a regional study by Yao *et al*. (2008) showed that frequent extreme precipitation events are found over South and Southeast Asia, with the exception of a narrow zone over the Indo-China peninsula along 100 °E. At low latitudes, there are both regional increases and decreases of rainfall over land areas, and increased rainfall intensity, particularly during the summer (southwest) monsoon, could increase the extent of flood-prone areas in temperate and tropical Asia (Houghton *et al*. 2001; Yao *et al*. 2008). Myanmar's location in the transition zone between the South Asian and East Asian monsoon systems results in a particularly complex spatial pattern of precipitation variability which is not very well understood (D'Arrigo *et al*. 2013). With a distinct nature, Myanmar's rainfall has no significant relationship with the contiguous area of India and Bangladesh, even though all of them are under a similar weather system (Sen Roy & Kaur 2000). According to the study of the Association of Southeast Asian Nations Disaster Risk Management Initiative (ASEAN DRMI 2010), a catastrophic 200-year flood (0.5% annual probability of exceedance) would have a major impact on ASEAN countries' economies, which are already fragile. In a comparative analysis of social vulnerability to disaster risks, among ASEAN countries Myanmar is the second worst-affected country after Indonesia, with 3,480 killed per year from natural hazards.

To the knowledge of the authors, few works on the hydrologic characteristics of the large-scale basins in Myanmar have been reported and particularly the Chindwin catchment has received relatively little attention. Further motivation is the public consensus on an increase in flood damage and risk in recent decades. This paper is intended to assess the hydrologic aspects of monsoon floods along the Chindwin River in northern Myanmar. An attempt was also made to identify the flood probability of the mesoscale Chindwin River Basin in the tropical monsoon country. As floods are complex and dynamic processes characterized by spatial and temporal variations, in this paper special attention was paid to the understanding of runoff behavior and its changes which play a crucial role in operational flood assessment.

Regional situation and monsoon floods

Myanmar is located in the northwestern part of the Indo-China peninsula, between 9°32′N and 28°31′N latitudes (with most of the area between the Tropic of Cancer and the Equator) and between 92°10′E and 101°11′E longitudes. Based on topographic conditions, Myanmar is divided into three parts – the western ranges (Himalayan ranges that divide India and Myanmar), the central plains (Ayeyarwaddy delta and other river basins) and the eastern hilly regions (Shan Plateau). River basin characteristics in Myanmar are quite variable due to the physiographic differences (Ti & Facon 2004).

Myanmar is the second biggest country in Southeast Asia, which is characterized by tropical rain forest and monsoon climates with a high and constant seasonal rainfall (Parry *et al*. 2007). Due to the diverse topographic conditions the climate varies across the country. As stated by Htway &

Matsumoto (2011) the southwest monsoon advances in southern Myanmar and onset date is end of May, though the onset date may differ year to year. The monsoon periods with their areal average monthly rainfalls and temperatures (1960–2009) are shown in Figure 1. There is the southwest (summer) monsoon (June to September) with a cloudy, rainy, hot, humid summer and the northeast (winter) monsoon (December to April) with less clouds, scanty rainfall, lower humidity and moderate temperatures. Annual rainfall ranges from as high as 4,000–6,000 mm along the coastal reaches and in the western mountainous region to as low as 500–1,000 mm in the central dry zone. Two-thirds of the country lies in the tropics and one-third in the temperate zone. Lying within the tropics and the great Asiatic continent to the north and the wide expanse of the Indian Ocean to the south, Myanmar furnishes one of the best examples of a monsoon country. Extreme events in Myanmar such as heavy precipitation during the southwest monsoon vary across the country, depending on the monsoon intensity in the Bay of Bengal, while droughts are related to El Niño and El Niño Southern Oscillation on a global scale as well as to the regional monsoon trough and synoptic situations (Houghton *et al*. 2001; Myint *et al*. 2011).

The complex topography of this mountainous country, high rainfall intensities and the large number of glaciers mean that Myanmar is highly exposed to flood hazards. While the contrast between the Asian continent and the surrounding oceans drives the large-scale swing of the monsoon, the regional distribution of monsoon rain is governed, to a large part, by orography (Liu *et al*. 2005). According to the Department of Meteorology and Hydrology (DMH) Myanmar, flood occurrence in Myanmar can be generally recognized as 6% in June, 23% in July, 49% in August, 14% in September and 8% in October. Recorded data by the DMH reveals that several severe floods have occurred in major rivers in Myanmar during recent decades: for example 2004 Ayeyarwaddy; 1991, 2002, 2011 Chindwin; 2002, 2011 Thanlwin; 1997, 2011 Sittaung and 1995, 2011 Bago. In the public's perception, there seems to be a trend of frequent hydrological extreme events, leading to a high risk of flood hazards. Floods usually occur every year in one river system or another during the southwest monsoon. The number of recorded floods with significant impacts continues to rise, making floods one of the most costly natural hazards. A hazard-specific distribution and the impacts of the various disasters that occurred in Myanmar during 1970–2009 are shown in Figure 2. In contrast to the prevailing flood hazards, the present flood management system in Myanmar is not satisfactory for most situations. Moreover, data scarcity still hampers the application of distributed hydrological models for predicting streamflow over a range of spatial scales.

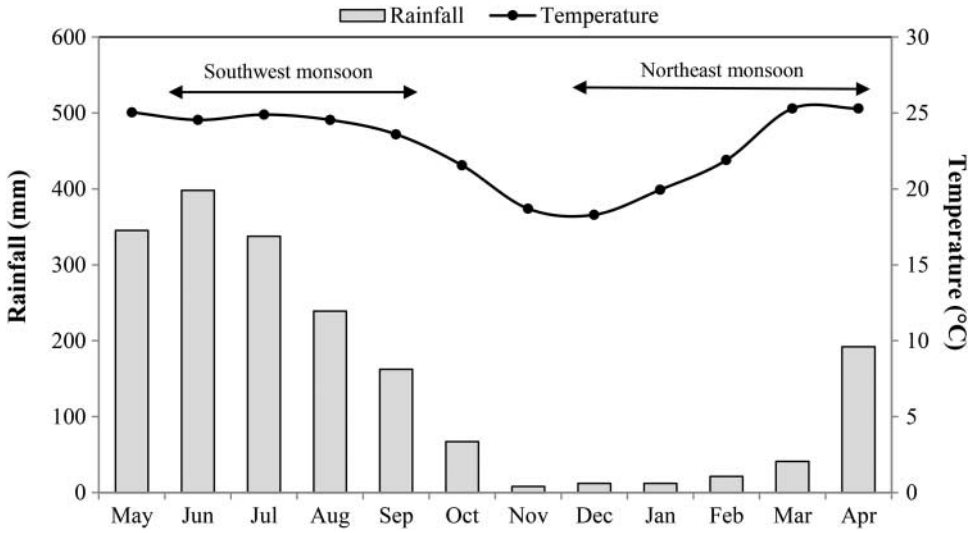

Figure 1 | Typical monsoon seasons of Myanmar.

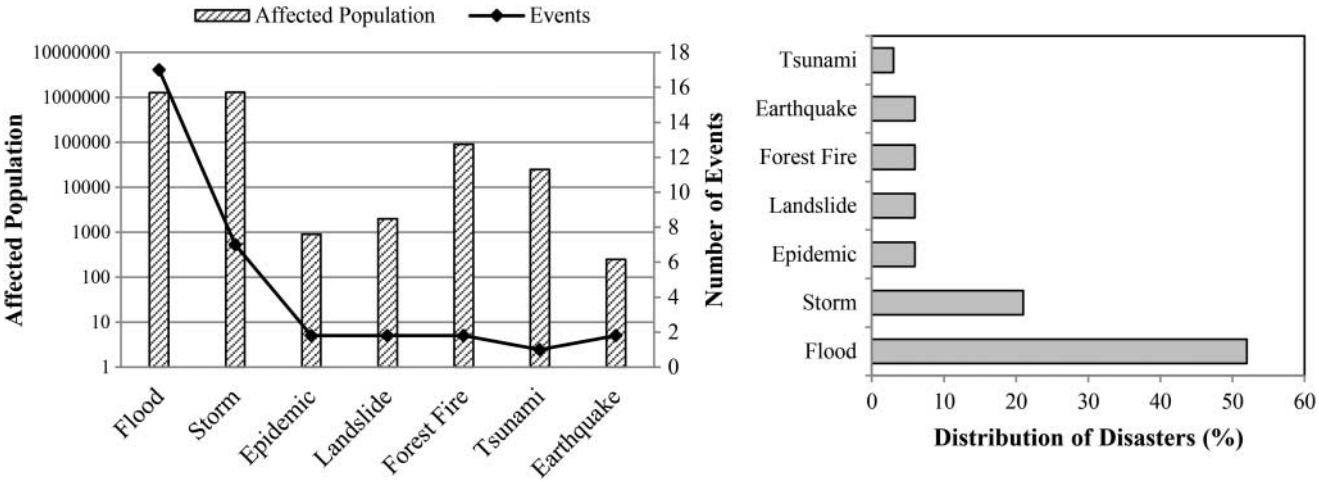

Figure 2 | Disaster impacts in Myanmar during 1970–2009 *Source*: ASEAN DRMI (2010).

Study area

The study was conducted for the Chindwin River Basin with a catchment area of 113,800 km^2 and a length of 985 km, in northern Myanmar as shown in Figure 3. It is the third largest river and one of the principal water resources of the country. It is comparable in size with the Elbe River, which has a catchment area of 148,268 km^2 and a length of 1,091 km, which is the fourth largest river in Europe. The Chindwin's catchment is a mountainous forested terrain with the exception of its lowest southern part, which comprises a wide flood plain. The Chindwin River flows down through the Hukaung valley, Hkamti, Homalin, and Mawlaik to the southwest and changes its course at Kalewa in the southeast, crossing a number of vast plains and finally joins the Ayeyarwaddy River which is one of the major rivers in Asia (Figure 4). The Chindwin River is 350 m wide near Hkamti, and spreading over the meridian direction. Downstream of the defile the river valley gets wider, with a width of 1,200 m near Monywa, and flow velocities slow down when flowing through the central flat terrain. The main tributaries are: the U Yu River just below the Homalin with a catchment area of 7,485 km^2, the Yu River above Mawlaik with 6,423 km^2 and the largest tributary, Myitthar River at Kalewa, with a 25,563 km^2 catchment. The Chindwin with its major tributaries is the most convenient means of communication within the basin connecting it with the main economically developed areas of the country. The river basin occupies almost the entire northwestern part of Myanmar and is important to the development of the country.

Chikamori *et al.* (2012) reported that the Chindwin basin is mainly formed by tertiary continental sediments such as sandstones of different hardness, shale and limestone. There is also exposure of crystalline rocks (granite, granite-gneisses, diorites, etc.) stretching to the east of Chindwin and a range of hills to the north of Monywa station. Closed forest covers 50% of the basin area. The second dominant land type is degraded forest including shrubs which covers about 33%. Agricultural land, alluvial island cultivation and homestead gardening cover 15% of the basin area while shifting cultivation and swamp areas represent 2%. Though the social and economic conditions have changed and the population in the basin has increased in recent years, urbanization effects do not seem to have greater impacts on the basin hydrology compared with the geomorphic conditions. The important role of the basin in national socio-economic development is hampered by flood hazards due to climate conditions. Severe floods hit the Chindwin basin every year at one place or another due to high rainfall intensities during the southwest monsoon. Since 1965 flood occurrences in the Chindwin basin have been highest in July and August contributing 72% of the total number of floods in the basin.

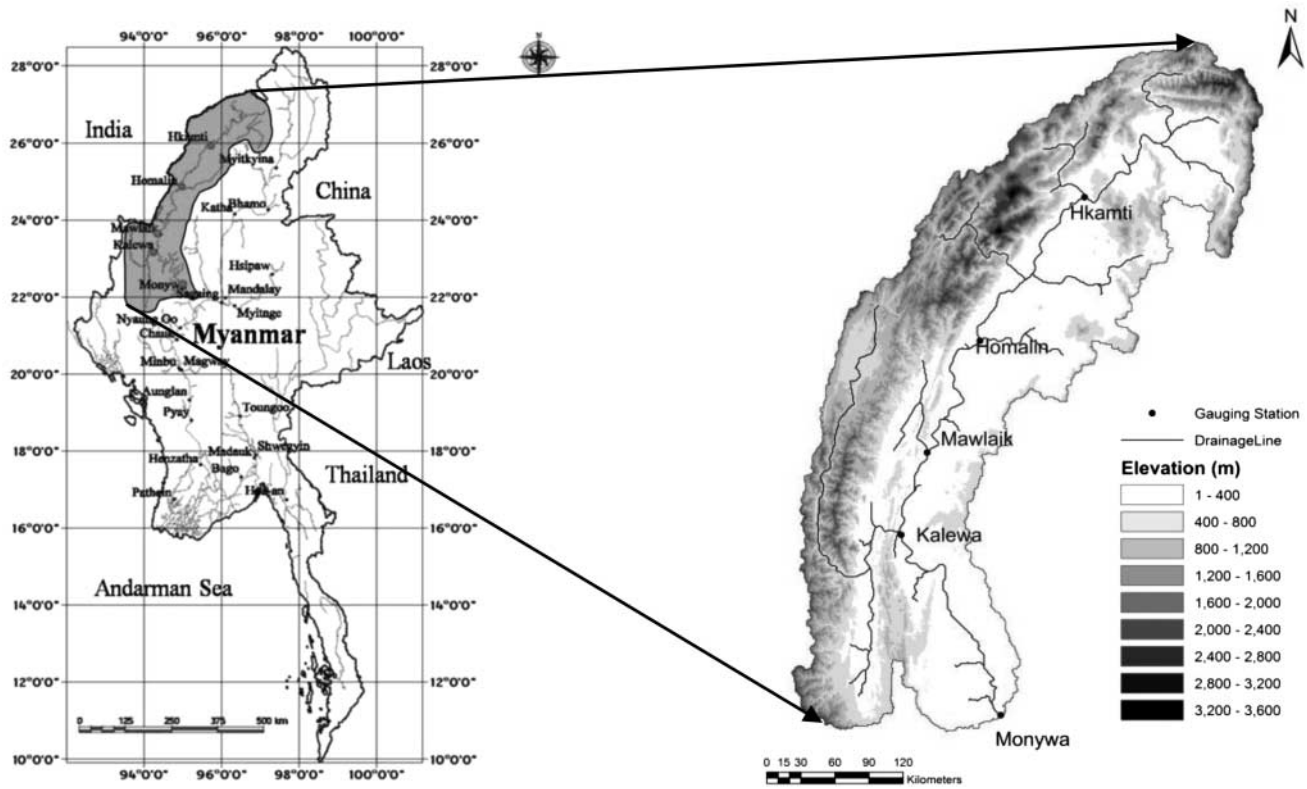

Figure 3 | Location of the Chindwin River Basin.

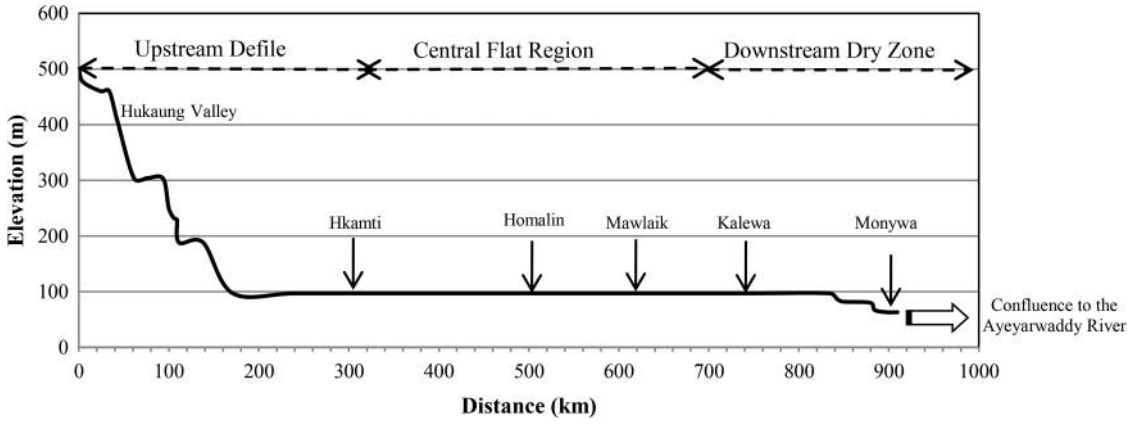

Figure 4 | Longitudinal profile of the Chindwin River from head to confluence.

MATERIALS AND METHOD

Data analyzed in this paper mainly consist of daily discharges and rainfall (1966 to 2011) at five gauging stations and relevant hydro-meteorological data of the basin. The gauging stations also refer to the outlets of the sub-basins of the Chindwin catchment along its main course. Geographic information system (GIS) was used to characterize catchment parameters. The hydro-meteorological data are mostly obtained from the DMH in Myanmar and from the

numerous research articles and published reports which are cited in the reference list. A simple and straightforward approach was applied to characterize the rainfall and flood runoff patterns over the basin based on the analysis of observed hydro-meteorological records and catchment characteristics.

Data review and analysis

Through a GIS process, catchment characteristics were extracted from the global digital elevation model (DEM) available from the USGS (EROS) Hydro 1 K Asia database as well as from ground survey data and maps. EsriArcGIS 10 software was used to analyze spatial parameters of the watershed. First raw DEM data was corrected to create a depressionless DEM by filling the sinks. Then watershed characterization was done by using the ArcHydrol Tools function in ArcGIS which processes and analyzes the corrected DEM data to characterize topography, measure basin parameters, identify surface drainage, subdivide watersheds, and quantify the drainage network. Base flow index (BFI) program was used for identification of annual base flow contributions of the total annual runoff. Among several hydrograph separation methods, the program implements a deterministic procedure developed by the British Institute of Hydrology and the method combines a local minimums approach with a recession slope test (Wahl & Wahl 1995). This program was included in the Developments in Water Science Series, volume 48, edited by Tallaksen & van Lanen (2004). Long-term variability of annual maximum floods in the Chindwin River was studied using flash flood magnitude index (FFMI), suggested by Kale (2003), which is the standard deviation of the logarithms of annual peak discharge, for defining the interannual variability of monsoon floods. A literature review on different aspects of water resources in Myanmar (Ti & Facon 2004; ADB 2009; ASEAN DRMI 2010; Chikamori *et al*. 2012) helps in understanding the study area and provides some preliminary conclusions. Particular attention was paid to information on flood hydrology. Statistical and regional analysis was applied to the observed streamflow and rainfall data at the five gauging stations of the Chindwin River. Mean, standard deviation and coefficient of variation were mainly used to understand the general hydrology of the watershed. Statistical analysis was done using SPSS 19 software and Microsoft Excel 2010.

Time series analysis

Time series analysis involves applying a linear regression to detect the trends of annual maxima (AM) series and their deviation trends. The significance of a linear trend was assessed using a linear regression function in SPSS 19. The issue of a linear trend is whether the slope value is significantly different from zero (i.e. no trend). The slope is the average rate of change over the years being examined. For the test of significance, the *P*-value was determined by referring to a *t*-distribution. The test statistic was calculated dividing the estimated slope coefficient by the estimated standard error. The null hypothesis of no trend is rejected if the *p* value is smaller than the significance level. In this study, a trend was considered to be significant at 5% significance level. If the *p* value is less than or equal to 0.05, there is a significant trend. If not, there is not enough evidence of a meaningful trend at this significance level.

Frequency analysis

Frequency analysis was applied to evaluate the probability of flood occurrences and possible trends during the observation period. Having listed a series of annual maximum floods, they were then ranked in descending order. The empirical recurrence interval (T) and probability (P) of the data could be computed using a plotting position and fitted by Log-Pearson Type III (LP-3) distribution. LP-3 distribution is mostly recommended in flood frequency analysis and is used for design purposes. It is determined by three parameters: mean, standard deviation and the skewness coefficient. Using the AM of the entire study period (1966 to 2011), the hypothetical floods were determined for the return periods of 2 to 1,000 years and then the flood risks were defined in terms of probability for each station along the main river. In the next step, the time series was split into two time phases: TP-1 (1966 to 1990) and TP-2 (1991 to 2011). The moving average method was used to determine at which year time series were split best into two periods. The moving average method smoothes the fluctuations of AM series. The year

at which an obvious change occurs in the moving average series was taken as the trend change year. With this, the time series are also divided into two partial series of similar length. To detect the changes in flood quantiles, the relative differences of flood quantiles in two time phases with respect to the entire observation period were compared.

Based on the flood frequencies, the index flood method could be applied to derive the regional frequency curve (Riggs 1982). The basic premise of this method is that a combination of streamflow records obtained at a number of gauging stations will produce a more reliable, not a longer, record, and thus will increase the reliability of frequency analysis within a region (Jain & Singh 2003). A dimensionless frequency curve representing the ratio of the flood of any frequency to an index flood, which is the mean annual flood, was generated.

RESULTS AND DISCUSSION

Hydrology

Orographic effects, as a natural barrier to the southwest monsoon in the meridian direction, cause much greater precipitation on the west side of the mountains and a rain shadow on the east side. Further, from the source of the Chindwin to its mouth the amount of rainfall also decreases because of the western disturbance and tropical cyclones in the Bay of Bengal. Assessment of the long-term average annual rainfall demonstrates that the spatial variation of rainfall was also influenced by topography. As a monsoon-dominated catchment, riverine floods and flash floods are most common to the Chindwin River when intense rainfall persists at the headwaters of the basin seasonally and annually. Generally the northern part of the Chindwin basin receives an average of 3,800 mm per year, while the lower (southern) part of the basin gets only 760 mm. Nearly 90% of the rainfall in the northern part and 75% in the southern part of the basin falls between June and October. In a flood warning context, floods are expected when critical values are exceeded. The DMH has defined the threshold discharge for a given cross-section of the Chindwin River. Threshold runoffs are 13,500 $m^3 s^{-1}$ at Hkamti, 14,200 $m^3 s^{-1}$ at Homalin, 16,200 $m^3 s^{-1}$ at Mawlaik, 16,800 $m^3 s^{-1}$ at Kalewa and 19,000 $m^3 s^{-1}$ at Monywa.

Figure 5 shows the annual rainfall comparison at different stations and typical rainfall pattern and streamflow of the upper Chindwin basin. It can be seen that intense rain falls almost every day during the southwest monsoon season. Lag or response time of rainfall to flow is about 1 to 3 days depending on the rainfall distribution. While single peak floods are characteristic during the southwest monsoon season especially in the lower basin, sometimes multiple peak events occur due to rain on successive days mostly in the upper Chindwin basin. They are imposed on the annual flood hydrograph, which is unique for any given year but similar in shape between different years. Annual cycle and flood season are stable and defined by monsoon precipitation that arrives approximately at the same time of the year. The high fluctuation of streamflow patterns in the Chindwin catchment is influenced by the extreme variation of rainfall in the region.

Generally monsoon floods display temporal patterns characterized by long period fluctuations and non-random behavior in terms of discrete periods of low and high floods (Kale 1999). The high rises of water levels and discharges are often noticed in July and August, the mid-season of the monsoon when soils are saturated with water concurrently and infiltration during intense rainfall is less. Nevertheless, early and late monsoon floods should also be considered as common events. According to past flood events since 1966, the highest river level reached 4 m above the danger level at the upper Chindwin basin contributing discharges of 19,613 $m^3 s^{-1}$ and 19,400 $m^3 s^{-1}$ at Hkamti in 1991 and 1997, 26,773 $m^3 s^{-1}$ and 26,443 $m^3 s^{-1}$ at Mawlaik in 1976 and 2002, and 26,220 $m^3 s^{-1}$ at Kalewa (lower basin) in 2002. The severe floods, which were over critical levels on 22 July 2004 (17,673 $m^3 s^{-1}$) at Hkamti, 15 July 1997 (19,470 $m^3 s^{-1}$) at Homalin, 01 September 1999 at Mawlaik (24,093 $m^3 s^{-1}$), 10 July 2008 (23,720 $m^3 s^{-1}$) at Kalewa and 19 August 2002 (23,957 $m^3 s^{-1}$) at Monywa, lead to the assumption that extreme events have occurred more often in the last two decades. Duration of floods above the danger levels varied from 9 to 18 days. The danger level corresponds to the crest height of the levees. Historical flood records indicated that the middle part of the basin also has a high potential flood

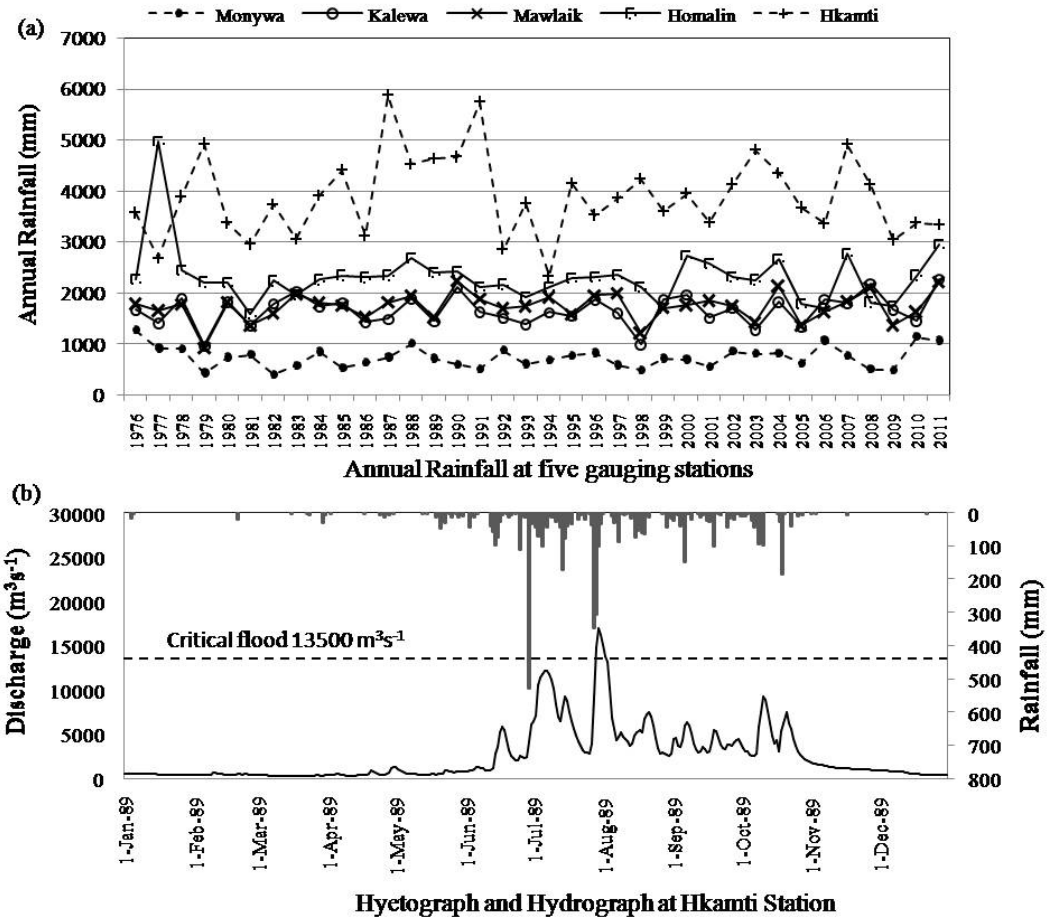

Figure 5 | Annual Rainfall and Typical Rainfall Pattern of the Chindwin River (a) Annual rainfall and (b) typical rainfall and streamflow pattern of the Chindwin River.

hazard although rainfall is not as high as in the most upstream catchment. During the southwest monsoon, flood flows at the middle station (Mawlaik) are moderately correlated with those of the upstream station, Hkamti ($R^2 = 0.5$), but strongly correlated with the lower station, Monywa ($R^2 = 0.8$). The latter situation is likely due to the similar geomorphic condition and rainfall distribution over these areas.

According to Kondoh *et al.* (2004) Myanmar belongs to region B2 of Monsoon Asia where the climate is characterized by distinct wet and dry seasons with a large water deficit in the dry season. Maximum mean annual temperature at the Monywa station (lower part of the basin) is 29 °C whereas the minimum mean annual temperature amounts to 25 °C. Average annual evaporation is high with about 1,400 mm/a in the southern part of the basin to 1,000 mm/a in the north. This causes an average basin loss of about 45% of total rainfall. From daily streamflow records, annual base flow contributions were determined and expressed in BFI, which is the ratio of base flow to total flow volume for a given year. The average specific discharge at five stations ranges between 0.20 $m^3 s^{-1} km^{-2}$) and 0.53 ($m^3 s^{-1} km^{-2}$). Basin area and slope, river length and slope are determined using GIS based on the DEM of 1 km^2 resolution. All parameters, together with basin properties, are shown in Table 1.

Figure 6(a) shows the FFMI against the ratios of observed highest discharge and average annual maximum discharge at different stations. FFMI values range between 0.08 and 0.1 showing that the interannual variability in

Table 1 | Catchment characteristics of the Chindwin Basin

Parameter	Hkamti	Homalin	Mawlaik	Kalewa	Monywa
Location	N-26° 00′ E-95° 42′	N-24° 52′ E-94° 55′	N-23° 38′ E-94° 25′	N-23° 12′ E-94° 18′	N-22° 06′ E-95° 08′
Basin area (km^2)	27,210	49,137	69,057	99,072	113,814
River length (km)	347	546	660	741	985
River slope	0.0013	0.0002	0.0004	0.0002	0.0003
Basin slope	0.104	0.122	0.118	0.120	0.114
Mean annual rainfall (mm)	3,830	2,287	1,738	1,685	764
Mean annual max flow ($m^3\,s^{-1}$)	14,387	16,243	19,542	20,054	20,603
Specific discharge ($m^3\,s^{-1}\,km^{-2}$)	0.53	0.33	0.28	0.20	0.18
BFI	0.61	0.69	0.73	0.74	0.77

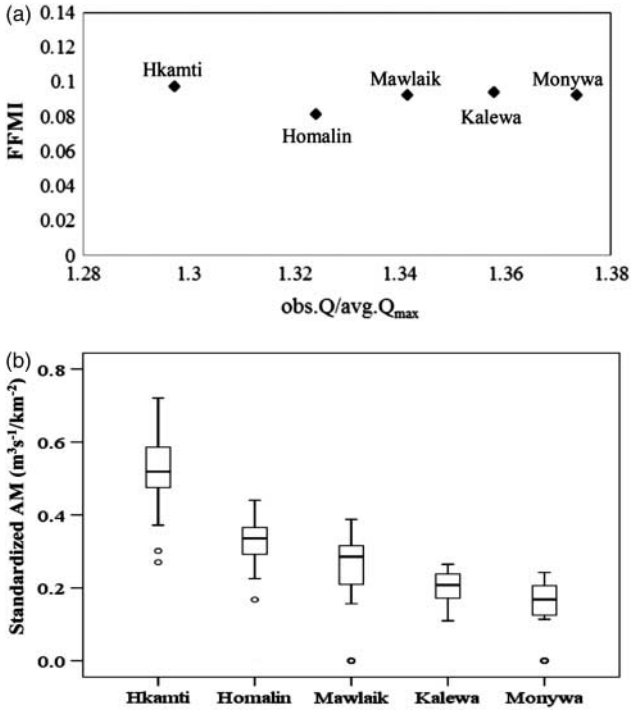

Figure 6 | Variability of annual floods: (a) FFMI against the ratio of observed largest floods to mean annual maximum discharges; (b) distribution of standardized AM.

flood peaks was not very different from station to station. Figure 6(b) shows the box plot of AM standardized by the basin area. The annual maximum flood relative to the basin area is highest at Hkamti followed by Homalin, Mawlaik, Kalewa and Monywa. Flood generation decreases with the increase in the catchment area. The standardized AMs are more variable over time at Hkamti and Mawlaik, with higher standard deviations than at other stations.

Time series and frequency analysis of floods

The trends in AM and variability of extreme floods were evaluated. Temporal trends of AM series and their deviations were detected at five stations along the Chindwin River using a linear regression. Annual maximum discharges (Qmax) and deviation trends (1967–2011) at two selected gauging stations are shown in Figure 7. Table 2 shows the slope factors and *p*-values as the significance test for a linear trend.

AM series at all stations show slightly decreasing trends with negative slopes. But trends were not significant as *p*-values are much greater than 0.05. Thus, the AM series of the Chindwin River can be regarded as stable for the observation period. The statistical mean value was not changing with time and there was no significant trend. However, the deviation of annual peaks from their mean (regardless of positive or negative) showed increasing trends with positive slopes at all stations. Deviation trends at Hkamti and Mawlaik stations were highly significant at the 5% level with *p*-values of 0.001 and 0.05, respectively. At Monywa station, the deviation of AM series showed an increasing trend with a marginal significance ($p = 0.068$). At Homalin and Kalewa stations, there was not enough evidence for meaningful trends at the 5% significant level.

The trend to a higher deviation and thus variation of annual maximum floods is in accordance with the hypotheses of climate change, making the region experience more extreme events. For example, ADB (2009) reported that Southeast Asia is one of the world's most vulnerable

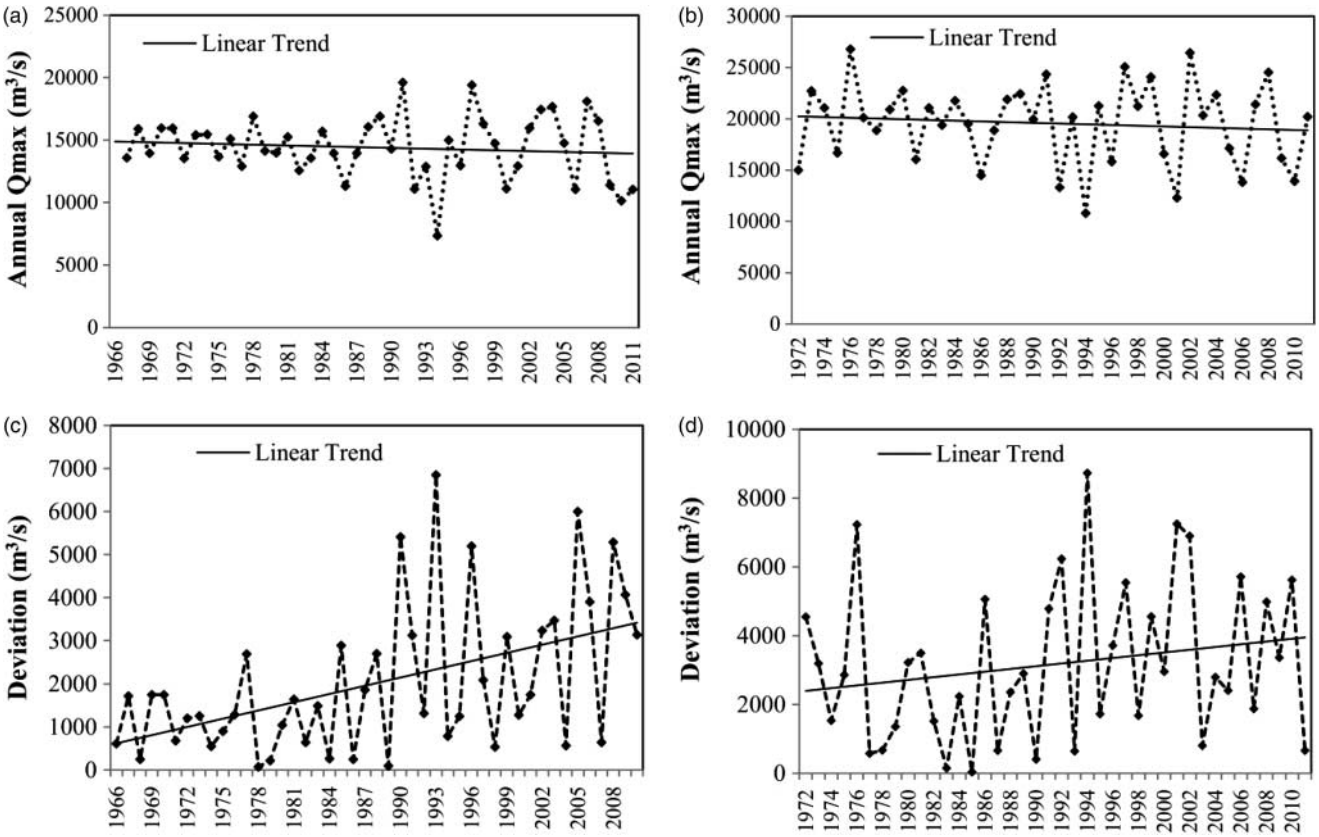

Figure 7 | Linear trends of annual Q_{max} at (a) Hkamti (b) Mawlaik and deviation of annual Q_{max} from mean value at (c) Hkamti (d) Mawlaik.

Table 2 | Linear trend statistics of two time series for different stations

	AM		Deviation of AM from the means	
Station	**Slope**	***P*-value**	**Slope**	***P*-value**
Hkamti	−21	0.6	55	0.001
Homalin	−28	0.4	30	0.150
Malwaik	−42	0.5	68	0.050
Kalewa	−28	0.6	25	0.320
Monywa	−10	0.8	45	0.068

regions to the impact of climate change in terms of frequency and intensity of extreme weather events which are projected to increase. Furthermore, frequent extreme precipitation over Southeast Asia is predicted in the next few decades due to climate change and that is definitely going to worsen the flooding situation in the region (Houghton *et al.* 2001; Yao *et al.* 2008; Turral *et al.* 2011). Statistically, the time series are thus not homogeneous.

In many cases large rivers with the highest annual variability may have potential impacts from dams because of substantial control over downstream hydrology (Graf 2006). However, flow changes by dam building were not evident in the Chindwin watershed. According to the collected data from the Myanmar Irrigation Department, there is no dam across the main stream yet and only three dams have been implemented in recent years on the Chindwin's tributaries. Locations of the dams are on the Neyinsara River (23°31′ N and 94°06′ E), on the Manipur River (22°58′ N and 93°58′ E), and on the Myitthar River (22°00′ N and 94°02′ E). But none of these dams is finished yet and regulated controls are not capable of exerting substantial influence on downstream hydrology. Although their impacts could not be fully assessed, the damming was not a prime influencing factor for the variability of floods whose magnitudes have increased in the last two decades. Furthermore, as stated by Bruijnzeel (2004), it is difficult to evaluate the effects of land use change on flood peaks in large rivers

because such changes are rarely fast and consistent with the exception of high population pressure and thus often compounded by climatic variability. High variability of streamflow could be expected as an effect of an interannual structure in regional climate as well as changes in monsoon intensity. Regarding other monsoon-dominated rivers in Southeast Asia, Delgado *et al.* (2010) came to a similar conclusion that the variation of extreme floods in the Mekong River was validated with the precipitation data, which suggests climatic causes for the increase in variability.

Frequency analysis was then applied to annual maximum discharges of five stations during 1966 to 2011. Although not all stations covered the same data length, all streamflow data used span over 40 years of records. Mean, standard deviation, skewness coefficients and coefficients of variation (CV) of the annual maximum series of the different stations are shown in Table 3. Probable floods at each gauging station were computed by using the LP-3 distribution for different return periods of 2 to 1,000 years. The expected hypothetical floods were compared with the highest observed flows in the past 40 years as shown in Figure 8. Comparing the expected floods with the highest observed floods, suggests that these correspond in the upper mountainous catchment (Hkamti and Homalin) to about 100-year events. In the central flat terrain with medium elevations (Mawlaik) the maximum observed flood has a statistical return interval of about 50 years, while in the lower part of the dry zone area (Kalewa and Monywa) it is about 15 years. It is generally assumed that the reliability of statistical analyses increases with the length of time series or the number of data. An important precondition for this, however, is that the set of data is homogeneous, drawn from a single data population. As found above, this condition is not fulfilled for the flood data of the Chindwin River. There was a rise in standard deviation particularly in the last two decades caused by outer (most extreme) influences (Table 3). The most likely effects on this high flood variability are the changes in rainfall intensity and pattern in the region, as discussed above. The standard deviations of AM series for the data from the last two decades are 2.4, 1.5, 1.5, 1.3 and 1.4 times greater than that of the period 1966–1990 at Hkamti, Homalin, Mawlaik, Kalewa and Monywa, respectively.

Taken strictly, the frequency analysis of the entire observation period was not admissible. Therefore, the AM series should be analyzed in different time phases. A moving average with seven spans was used to check the trend change at all stations. The year when the AM series were split is the year in which a trend of flood variability changes. Moving average series for five stations are given in Figure 9. Although the trend change years for all stations are not identical, with less fluctuation, the moving average series for all stations are generally smooth till 1990 and the higher fluctuations occurred in the later periods. In this study, detecting exact change points using possible statistical tests is not the main focus. Instead, the authors would like to point out that the deluge of extreme floods frequently occurred after 1990, especially concentrated in the last 20 years of the time series.

In Monsoon Asia, substantial regional features are associated with the changes in precipitation amounts and duration, and in southeast China, a sharp increase in extreme precipitation (>50 mm per day) occurred in 1993 (Yao *et al.* 2008). The change point for annual maximum flood series of the Wijiang River in South China was found in 1991with an increase in mean of AM by 45% due

Table 3 | Statistical parameter of annual maximum series

	Mean ($m^3 s^{-1}$)			Standard deviation ($m^3 s^{-1}$)			Skew coefficient			CV
Station	Entire period	1966–1990	1991–2011	Entire period	1966–1990	1991–2011	Entire period	1966–1990	1991–2011	Entire period
Hkamti	14,387	14,582	14,165	2,481	1,404	3,343	−0.31	−0.24	−0.80	0.17
Homalin	16,243	16,782	15,653	2,715	2,128	3,189	−0.64	0.32	−0.66	0.17
Mawlaik	19,542	20,017	19,113	3,931	3,001	4,650	−0.31	−0.05	−0.20	0.20
Kalewa	20,054	20,504	19,518	4,175	3,663	4,750	- – 0.36	−0.40	−0.21	0.21
Monywa	20,603	20,804	20,362	4,103	3,480	4,820	−0.02	0.16	0.07	0.20

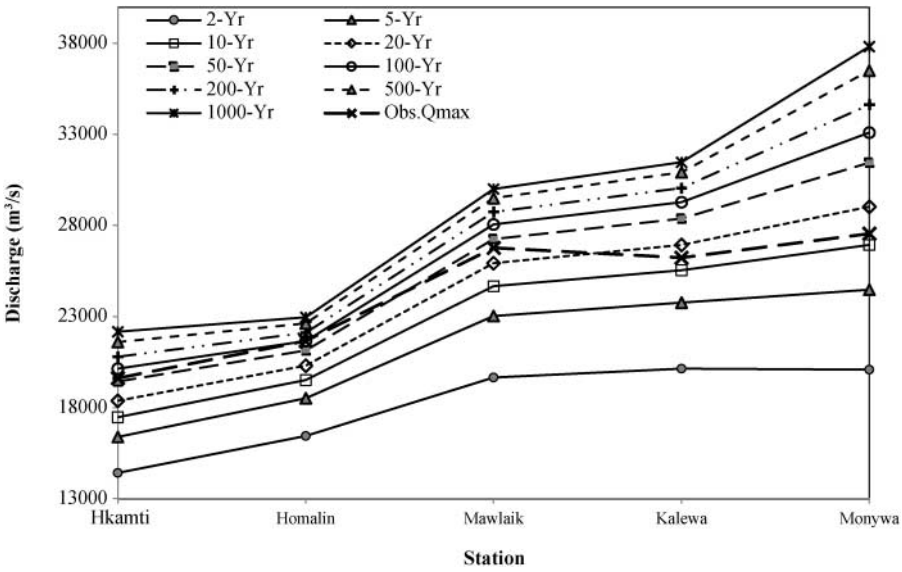

Figure 8 | Observed maximum floods and expected flows with different return periods.

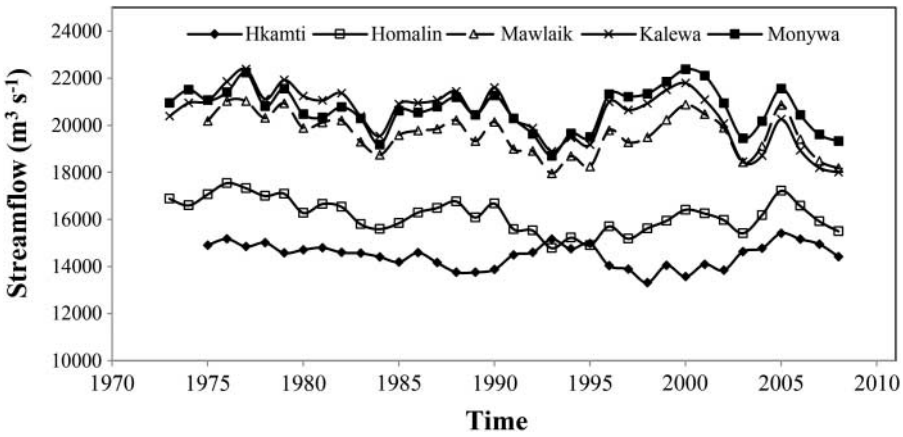

Figure 9 | Moving average series of annual maxima at five stations.

to increased rainstorms (Chen *et al*. 2013). In Southeast Asia, extreme weather events associated with El Niño were more frequent and intense in the past 20 years (Parry *et al*. 2007). Interannual rainfall and temperature variability in Myanmar is affected by the ENSO (El Niño Southern Oscillation) patterns (Lwin 2006; Baroang 2013). With the effects of warmer temperature, the increased water vapor will possibly result in an increase in precipitation amount and intensity (Houghton *et al*. 2001; Wang *et al*. 2008). Thus extreme floods in the Chindwin catchment were found not only in strong La Niña but also in strong El Niño years, and the extreme floods associated with moderate to strong El Niño years have been observed since 1991.

A sharp increase in the maximum flood level (4.3 m above danger level) at Hkamti station occurred in 1991 and the occurrences of extreme floods (>2 m above the danger levels) are more frequent at Hkamti, Mawlaik and Kalewa stations from 1991 onwards. These regional and local situations show that higher interannual variations of streamflows in the Chindwin catchment are expected in the past 20 years. Through this reasoning, AM series are analyzed with two time phases: TP1 (1966–1990) and TP2

(1991–2011). Overall, 1990 was considered the trend change year for the Chindwin watershed because the deviations of AM series at all stations are also getting larger around this year. Modification of the rating curve for the Monywa station was carried out in 2009 and any changes of monitoring method which affect the rating curves could not be observed for all stations. Sometimes human activities are more important in the regional hydrologic regime (Yang *et al.* 2004); however the variation of extreme floods in the Chindwin catchment after 1990 is probably due to climatic causes especially precipitation since the major human-induced impacts such as damming and land use changes were not evident in the catchment.

The two respective frequency curves, along with the plotting positions, for Hkamti and Mawlaik stations are shown in Figure 10. Parameters are given in Table 3. As expected, the frequency curves based on 1991–2011 records, with the exception of Homalin, provided higher floods. Hypothetical floods of the two frequency curves were then compared for the return periods. The increase of flood magnitudes in TP-2 with respect to TP-1 was expressed as a percentage as shown in Figure 11. Beyond the 5-year return period, expected floods are 2.5% to 26% higher for the data of TP-2. Only at Homalin station was no significant difference found.

To analyze the change in flood peak series, relative differences of flood quantiles in two periods were compared with respect to that of the entire period and results are shown in Figure 12. In the latter period (1991–2011), flood values are increasing 3% to 15% at different stations while the flood values of the former period (1966–1990) are decreasing up to 13% with the exception of Homalin station. In both comparisons of relative differences in flood values of two series with respect to the entire series, the highest difference (either high or low values) was found at the Hkamti station followed by Mawlaik, Monywa and Kalewa, respectively. This significance shows that the change in flood quantiles of the Chindwin River is decreasing from upstream to downstream.

The index-flood method was also applied here as a tool for regionalization of the basin using five station data. Dawdy & Gupta (1995) assess this method as unrealistic with its assumption of simple scaling, that the coefficient of variation is not changing with the increasing catchment area. Normally, CV decreases with the increasing catchment scale due to damping effects (Kuzuha *et al.* 2009). In the Chindwin basin, mean annual flood rises with the increase of catchment areas and CV is changing with increasing catchment as shown in Table 3. This agrees with the former argument. Flood indices (FI) were calculated as the ratios of expected floods with different return periods (Q_e) to the mean of observed annual maximum series (Table 4). The regional frequency curve is shown in Figure 13. In averaging the entire basin, the expected floods may range

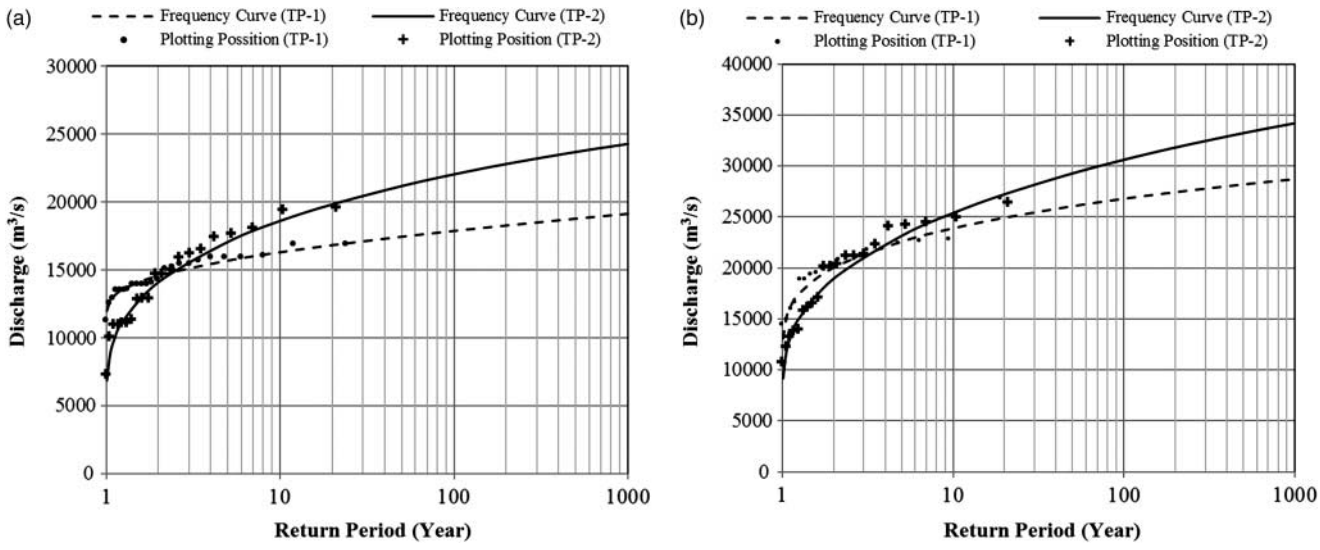

Figure 10 | Comparison of frequency curves with the most significant differences: (a) Hkamti (b) Mawlaik.

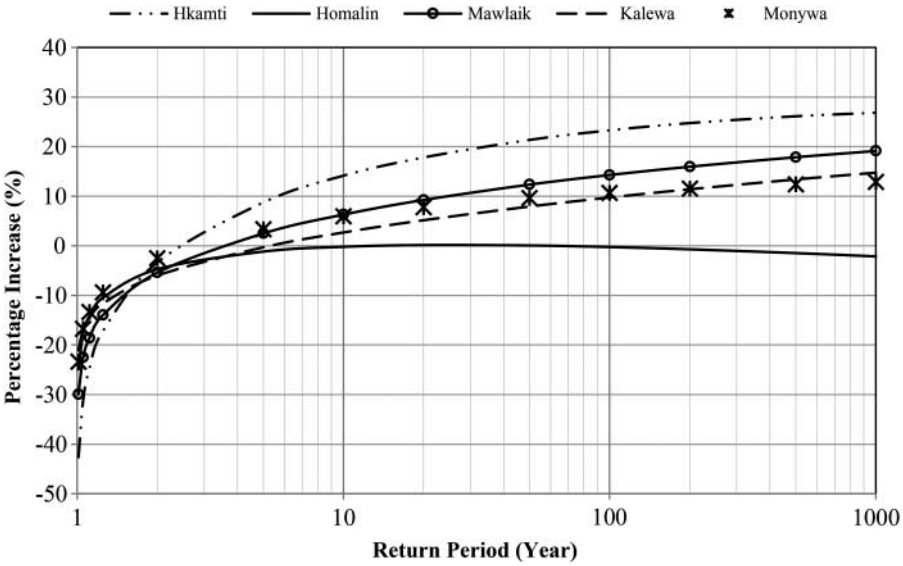

Figure 11 | Percentage increase of flood quantiles in comparison with TP-1 and TP-2 series.

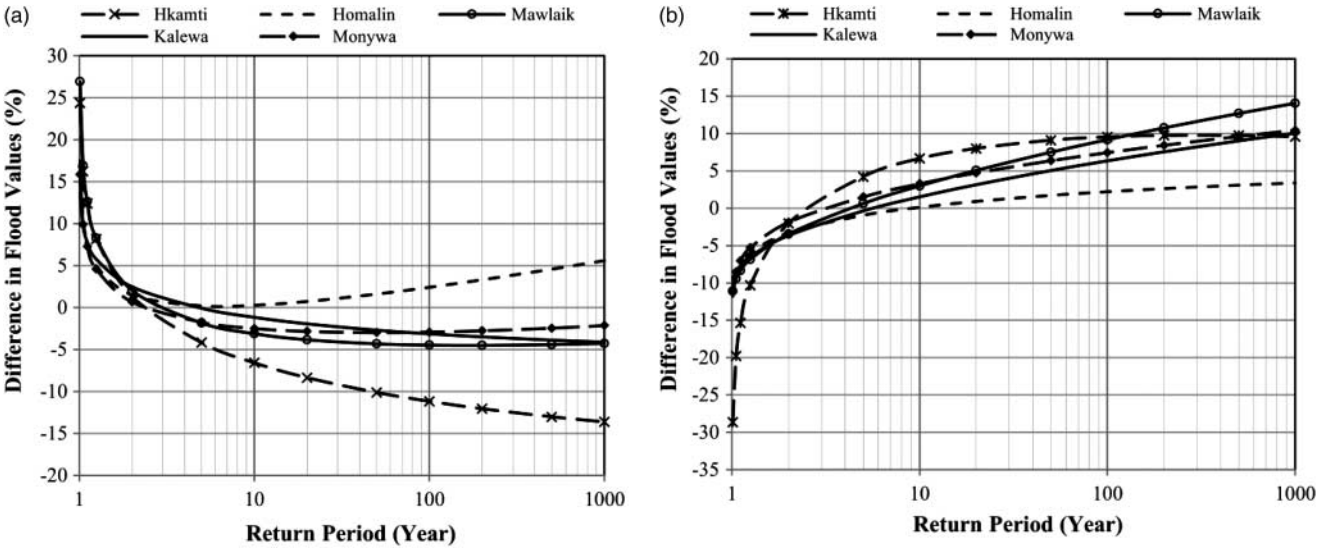

Figure 12 | Comparison of flood quantiles: (a) TP-1 and entire period; (b) TP-2 and entire period.

between 0.6 and 1.5 times the mean annual maximum discharge. Average FI for all return periods at each station lie within 1.2 to 1.3, from upstream to downstream. The average value of the highest expected floods would not be much different from station to station. It is also noticeable that the expected floods, even with higher return periods, are not largely different from the average annual maximum floods of the basin.

CONCLUSIONS

Severe floods with high rainfall during the southwest monsoon are the most serious natural disasters in Myanmar. Flood risk management, however, is not yet well-developed. Flood characteristics and trends at five gauging stations along the Chindwin River are evaluated. Under the regional climate the Chindwin is a perennial river with high seasonal

Table 4 | FI at different stations

	Hkamti		Homalin		Mawlaik		Kalewa		Monywa		Average FI
Return period (yr)	Q_e ($m^3 s^{-1}$)	FI	Q_e ($m^3 s^{-1}$)	FI	Q_e ($m^3 s^{-1}$)	FI	Q_e ($m^3 s^{-1}$)	FI	Q_e ($m^3 s^{-1}$)	FI	
1	7,759	0.54	10,162	0.63	9,844	0.50	9,929	0.50	11,568	0.56	0.55
2	14,436	1.00	16,438	1.01	19,640	1.01	20,126	1.00	20,130	0.98	1.00
5	16,543	1.15	18,545	1.14	23,088	1.18	23,819	1.19	23,703	1.15	1.16
10	17,520	1.22	19,591	1.21	24,789	1.27	25,659	1.28	25,687	1.25	1.24
20	18,256	1.27	20,423	1.26	26,129	1.34	27,116	1.35	27,393	1.33	1.31
50	18,988	1.32	21,310	1.31	27,530	1.41	28,651	1.43	29,381	1.43	1.38
100	19,425	1.35	21,876	1.35	28,408	1.45	29,618	1.48	30,754	1.50	1.42
200	19,783	1.38	22,371	1.38	29,159	1.49	30,450	1.52	32,042	1.56	1.46
500	20,175	1.40	22,949	1.41	30,017	1.54	31,406	1.57	33,654	1.64	1.51
1,000	20,411	1.42	23,328	1.44	30,555	1.56	32,019	1.60	34,807	1.69	1.54
Average FI		1.20		1.21		1.29		1.27		1.31	

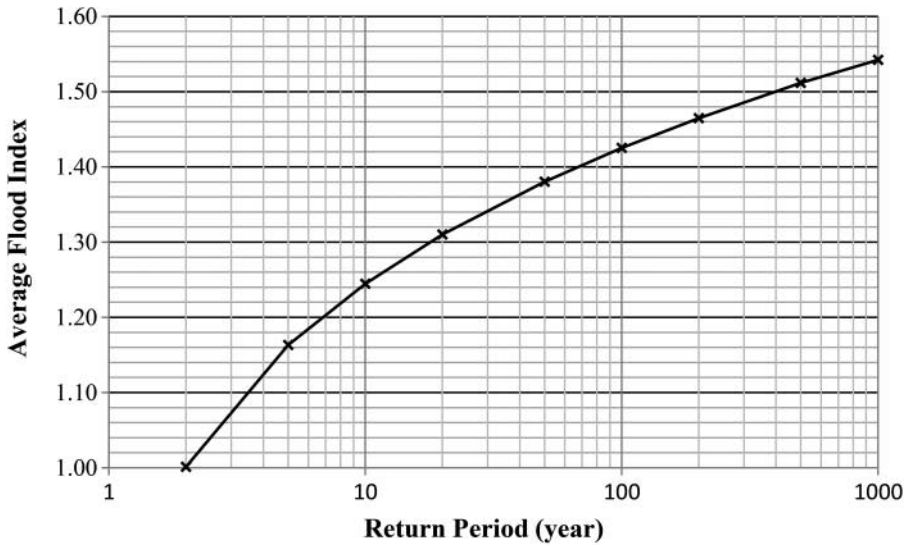

Figure 13 | Flood regionalization of the Chindwin River Basin.

variation in discharge and rainfall, since up to 90% of rainfall occurs during the southwest monsoon. In the past flood levels have reached up to 4 meters over the bank level at Hkamti in 1991 and 1997, at Mawlaik and Kalewa in 2002, resulting in relatively large inundations. Duration of most floods generally lasts over 10 days and such long-lasting floods are frequent occurrences in the basin seasonally and annually.

Statistical analysis shows that there are no trends of the mean values of annual maximum discharges but strong trends in standard deviation and probability curves along the main stream. Particularly at the upper station (Hkamti) and the middle station (Malwaik), over the last two decades the standard deviations of AM have significantly increased 2.4 and 1.5 times, respectively, compared with the period 1966–1990. The study pointed out the remarkable increase in flood occurrence as well as the increasing trend of deviation of annual maximum floods with time since 1990. Frequency analysis of the entire observation period indicates that the river has already experienced a 100-year flood in the

upper part, 50-year flood in the middle and a 15-year flood in the lower part. The paper also concludes that flood risk is high in the upper and middle regions of the basin. To detect the changes in flood quantiles, two distinct phases were studied: 1966 to 1990 with small deviation of annual maximum discharge and 1991 to 2011 with increasing trend of high floods. As the basin is not well industrialized and urbanized, except in Monywa, any substantial changes in land management were not evident in the catchment. However, the cause for the increasing variability in annual peaks is probably the interannual structure of regional climate and changes in monsoon intensity. It is recommended that interannual variation of streamflow should be validated with the detailed spatial precipitation data at the regional level. Attention should also be paid to human activities which alter regional hydrologic regimes, affecting long-term changes in streamflow at both seasonal and regional scales.

As a result better understanding of monsoon flood characteristics of the Chindwin River Basin would contribute to improved flood hazard management because an effective mitigation plan could never be realized without a proper understanding and assessment of the regional characteristics. The study also gives motivation for further analysis of flood extents in this poorly gauged basin with finer spatial scale. It also suggests that flood management could benefit by paying more attention to the area with relatively high probability floods with the application of reliable forecasting methods coupling with inundation assessments.

ACKNOWLEDGEMENTS

The study was funded by the Deutscher Akademischer Austausch Dienst (German Academic Exchange Service). The hydrometric data used in this analysis was provided by the DMH, Myanmar.

REFERENCES

ADB 2009 *The Economics of Climate Change in Southeast Asia: A Regional Review*. Asian Development Bank, Manila.

ASEAN Disaster Risk Management Initiative 2010 *Synthesis Report on Ten ASEAN Countries Disaster Risks Assessment*. World Bank, Association of Southeast Asian Nations (ASEAN), United Nations Office for Disaster Risk Reduction – Regional Office for Asia and Pacific (UNISDR AP), Global Facility for Disaster Reduction and Recovery (GFDRR).

Baroang, K. 2013 Myanmar Bio-Physical Characterization: Summary Findings and Issues to Explore. Background paper No.1. Report for USAID/Burma.

Borga, M., Anagnostou, E. N., Blosch, G. & Creutin, J. D. 2011 Flash flood forecasting, warning and risk management: the HYDRATE project. *Environmental Science & Policy* **14** (7), 834–844.

Bruijnzeel, L. A. 2004 Hydrological functions of tropical forests: not seeing the soil for the trees? *Agric. Ecosyst. Environ.* **104**, 185–228.

Chen, X., Zhang, L., Xu, C. Y., Zhang, J. & Ye, C. 2013 Hydrological design of nonstationary flood extremes and durations in Wijiang River, South China: changing properties, causes, and impacts. *Math. Probl. Eng.* 2013, Article ID 527461.

Chikamori, H., Heng, L. & Daniell, T. (eds) 2012 *Catalogue of Rivers for Southeast Asia and the Pacific Volume VI*. UNESCO-IHP Regional Steering Committee for Southeast Asia and the Pacific, Indonesia.

D'Arrigo, R., Palmer, J., Ummenhofer, C., Kyaw, N. N. & Krusci, P. 2013 Myanmar monsoon drought variability inferred by tree rings over the past 300 years: linkages to ENSO. In: *El Nino-Southern Oscillation* (P. Braconnot, C. Brierley, S. P. Harrison, L. von Gunten & T. Kiefer, eds). PAGES news 21(2), pp. 50–51.

Daniel, T. M. & Daniel, K. A. 2006 Human impacts, complexity, variability and non-homogeneity: four dilemmas for the water resources modeler. In *Climate Variability and Change: Hydrological Impacts. Proceedings of the Fifth FRIEND World Conference*, IAHS Publ. 308, pp. 10–15.

Dawdy, D. R. & Gupta, V. K. 1995 Multiscaling and skew separation in regional floods. *Water Resour. Res.* **31** (11), 2761–2767.

Delgado, J. M., Apel, H. & Merz, B. 2010 Flood trends and variability in the Mekong river. *Hydrol. Earth Syst. Sci.* **14**, 407–418.

Dhital, Y. P. & Kayastha, R. B. 2012 Frequency analysis, causes and impacts of flooding in the Bagmati River Basin, Nepal. *J. Flood Risk Manage.*

Dutta, D. & Herath, S. 2004 Trends of floods in Asia and flood risk management with integrated river basin approach. *Proceedings of the Second International Conference of Asian-Pacific Hydrology and Water Resources Association*, Singapore. 1, 55–63.

Graf, W. L. 2006 Downstream hydrologic and geomorphic effects of large dams on American rivers. *Geomorphology* **79**, 336–360.

Houghton, J. T., Ding, Y., Griggs, D. J., Noguer, M., van der Linden, P. J., Dai, X., Maskell, K. & Hohnson, C. A. (eds) 2001 *Climate Change 2001: The Scientific Basis*. Contribution of Working Group I to the Third Assessment Report of the Intergovernmental Panel on Climate Change. Cambridge University Press, Cambridge.

Htway, O. & Matsumoto, J. 2011 Climatological onset dates of summer monsoon over Myanmar. *Int. J. Climatol.* **31**, 382–293.

Huntington, T. G. 2006 Evidence for intensification of the global water cycle: review and synthesis. *J. Hydrol.* **319** (1–4), 83–95.

Jain, S. K. & Singh, V. P. 2003 Water resources systems planning and management. *Dev. Water Sci.* **51**.

Kale, V. S. 1999 Long-period fluctuations in monsoon floods in the Deccan Peninsula, India. *J. Geol. Soc. India* **53**, 5–15.

Kale, V. S. 2003 Geomorphic effects of monsoon floods on Indian Rivers. *Nat. Hazards* **28**, 65–84.

Kondoh, A., Harto, A. B., Eleonora, R. & Kojiri, T. 2004 Hydrological regions in monsoon Asia. *Hydrol. Process.* **18**, 3147–3158.

Kuzuha, Y., Tomosugi, K., Kishii, T. & Komatsu, Y. 2009 Coefficient of variation of annual flood peaks: variability of flood and rainfall intensity. *Hydrol. Process.* **23**, 546–558.

Liu, W. T., Xie, X. & Tang, W. 2005 Monsoon, orography, and human influence on Asian rainfall. *Proceedings of the First International Symposium in Cloud-prone & Rainy Areas Remote Sensing (CARRS)*, Chinese University of Hong Kong.

Lwin, T. 2006 The impact of El Nino and La Nina events on the climate of Myanmar. 12th Pacific Congress (PACON) on Marine Science and Technology in Asia.

Marchi, L., Borga, M., Preciso, E. & Gaume, E. 2010 Characterization of selected extreme flash floods in Europe and implications for flood risk management. *J. Hydrol.* **394** (1–2), 118–133.

Myint, U. T., Thaw, S. H. & Nyein, Y. Y. 2011 Overview of droughts in Myanmar. In: *Drought in Asia Monsoon Regions* (R. Shaw & H. Nguyen, eds). Community, Environment and Disaster Risk Management Series, Volume 8. Emerald Group Publishing, UK, pp. 87–95.

Parry, M., Canziani, O., Palutikof, J., Linden, P. & Hanson, C. (eds) 2007 Climate change 2007: impacts, adaptation and vulnerability. Contribution of Working Group II to the Fourth Assessment Report of the Intergovernmental Panel on Climate Change. Cambridge University Press, Cambridge.

Riggs, H. C. 1982 *Regional Analysis of Streamflow Characteristics*. *Techniques of Water Resources Investigation of the United States Geological Survey*. United States Government Printing Office, Washington, DC.

Sanyal, J. & Lu, X. X. 2004 Application of remote sensing in flood management with special reference to Monsoon Asia: a review. *Nat. Hazards* **33**, 283–301.

Sen Roy, N. & Kaur, S. 2000 Climatology of monsoon rains of Myanmar (Burma). *Int. J. Climatol.* **20**, 913–928.

Sharma, D. 2012 Situation analysis of flood disaster in south and Southeast Asia: a need of integrated approach. *Int. J. Sci., Environ. Technol.* **1** (3), 167–173.

Sharma, R. J. & Shakya, N. M. 2005 Hydrological changes and its impacts on water resources of Bagmati watershed, Nepal. *J. Hydrol.* **327** (3–4), 315–322.

Tallaksen, L. M. & van Lanen, H. A. J. (eds) 2004 Hydrological Drought: Processes and Estimation Methods for Streamflow and Groundwater. *Developments in Water Science Series*, vol. 48, Elsevier Science BV.

Ti, L. H. & Facon, T. 2004 *From Vision to Action: A Synthesis of Experiences in Least-Developed Countries in Southeast Asia. FAO-ESCAP Pilot Project on National Water Vision Phase II*. RAP Publication 32, Bangkok.

Turral, H., Burke, J. & Faurès, J. 2011 Climate Change, Water and Food Security. FAO Water Reports 36, Rome.

Wahl, K. L. & Wahl, T. L. 1995 Determining the Flow of Comal springs at New Braunfels, Texas. In *Proceedings of Texas Water '95, American Society of Civil Engineers*, San Antonio, Texas, pp. 77–86.

Wang, W., Chen, X. & van Gelder, P. H. A. J. M. 2008 Detecting changes in extreme precipitation and extreme streamflow in the Dongjiang River Basin in southern China. *Hydrol. Earth Syst. Sci.* **12**, 207–221.

Yang, D., Ye, B. & Shiklomanov, A. 2004 Discharge characteristics and changes over the Ob River watershed in Siberia. *J. Hydrometeorol.* **5** (4), 595–610.

Yao, C., Yang, S., Qian, W., Lin, Z. & Wen, M. 2008 Regional summer precipitation events in Asia and their changes in the past decades. *J. Geophys. Res.* **113**, D17107.

Zhou, T., Zhang, L. & Li, H. 2008 Changes in global land monsoon area and total rainfall accumulation over the last half century. *Geophys. Res. Lett.* **35**, L16707.

First received 21 May 2013; accepted in revised form 25 May 2014. Available online 8 August 2014

Supplementary Materials

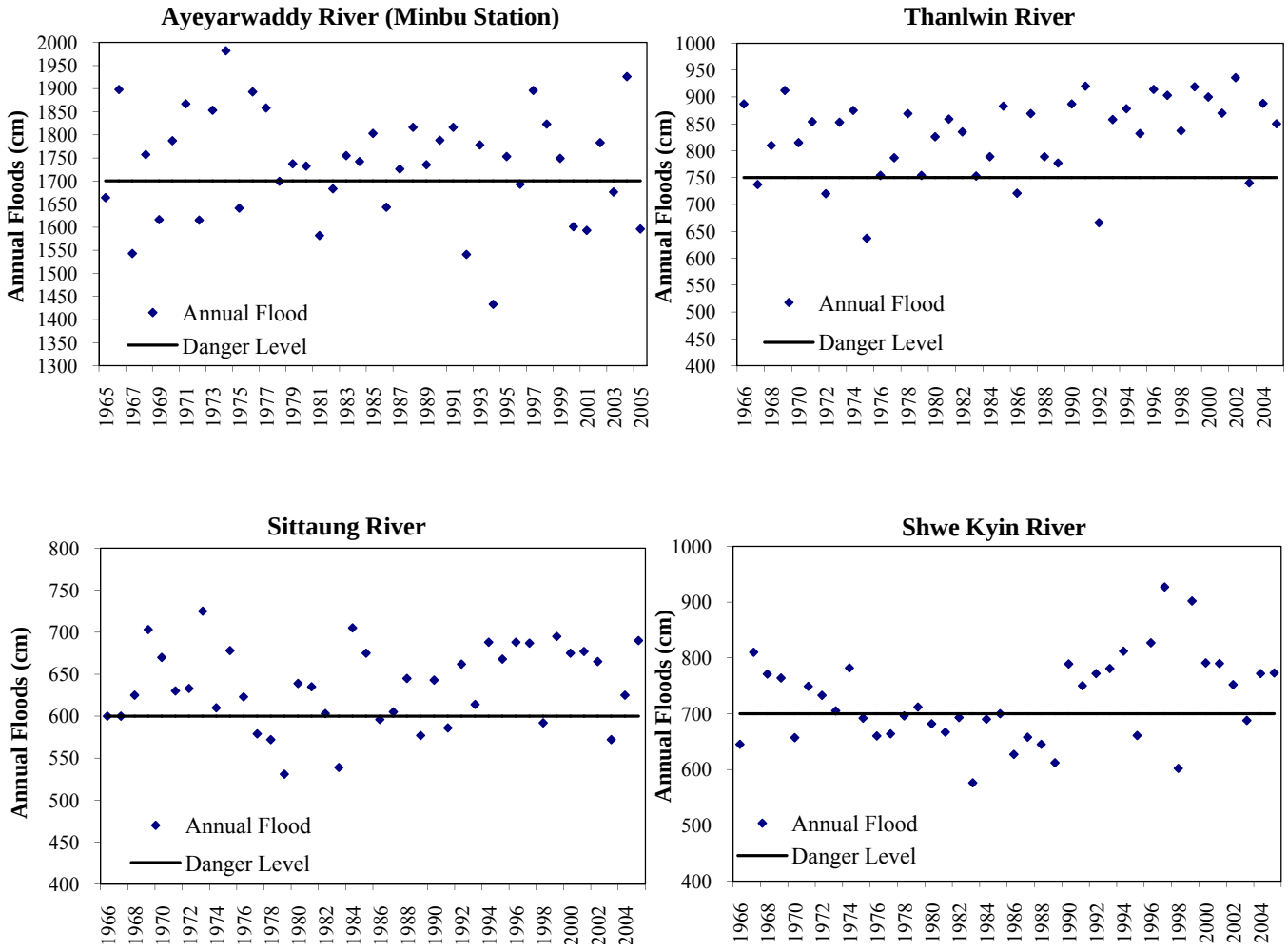

Fig. S1 Maximum Flood Levels of the major Rivers in Myanmar

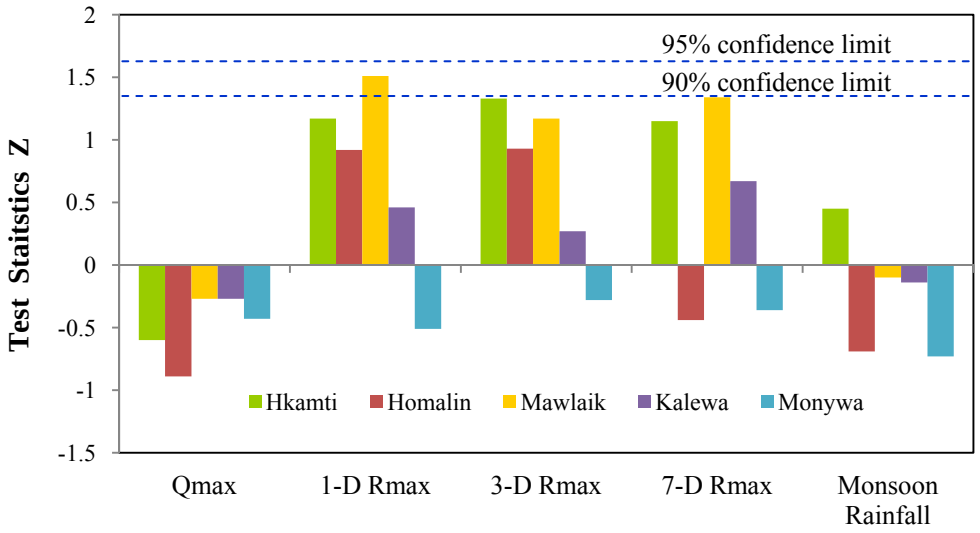

Fig. S2 Mann-Kendall Statistics for streamflow and rainfall series at five stations along the Chindwin River

Fig. S2 shows the Mann-Kendall (MK) trend analysis, indicating the test statistic for each variable at five stations. The results show that Qmax at all stations and Rmax at four stations, excluding Hkamti, has a slightly decreasing trend with negative values. Other rainfall parameters (1-D, 3-D and 7-D Rmax) show an increasing trend at four stations, excluding Monywa. Neither positive or negative trends are highly significant at 5% as test statistics are less than Zc. 3-D Rmax at Hkamti station and 1-D and 7-D Rmax at Mawlaik station shows significant increasing trend with 90% probability. Sen's slope values also indicate increasing and decreasing trends in correspondence with MK tests. Overall, both linear regression and MK tests suggested that Qmax and monsoon rainfall series are stable as the slightly decreasing trends are not much significant. The remaining parameters anyhow show increasing trends with marginal significant level. According to trend analysis, there is an evidence of increasing trends in moving average rainfall series with different daily spans, except for the Monywa station, where all series show a decreasing trend.

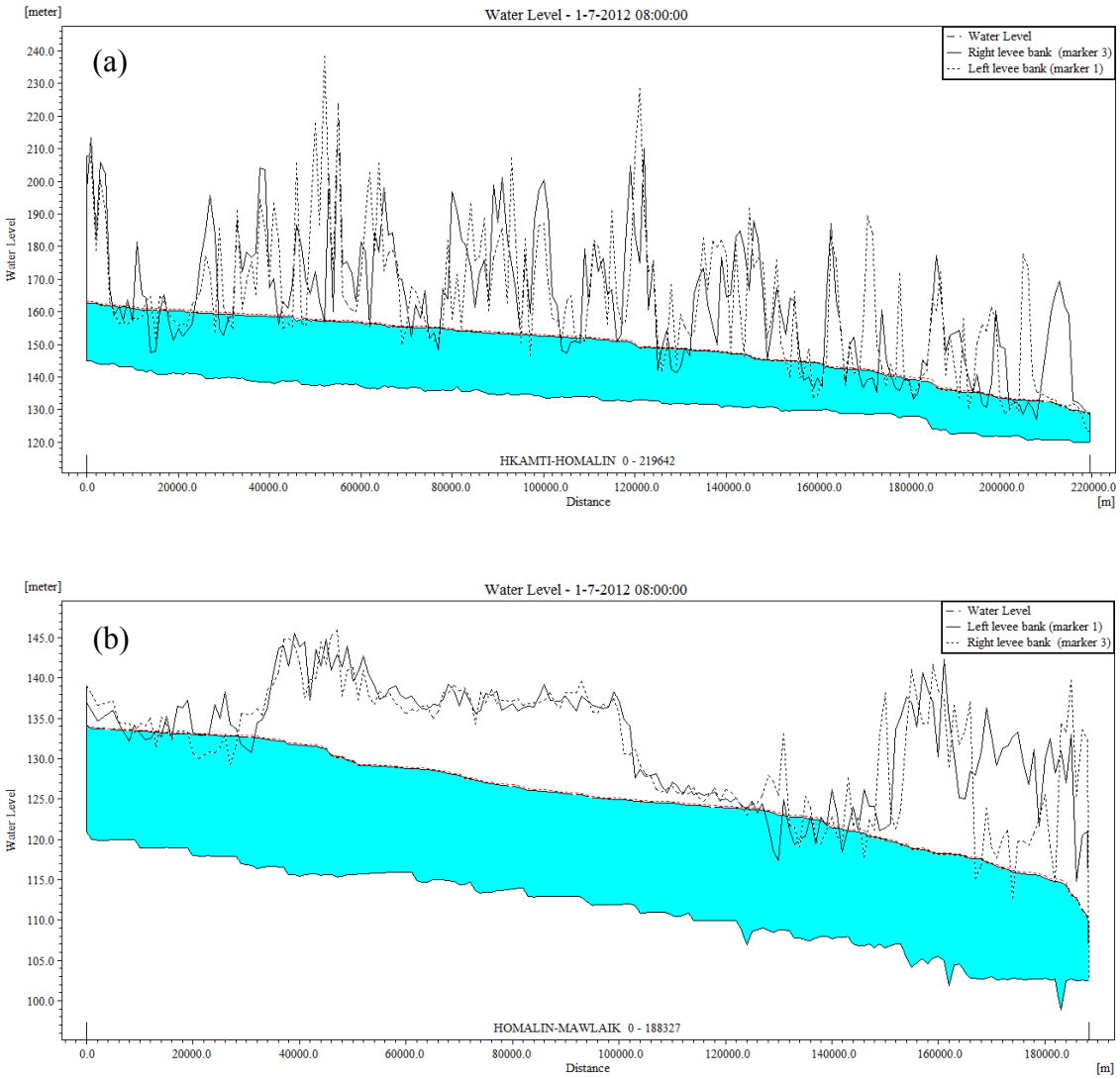

Fig. **S3** Simulated water level profiles for 2-Yr floods by one-dimensional (MIKE 11) hydraulic model for flood prone reaches (a) Hkamti to Homalin (b) Homalin to Mawlaik

Water levels with respect to 2-year flood discharges at each station are approximately close to the danger levels at the respective stations. Therefore, water level profiles for 2-year floods are calculated using one-dimensional MIKE-11 hydraulic model for the flood prone reaches of the upper Chindwin basin, and the results are shown in Fig. S3. As evidenced by the results, the simulated discharges spill over the some portions of bank levels along the reaches, despite low inundations. As a supplement, the hydraulic simulation results also agree that the upper half of the basin has a higher potential flood risk, even if streamflows with small return periods will come.

Article II

Improving Flood Forecasting in a Developing Country: A comparative Study of Stepwise Multiple Linear Regression and Artificial Neural Network

Zaw Zaw Latt, Hartmut Wittenberg

Reprinted from Journal of Water Resources Management 28(8)
doi: 10.1007/s11269-014-0600-8, pages 2109-2128,

Water Resour Manage (2014) 28:2109–2128
DOI 10.1007/s11269-014-0600-8

Improving Flood Forecasting in a Developing Country: A Comparative Study of Stepwise Multiple Linear Regression and Artificial Neural Network

Zaw Zaw Latt · Hartmut Wittenberg

Received: 5 September 2013 / Accepted: 16 March 2014 /
Published online: 18 April 2014

Abstract Due to limited data sources, practical situations in most developing countries favor black-box models in real time operations. In a simple and robust approach, this study examines performances of stepwise multiple linear regression (SMLR) and artificial neural network (ANN) models, as tools for multi-step forecasting Chindwin River floods in northern Myanmar. Future river stages are modeled using past water levels and rainfall at the forecasting station as well as at the hydrologically connected upstream station. The developed models are calibrated with flood season data from 1990 to 2007 and validated with data from 2008 to 2011. Model performances are compared for 1- to 5-day ahead forecasts. With a high accuracy, both candidate models performed well for forecasting the full range of flood levels. The ANN models were superior to the SMLR models, particularly in predicting the extreme floods. Correlation analysis was found to be useful for determining the initial input variables. Contribution of upstream data to both models could improve the forecasting performance with higher R^2 values and lower errors. Considering the commonly available data in the region as primary predictors, the results would be useful for real time flood forecasting, avoiding the complexity of physical processes.

Keywords Artificial neural network · Flood forecast · Rainfall · Real time operation · Stepwise regression · Water level

1 Introduction

As a non-structural measure, flood forecasting (such as discharge, water level, or flow volume) is a crucial part of flow regulation and water resources management. Worldwide, flood disasters account for about one-third of all natural disasters in terms of number and economic losses (Berz 2000). As stated by Dutta and Herath (2004), out of the total number of flood events in the world during the past 30 years, 40 % occurred in Asia and Southeast Asia countries stood for the second worst region in Asia. ASEAN Disaster Risk Management

Z. Z. Latt (✉) · H. Wittenberg
Faculty of Sustainability, Institute of Ecology, Leuphana University of Lueneburg,
Scharnhorststr. 1, C13.112, Lueneburg 21335, Germany
e-mail: zawzawlatt@khalsa.com

Initiative (2010) reported that a catastrophic 200-year flood (0.5 % annual probability of exceedance) would have a major impact on the economies of the Southeast Asian countries, including Myanmar, which are already fragile. The process of floods is basically complex, uncertain and unpredictable, due to its nonlinear dependency on meteorological and topographic parameters (Thirumalaiah and Deo 1998). While distributed hydrological modeling involves multidisciplinary and complex issues, simple, robust and sustainable approaches in flood forecasting system are needed, without much effort in continuous updating such models. For flood forecasting to be effective, it must provide flood warnings with a reasonable lead time. Furthermore, for real time operation, the authorities may require to access the gauges of significant predictors (Corani and Guariso 2005), thus saving considerable costs, a critical issue in developing countries.

Since a flood warning and forecast system does not primarily aim at providing explicit knowledge of rainfall–runoff processes, black-box models have been widely used in addition to the physical based models (Abudu et al. 2010; Magar and Jothiprakash 2011). The main focus of this paper is on the application of data driven models in the context of real time forecasting for developing countries, with the example of Myanmar. As real time flood forecasting systems of Myanmar still provide river stage forecasts for 1-day lead time, provision of more lead times is an interest of this study. Myanmar is one of the tropical countries characterized by the monsoon climate and river flooding is a recurrent natural phenomenon, particularly during monsoon (Sanyal and Lu 2004). Severe floods have occurred in major rivers in Myanmar during the last decades and there seems to be a trend of frequent hydrological extreme events, leading to a high risk of flood hazards. When implementing a flood forecasting system in a developing country, special attention should be paid to the sustainability of its operation (Shamseldin 2010) and availability of hydrometric data which are commonly monitored in the region. While conceptual or physically based models are vital for the understanding of hydrological processes, there are practical situations where the main focus is to provide accurate predictions at specific locations, especially for the river basins where catchment properties are not fully monitored. Sometimes, a model is valued for its simplicity and robustness in solving the local problems. In the Myanmar context, such a strong predictive model would benefit to the key flood management actions.

In recent years, a great deal of work has been done in applying data driven models like multiple regressions and neural networks for water resources research. Conventional multiple linear regression (MLR) methods and time series models have been widely used in real time flood forecasting and warning. MLR (deterministic) and autoregressive integrated moving average models, which are stochastic and special cases of MLR, perform well if the data length is sufficiently long with a high persistence (Magar and Jothiprakash 2011). National flood forecasting centers, especially those in developing countries such as Myanmar and the Mekong River Commission in Southeast Asia still widely use MLR methods for daily water level forecasting at most gauging stations. Linear regression models are quite applicable to forecasting, however, they require a prior assumption about the type and consistency of the relation between dependent and independent variables. In the real world, temporal variations in data do not always exhibit simple regularities and may not always satisfy this assumption. Thus, the complexity and nonlinear problems make it attractive to try artificial neural network (ANN) approaches. There are a number of reasons why ANN applications solve one or more specific problems. ANNs neither presuppose a detailed understanding of a river's physical characteristics, nor do they require extensive data pre-processing (Dawson et al. 2002). Over the last decade, ANNs have been increasingly used in water resources management, such as rainfall-runoff modeling (Minns and Hall 1996; Dawson and Wilby 2001; Rajurkar et al. 2002; Shamseldin 2010; Sattari et al. 2012), stream flow forecasting (Thirumalaiah and Deo 1998;

Cigizoglu 2003; Haddad et al. 2005), and reservoir inflow prediction (Othman and Naseri 2011; Sentu and Regulwar 2011). Recent studies have also supported application of different ANN techniques as an efficient alternative tool for real time forecasting of river stages and discharges (Chang et al. 2007; Kisi 2007; Dawson and Wilby 1999; Dawson et al. 2002). Cigizoglu (2003) examined the forecasting and the extrapolation ability of ANN for multi-step forecast using daily flows and proved that multilayer perceptron network could capture the nonlinear dynamics and generalize the structure of the whole data set. Concepts of ANN application have been extensively reviewed, and ANN was shown to be an alternative modeling tool in hydrology (ASCE Task Committee 2000a; b).

In addition, several researchers have also considered ANNs as a competitive alternative to conventional statistical methods. For example, Asati and Rathore (2012) compared the ANN with autoregressive (AR) models and multiple-linear regression (MLR) for short-term flow prediction. In their study, the AR models provided the best performance beyond one-step lead time. Furthermore, Dawson and Wilby (1999) demonstrated that multi-layered perceptron has a better performance than MLR method in one-step ahead river flow predicting, using past rainfalls and discharges. Bisht et al. (2010) also presented that multilayer feed-forward ANN models are superior to MLR models in forecasting one-step ahead discharge, using past river stages and discharges. In this comparison, however, benchmark regression models did not seem to have the best performance because the criteria of input data selection were not explained, and the ANN and the regression models were solely developed using different inputs from the river stage and discharge data series, whose first few antecedent data were believed to have a strong correlation to output discharges in regression models. Since performances of different models differ for different rivers and the choice of input vector has a significant impact on model accuracy (Rezaeianzadeh et al. 2013), the superiority of the ANN approach towards benchmark regression methods could not be expected in every forecasting case. Islam (2010) developed a feedforward ANN with a high accuracy in river stage forecasting of the Buriganga River in Bangladesh, but the regression model outperformed the ANN model in the validation. Moreover, there was a mixed fortune of model performance in multi-step forecasting for both ANN and regression models (Tareghian and Kashefipour 2007; Daud et al. 2011). Despite several efforts in comparing forecasting models, a conclusive comparison could not be achieved because different input data were used for different types of model, which makes the comparison unfair (Wang 2006).

Keeping the above scenario of real time flood forecasting, the present study aims to develop multi-step river stage forecasting models using past water levels and rainfall. A further motivation is that ANN is well suited for problems whose underlying process cannot be fully specified, but for which there are sufficient observations. This study has not only presented the robustness of ANN models in multi-step flood forecasting with limited data types, but also assessed their clear-cut superiority to regression models, for the conditions under which the regression technique has the best performance. To establish the true merits of ANNs relative to conventional statistical techniques, comparisons are made between the forecasting performance of ANN and stepwise multiple linear regression (SMLR) models. Two conditions are addressed in the comparison of forecasting skills: (a) using a-site data only and (b) using at-site and upstream data. This paper is an effort to improve national flood forecasting systems in Myanmar by applying ANN models which offer more advantages than the conventional regression models. Additionally, the results of this study can be applied to similar basins and further researches.

2 Study Area

All forecasting models were applied to the Chindwin river basin in northern Myanmar, located between the latitudes 22° and 26° north, and the longitudes 94°and 96° east. It is the largest tributary of the well-known Ayeyarwaddy River, which is one of the principle water resources of Asia. As the third largest river of Myanmar, the Chindwin River has a catchment area of 113,800 km^2 and a length of 985 km. The average slope of the basin is 13 % and the flow slope is 0.05 %. Along the main river, there are five hydro-meteorological stations namely Hkamti, Homalin, Mawlaik, Kalewa and Monywa as shown in Fig. 1. All gauging stations are hydrologically connected which means that the flow from upstream stations directly affect the flow at downstream stations. The Chindwin's catchment is a mountainous forested terrain with the only exception of its lowest southern part which comprises a wide flood plain. The catchment receives average annual rainfall between 760 mm (in the lower basin) to 3,800 mm (in the upper basin), out of which 80 % falls during monsoon season i.e. June to October. Mean annual maximum flows vary from 14,000 m^3 s^{-1} in the upstream region to 20,000 m^3 s^{-1} in the downstream. During the southwest monsoon, severe floods mostly occur in July and August when the intense rainfall hits the basin seasonally and annually at one place or another. The river is an important water resource and transport artery of the country. However, challenging reason against to its important role in the country's socio-economic is flood hazard due to climate conditions. In the last two decades, severe floods along the Chindwin River occurred on 15 July 1997, 1 September 1999, 19 August 2002, 22 July 2004 and 10 July 2008.

In this study, multi-step river stage forecast models were developed for the Mawlaik station (N 23° 38′and E 94° 25′), whose elevation is 102 m above mean sea level. In recent years, flood prone effects on this station have been more critical than other stations. The reason for using water level instead of discharge is that they are more practical and useful indicators as they directly reflect the expected flood levels with which the community is more familiar. The drainage area and the river length at this site are 69,339 km^2 and 660 km, respectively. Observed daily water level and rainfall data (1990 to 2011) at Mawlaik (forecast station) and Homalin (upstream station) were used in model development. The distance from Homalin station to Mawlaik station is 114 km.

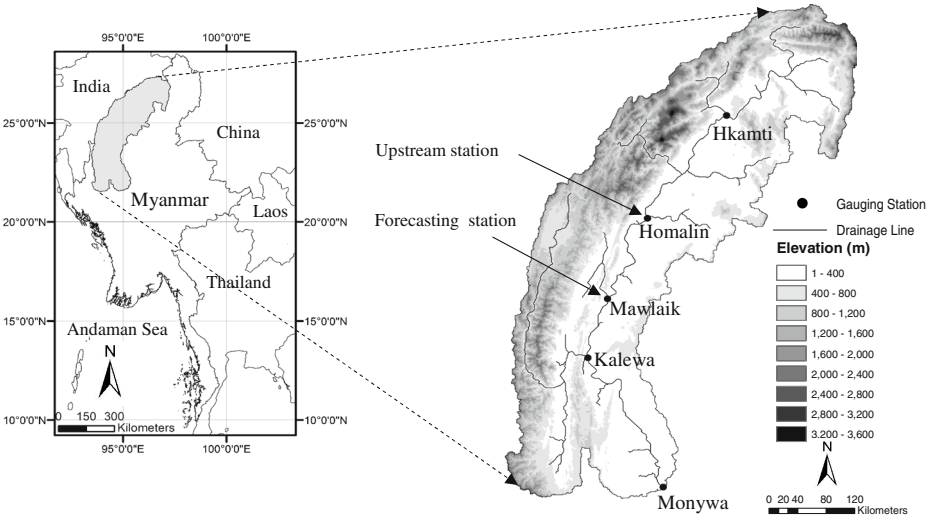

Fig. 1 Location of the Study Area

3 Data Processing and Selection of Predictor Variables

For water level forecasting especially in the flood period, the data were selected only from July to October which is a regular monsoon flood season in Myanmar and most Asian countries. In order to characterize the variation of water level at Mawlaik station, descriptive statistics were calculated. As shown in Fig. 2, the frequency distribution exhibits almost a normal distribution, although the data was slightly skewed. The Kolmogorov-Smirnov test was also used to numerically check the normality of the data whose size is 2706. The null hypothesis of normality is rejected if the probability (p) value is smaller than the significance level of 0.05. Since the p value associated with the normality test is 0.001, the test statistically detected a non-normal distribution of the large data set. However, with a low skewness (0.3) and small kurtosis (−0.56), there seem to be trivial departures from normality for the water level series at Mawlaik station and the distribution is reasonably close to the normality. For large sample sizes, significant results would be derived even in the case of a small deviation from normality, but detecting non-normality would not affect any statistical analysis (Ghasemi and Zahediasl 2012). It is also imperative that the training and validation sets are representative of the same population. In the model development 80 % of the flood season data (1990–2007) were used for calibration while 20 % (2008–2011) were used for validation. For ANN models, the calibration data were further randomly divided into 80 % for training set and 20 % for the testing set. Before applying the ANN models, the calibration data sets of river stage and rainfall were standardized in a linear scale subtracting the mean and divided by the standard deviation in order that numerical difficulties, such as slow convergence of optimization algorithms and getting stuck in local minima, during the calculation could be overcome. Standardization of the data in the training process can remove the scale dependence problem of initial weights and improve the model accuracy. The input variables used in models included various combinations of two major variables: daily water levels and rainfalls at the forecasting station (Mawlaik) as well as at the hydrologically connected upstream station (Homalin). For accurate model development, the selection of appropriate input variables is important. The addition of unnecessary variables would create a more complex model than required and is susceptible to over fitting of training (Wu et al. 2008). Determining the number of

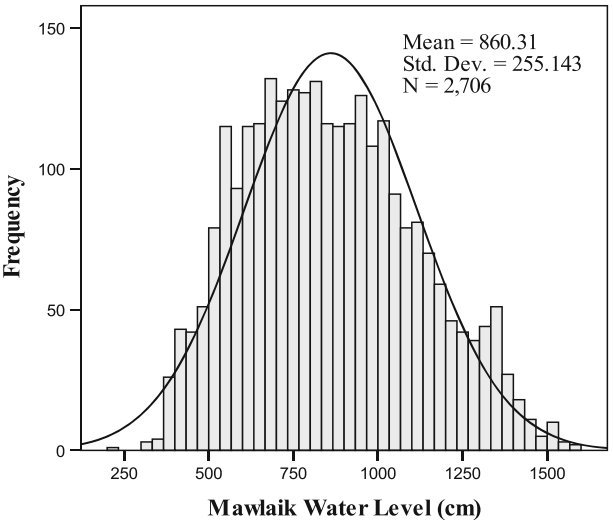

Fig. 2 Frequency distribution of water level data at Mawlaik station

input parameters involves finding the lags of water level and rainfall that have a significant influence on the predicted next day's water levels. In order to reduce the dimensionality of inputs, auto- and partial correlation functions (ACF and PACF) on water level series were generated. At the Mawlaik station on the Chindwin River, cross correlations (CCF) between the water levels and rainfalls were determined at several lags in order to detect the relationship between data values. In case of using upstream data, water levels at the forecasting station were cross correlated with water levels and rainfalls at the upstream station to detect the significant correlation. After the initial selection of input variables from PACF and CCF, stepwise regression models were used in determining optimal inputs from a view point of the linear relationship. While the ANN models' performances depend on network structure, learning method, and training procedure, the performances of the SMLR models will be by any means the best in a parsimonious manner since the regression models use the inputs, which have a strong correlation with the output, decided by the ACF, PACF and CCF. Therefore, significant predictors defined by the SMLR models constitute the inputs for the ANN models to have a conclusive comparison via a parallel assessment.

4 Multiple Linear Regression

Multiple linear regressions are the extended forms of simple linear regressions applied to the case of multiple explanatory variables. The purpose of MLR is to explain as much as possible of the variation observed in the response variable, leaving as little variation as possible to unexplained "noise" (Helsel and Hirsch 2002). The general form of a regression model for k independent variables is given by

$$Y = \beta_0 + \beta_1 X_1 + \beta_2 X_2 + \ldots\ldots\ldots + \beta_k X_k + \varepsilon \quad (1)$$

Where, Y is the response variable. $\beta_0, \beta 1, \beta_2, \ldots, \beta_k$ are the regression coefficients. ε is the error, and $X_1, X_2, \ldots, X_k$ are the independent variables. Based on least squares criterion, the regression coefficients are estimated by minimizing the sum of the squares of the vertical deviations of each data point to the best-fitting line.

An important step in choosing the best model is to determine how many variables and which particular variables should be in the final model. Stepwise regression permits re-examination, at every step, of the variables in previous steps. A variable that enters at an early stage may become superfluous at later stages because of its relationship with other variables subsequently added to the model (Kleinbaum et al. 1998). To check this possibility, at each step a partial F test is checked for each variable currently in the model, regardless of its actual entry point into the model. The variable with the smallest non-significant partial F statistic is removed, and the model is refitted with the remaining variables by checking the partial Fs. The whole process was repeated until no more variables can be added or removed. In this way, SMLR models were developed using statistically significant predictors.

5 Artificial Neural Network

Haykin (1994) defines a neural network as a massively parallel distributed processor that has a natural propensity for storing experiential knowledge and making it available for use. The black-box type flood forecasting can be classified under the category of pattern mapping (Sajikumar and Thandaveswara 1999). A feed-forward multi-layer perceptron (MLP) network (Rumelhart et al. 1986) is usually used for pattern mapping problems. As shown in Fig. 3, an

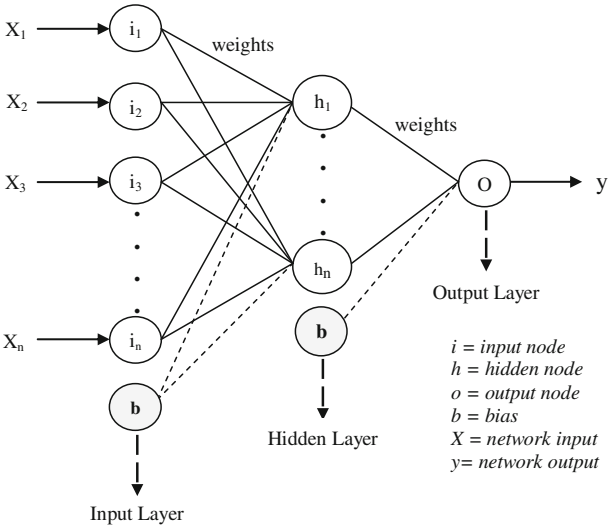

Fig. 3 Configuration of feed forward ANN (multi layer perceptron) network

MLP network used in this study consists of a set of sensory units that constitute the input layer, one or more hidden layers of computational nodes (neurons), and an output layer of computational nodes. A neuron consists of multiple inputs and a single output. The sum of the product of inputs and their weights (w) minus bias (b) leads to a net as follows:

$$net = \sum x_i \cdot w_i - b \tag{2}$$

Then the output of a neuron, $f(net)$ is decided by an activation function that determines a response of the node to the input signal it receives. The sigmoid and hyperbolic tangent functions, given as Eqs. (3) and (4) respectively, are mostly used in the hidden layers.

$$f(x) = \frac{1}{1 + e^{-x}} \tag{3}$$

$$f(x) = tanh(x) = \frac{e^{x} - e^{-x}}{e^{x} + e^{-x}} \tag{4}$$

In order to generate an output vector $Y=(y_1, y_2, \ldots\ldots, y_n)$, a training (learning) process is employed, making network outputs closer to the targets, to find optimal weight matrices and bias vectors that minimize a predetermined error function given as follows.

$$E = \sum_{p=1}^{p} \sum_{i=1}^{N} (y_i - t_i)^2 \tag{5}$$

Here, t_i and y_i represent target (observed) and ANN output at the i^{th} node respectively; N is the number of output nodes and p denotes the number of training patterns. Most hydrological applications have used a supervised learning that requires large number of inputs and corresponding outputs. The most frequently used learning rule in many ANN applications is error back propagation, which is essentially a gradient-descent algorithm that minimizes the network error function. Each input pattern of the training set is passed forward through the network. The network output is compared with the desired target, and the error is propagated

backward through the network to each node. Based on Eq. (6) (ASCE 2000a), the network weights and biases are adjusted by moving a small step in the direction of a negative gradient of the error function during each iteration (Thirumalaiah and Deo 1998). The iterations continue until a specified convergence or number of iterations is achieved.

$$\Delta w_{ij}(n) = -\eta * \frac{\partial E}{\partial w_{ij}} + \alpha * \Delta w_{ij}(n-1) \tag{6}$$

Where $\Delta w_{ij}(n)$ and $\Delta w_{ij}(n-1)$ are weight interconnections between node i and j during the n^{th} and $(n\text{-}1)^{th}$ pass or epoch. η and α denote learning rate and momentum, respectively.

In model building, various ANN models with one hidden layer were considered to the same data set. The different architectures of three-layered fed forward ANN models were trained with a gradient descent learning algorithm, looking for optimal performance by trial and error. Different learning rates were applied while momentum was set at 0.9. The number of hidden layer neurons was changed up to 20 through the training process. Through a trial and error process, the appropriate neuron number was selected depending on minimum standard error. In the training stage, an early stopping method was applied in order to avoid over fitting. By evaluating the objective function at each iteration on training and testing sets, the training process was stopped in correspondence with the minimum validation error. Sigmoid and hyperbolic tangent functions were applied in the hidden layer as well as in the output layer. The linear function (identity), given as $f(x) = x$, was used at the output layer, making the network take any values as predicted outputs may be distorted by non-linear activation functions.

6 Assessment of Model Performance

Judging the effectiveness of flood forecasting models is unavoidable in selecting the best models. Obviously, the selection criterion should be liberal to avoid missing useful predictors when reliable prediction of future observations is required (Kleinbaum et al. 1998). In selecting the best candidate models from each method, R^2 and error measures were used for the assessment of the selected models from the same approach during calibration. In validation, the performances of the best ANN and SMLR models were compared using four performance indices, namely coefficient of determination (R^2), root mean-square error (*RMSE*), coefficient of variation (*CV*) and mean absolute percent error (*MAPE*).

$$R^2 = \left[\frac{\sum_{i=1}^{n}(y_i-\bar{y})(\hat{y}_i-\bar{\hat{y}})}{\sqrt{\sum_{i=1}^{n}(y_i-\bar{y})^2\sum_{i=1}^{n}(\hat{y}_i-\bar{\hat{y}})^2}}\right]^2 \tag{7}$$

$$RMSE = \sqrt{\frac{1}{n}\sum_{i=1}^{n}\left(y_i-\hat{y}_i\right)^2} \tag{8}$$

$$CV = \frac{RMSE}{\bar{\bar{y}}} * 100 \tag{9}$$

$$MAPE = \frac{1}{n}\sum_{i=1}^{n}\frac{\left|y_i-\hat{y}_i\right|}{y_i} * 100 \tag{10}$$

In above equations, y represents the observed water level, $\hat{y}$ the forecasted water level, $\bar{y}$ and $\hat{\bar{y}}$ the average observed water level and average predicted water level, respectively and the number of observation in both calibration and validation stages.

R^2 provides the strength of linear relationships between observed and predicted values. *RMSE* represents the prediction error in the model. *CV* is an average error ratio. *MAPE* yields the relative error, providing how close the predicted values are to the respective observed ones and it is a measure of accuracy in a fitted series, expressed in percentages. A higher R^2, a lower *RMSE*, *CV* and *MAPE* imply good performance. Through these criteria, the ability of each candidate model can be properly understood. The unit of *RMSE* is the same as that of the predicted variable in the model.

7 Results and Discussion

7.1 Forecasting Models Using at-Site Data

Table 1 shows the statistical parameters of calibration and validation data. The maximum value of calibration period was larger than that of the validation range while the minimum value was less than that of validation. Thus extrapolation problems may not exist in this data set. The skewness in both calibration and validation data sets are not drastically different. At the forecasting station, the autocorrelation and partial autocorrelation functions of water level with corresponding confidence limits were estimated up to 20 lags as shown in Fig. 4. The ACF for many successive lags was quite high in the water level series as a signal of high persistence. The PACF indicates a significant correlation up to lag 4. Thereafter, correlations fell within the confidence limits. In this case, five delay water levels at times (t-1) to (t-5) were considered as inputs.

The cross correlations between water levels and rainfalls during flood season were also determined to estimate the degree to which two variables are correlated. It was found that the water level was less correlated with its at-site rainfall although the positive relation was shown up to 8 previous rainfalls. The CCFs of five antecedent rainfalls are 0.16, 0.17, 0.16, 0.15, and 0.13, respectively, and considered as predictor variables. The number of input was directly

Table 1 Descriptive Statistics for dependent water level (cm) at Mawlaik station

Parameter	Calibration (1990–2007)	Validation (2008–2011)
Number of observation	2214	492
Mean	864	842
Median	839	849.50
Mode	827	729
Standard Deviation	261	228
Variance	67916	52128
Skewness	0.30	0.22
Kurtosis	−0.60	−0.49
Range	1384	1124
Minimum	204	391
Maximum	1588	1515

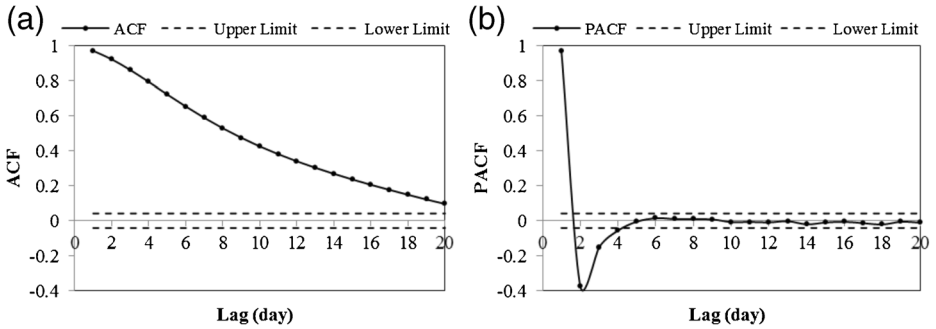

Fig. 4 Autocorrelation (**a**) and partial autocorrelation (**b**) functions of water level at the forecasting station during flood season

determined by the number of lagged values to be used for forecasting of the next value. The general function of input–output relations for both SMLR and ANN models are as follows:

Case—1 H_t *to* H_{t+4}=f[H_{t-1},H_{t-2},H_{t-3},H_{t-4},H_{t-5}]
Case—2 H_t *to* H_{t+4}=f[H_{t-1},H_{t-2},H_{t-3},H_{t-4},H_{t-5},R_{t-1},R_{t-2},R_{t-3},R_{t-4},R_{t-5}]

Where t = time (day), H = water level and R = rainfall

The output water levels (H) at time step t to t+4 were mapped with only past water levels of five lags as inputs in the case (1). For case (2), five previous rainfalls are considered in addition to the water levels to map with the output water levels. On the basis of R^2 and *RMSE* in calibration stages, the selected candidate models from each method were evaluated.

Initially simultaneous regression method was performed, taking five previous water levels all of which must be included in the model to forecast future water levels. Since over-fitting is a concern, only the variables explaining additional variance are required, without decreasing model performance. Consequently stepwise regression technique was applied to determine optimal inputs in the order of their explanatory power by linear relationships. The stepwise regression models with significant variables are shown in Table 2. In the 1- to 5-day forecast

Table 2 SMLR Models using at-site data

Data Used	Lead Time (day)	SMLR models	Calibration	
			R^2	*RMSE* (cm)
Water level	1	H_t=21.14+1.56H_{t-1}-0.52H_{t-2} -0.07H_{t-3}	0.98	36
	2	H_{t+1}=50.69+1.99H_{t-1}-1.06H_{t-2}	0.93	67
	3	H_{t+2}=88.87+2.19H_{t-1}-1.3H_{t-2}	0.86	97
	4	H_{t+3}=119.01+2.27H_{t-1}-1.25H_{t-2} -0.31H_{t-3}+0.15H_{t-5}	0.78	124
	5	H_{t+4}=152.77+2.27H_{t-1}-1.31H_{t-2} -0.36H_{t-3}+0.21H_{t-5}	0.70	149
Water level and rainfall	1	H_t=22.57+1.56H_{t-1}-0.5H_{t-2} -0.09H_{t-3} -0.17R_{t-3}	0.98	36
	2	H_{t+1}=53.35+1.95H_{t-1}-0.84H_{t-2} -0.22H_{t-3}-0.05H_{t-5}-0.2R_{t-2}-0.22R_{t-3}	0.93	67
	3	H_{t+2}=90.83+2.15H_{t-1}-1.02H_{t-2} -0.34H_{t-3}+0.1H_{t-5}-0.34R_{t-2}-0.38R_{t-3}	0.86	97
	4	H_{t+3}=137.16+2.31H_{t-1}-1.46H_{t-2} -0.35R_{t-2}-0.49R_{t-3}-0.3R_{t-5}	0.78	124
	5	H_{t+4}=165.26+2.27H_{t-1}-1.19H_{t-2} -0.49H_{t-3}+0.22H_{t-5}-0.6R_{t-2}-0.49R_{t-3}	0.70	148

models, the most significant predictors are two successive past water levels. R^2 values ranged from 0.70 to 0.98 and *RMSE* was between 36 and 149 cm. In addition to the water level data, five antecedent rainfalls were applied as input variables. After several runs using a different combination of variables, it was found that the incorporation of rainfall data of the respective station did not significantly improve the model in terms of R^2 and *RMSE*. The range of R^2 was 0.70 to 0.98 and *RMSE* could not be reduced. The model performances remain the same. As a result the models using water level and rainfall data did not provide better results than the ones applying water level only.

ANN models were also trained using the input vectors that were identified by the SMLR models for 1- to 5-day ahead forecasting. After testing the sigmoid and hyperbolic activation functions in the hidden layer, the results suggest that hyperbolic tangent was preferable in this forecasting case, providing less prediction error and high performance than sigmoid function. In addition, using the same function in both hidden and output layers was not heuristic and could not minimize the errors. Thus, the linear (identity) function was used in the output layer to ensure that target values have no bounded range. The combination of hyperbolic tangent in the hidden layer and identity function in the output layer provides the better performance in this case.

The best-fit network architectures were determined on the basis of the least errors produced during calibration. The performance statistics of selected ANN models are shown in Table 3. According to the ANN structures, there is only one predicted value by each model for every lead time. The number of hidden layer nodes in the models varies from 2 to 7, depending on the complexity of the input–output relation to be captured by the models. For all ANN models, the number of input data is same as that of the SMLR models given in Table 2. For example, in the ANN structure of 3-3-1 for 1-day lead time, input data refers to H_{t-1}, H_{t-2} and H_{t-3}, which have been used in the SMLR model for same lead time. R^2 for 1 to 5-day forecast was decreasing from 0.98 to 0.72 while *RMSE* increased from 36 cm to 143 cm. To improve the model performance, antecedent rainfalls at the forecasting station were included in the input patterns successively. Within ANN models, the performance of models would not be better as both R^2 and the *RMSE* did not consistently show a better indication with increasing lead times. However, ANN models showed their superiority to SMLR models in the calibration stage. Rainfall contribution in the ANN models slightly reduced *RMSE* while the models provided the same R^2.

Table 3 ANN models using at-site data

Data Used	Lead Time (day)	ANN Structure	Learning Rate	Calibration	
				R^2	*RMSE* (cm)
Water level	1	3-3-1	0.6	0.98	36
	2	2-7-1	0.6	0.94	66
	3	2-2-1	0.3	0.87	97
	4	4-4-1	0.7	0.80	120
	5	4-4-1	0.8	0.72	143
Water level and rainfall	1	4-4-1	0.8	0.98	34
	2	6-7-1	0.3	0.94	65
	3	6-3-1	0.8	0.87	93
	4	5-2-1	0.2	0.80	120
	5	6-5-1	0.2	0.72	142

7.1.1 Performance Comparison

In this experiment, the addition of station rainfall data to ANN and SMLR models could not improve the model performance as the aforementioned results have shown. Thus, performance of best SMLR and ANN models using only water level were compared in a parsimonious manner. As shown in Fig. 5, both SMLR and ANN models provided satisfactory performance in forecasting river stages throughout the flood season (July to October). Table 4 shows the performance statistics of candidate modes to judge the forecasting abilities. In both types of models, coefficients of determination (R^2) decreased from 0.99 to 0.7 for 1 to 5-day forecasts. The *RMSE* in these two models ranged from 28 cm for the 1-day forecast to 134 cm for the 5-day forecast. *MAPE* values were between 2.5 and 13.5 % for 1- to 5-day lead times. *CV*s of residuals range from 3 to 16 %. In general, no significant improvement could be observed for ANN models over SMLR models. This may be due to the fact that past water levels are used as inputs in the comparison of both models. With a high persistence in the water level data, SMLR models could capture linear relationships and provide forecasting performance as well as ANNs. Although the forecasting performances of SMLR and ANN models were not very different in this case, the results showed that ANN models were slightly superior to the conventional MLR models, providing higher R^2 and a lower *RMSE*, *MAPE*, and *CV* for 4 and 5-day forecasts.

To get an impression on extreme event forecasting, high floods over critical level (1,200 cm at the Mawlaik station) were selected during the validation period and compared with the predicted values by the models using at-site water level for 1-day lead time. The results of the SMLR model using the water levels at times t-1, t-2 and t-3 were compared with that of the ANN model with 3-3-1 structure as shown in Fig. 6. In the validation period, high flood over the critical level occurred four times, in every July and August of 2008 and 2011 respectively. These four flood events altogether took 32 days. For each severe event, both models provided satisfactory forecasts for the observed floods in July 2008 and 2001 while the predicted values marginally agreed with the observed ones in Aug 2008 and 2011. Overall, their performances are not very different in terms of R^2. It was found that both models slightly under predicted the high floods in rising limb while over predicted the falling limbs, caused by the effects of antecedent water levels. The models could not fully capture the underlying mechanism of the rising and falling rates of high floods. In the case of extreme events, the *MAPE* is 1.5 % for SMLR and 1.4 % for ANN models. Minimum and maximum percent errors ranged between 0.09 and 7.4 % in the SMLR models while 0.05 and 6.7 % in the ANN models, respectively. Thus, particularly ANN models have a lower error range than the SMLR in predicting high floods. It seems that ANN models better generalize the variability of high floods in the observation period than SMLR models.

7.2 Forecasting Models using Upstream Data

The second application was to predict the water level at the downstream station using upstream data. The existence of a strong correlation between downstream and upstream data can be useful for stream flow forecasting at downstream sites. Following the similar methodology in the previous section, SMLR and ANN models were developed and their abilities to forecast flood levels were compared. The current water level at the forecasting station (Mawlaik) was considered as a function of its past water level as well as previous water levels and rainfall of the upstream station (Homalin). In this part, at-site water level data, which were shown to be significant in the previous condition, were used again. In addition, appropriate input variables from the upstream station were initially selected using CCF. Figure 7 shows the correlation

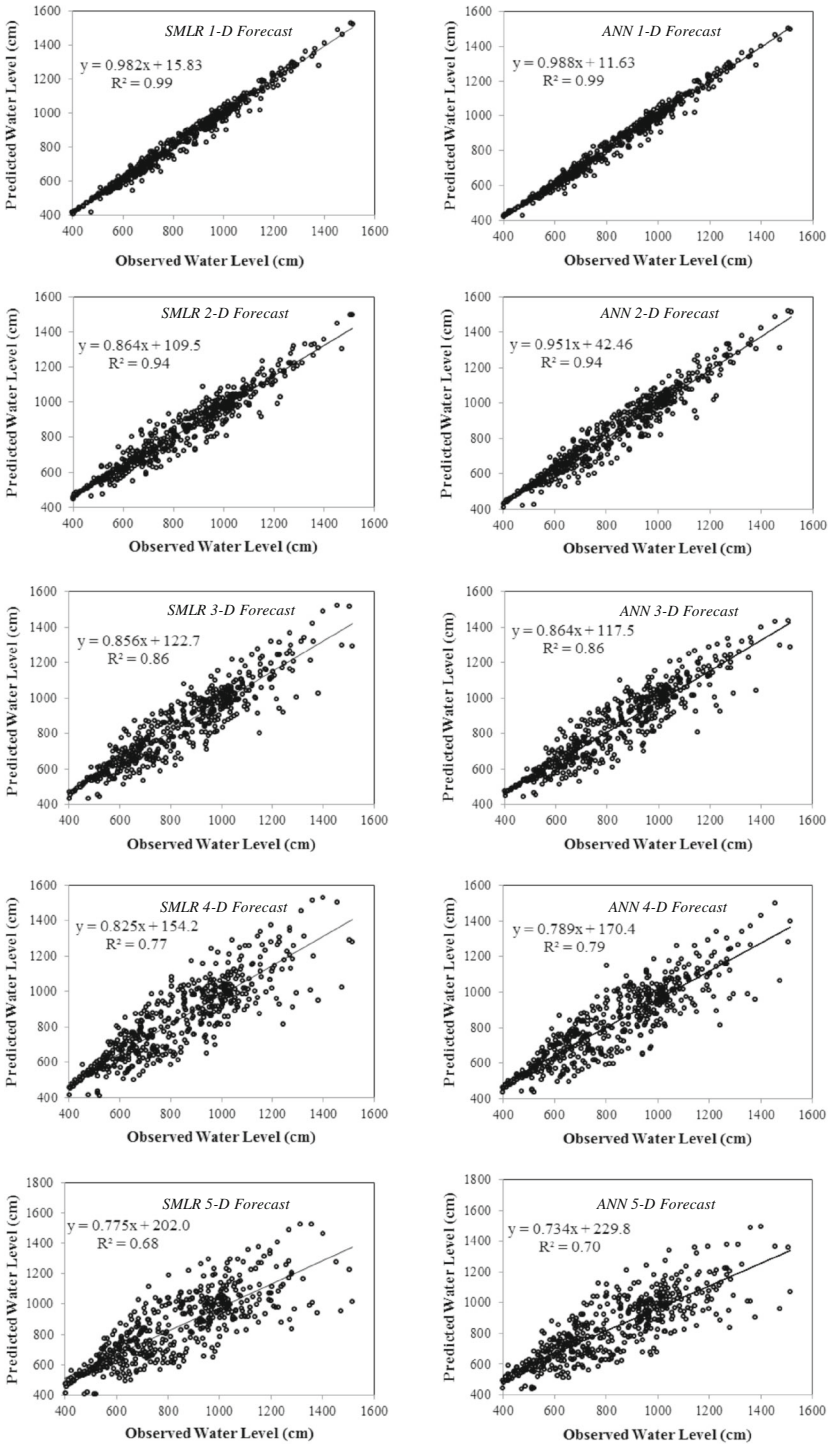

Fig. 5 Performance comparison of SMLR and ANN models using at-site water levels

Table 4 Performance Comparison of SMLR and ANN models using at-site water levels

Models	Lead Time (day)	Validation			
		R^2	*RMSE* (cm)	*MAPE* (%)	*CV*(%)
SMLR	1	0.99	28	2.54	3.33
	2	0.94	58	5.47	6.90
	3	0.86	88	8.52	10.45
	4	0.77	113	11.17	13.42
	5	0.68	134	13.47	15.91
ANN	1	0.99	28	2.54	3.33
	2	0.94	56	5.46	6.65
	3	0.86	87	8.52	10.33
	4	0.79	109	10.71	12.94
	5	0.70	132	13.45	15.67

between Mawlaik and Homalin stations. Water levels at Mawlaik are strongly correlated with its upstream river stage at Homalin station up to several lags as shown in Fig. 7a. Only lagged upstream water levels with CCF greater than 0.8 were taken. In this case, CCFs of past water levels between the upstream and downstream stations at t-1 to t-5 were 0.94, 0.94, 0.91, 0.87 and 0.81, respectively and thus considered as input. According to CCF in Fig. 7b, the water level at Mawlaik was less correlated with upstream rainfall at Homalin station. CCFs of five antecedent rainfalls from upstream station considered in the model are 0.19, 0.22, 0.24, 0.24, and 0.23.

Hence to predict the water level at the downstream station, all possible inputs consisted of five past water levels (H_{t-1} to H_{t-5}) and five antecedent rainfalls (R_{t-1} to R_{t-5}) at the upstream

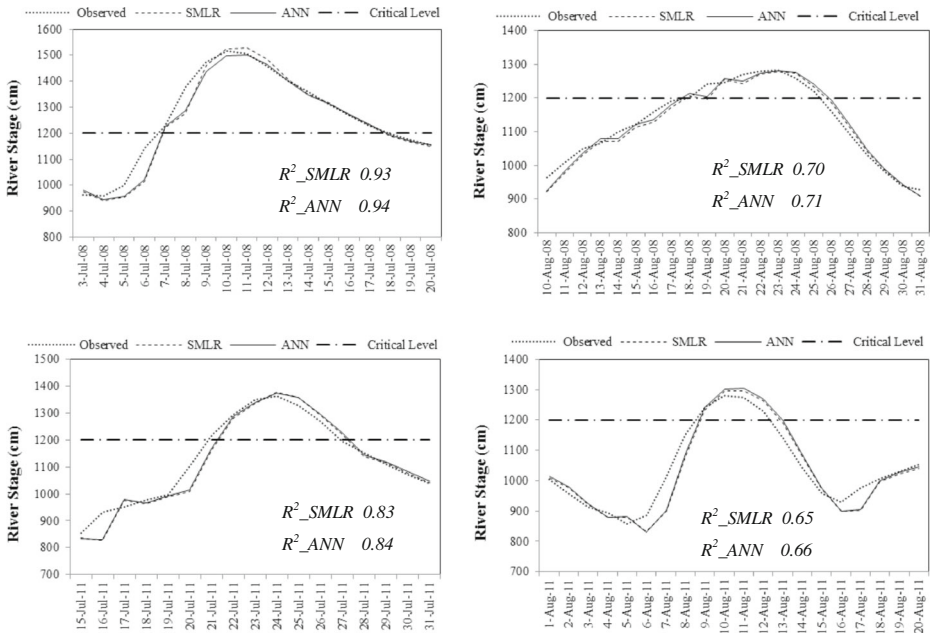

Fig. 6 High flood forecasting comparison of SMLR and ANN models using at-site water levels

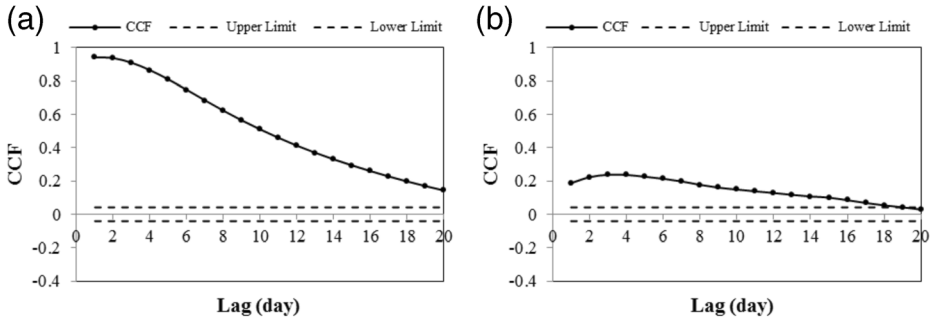

Fig. 7 Cross correlation function of water levels at Mawlaik and Homalin (**a**) and Water level at Mawlaik and rainfall at Homalin (**b**)

station, incorporating three lagged downstream water levels (H_{t-1}, H_{t-2} and H_{t-3}) at Mawlaik, which were the primary predictors in the previous case. These inputs were regressed with the output water levels using stepwise regression techniques through which only significant predictors were included in the models. The performances of selected SMLR models with significant inputs are shown in Table 5. The maximum R^2 is 0.99 for 1-day forecast while minimum R^2 is 0.81 for 5-day forecast. *RMSE* ranged from 27 to 116 cm. Residual variations varied from 2 to 11 %. The results are quite satisfactory both in terms of R^2 and error measures. Similar to the previous case, the feed forward MLP networks were created using these significant variables, as inputs, defined by the SMLR models. One hidden layer was used in the ANN models, which were trained with a gradient descent algorithm. As suggested by the previous analysis, the hyperbolic tangent function was used in the hidden layer and identity function in the output layer. Table 6 shows the developed ANN models which used upstream data. For 1- to 5-day forecasts, R^2 values are between 0.83 and 0.99. In the calibration stage, ANN could generalize the data set, providing higher R^2, lower *RMSE* and *MAP*E with increasing lead times, as ANN could identify the nonlinear contribution of upstream rainfall.

Comparing to the performance indicators in the previous section, R^2 values of the SMLR and ANN models increased in a similar pattern, with 1, 4, 8, 13 and 16 % higher than that of the previous R^2 for 1 to 5-day forecasts, respectively. Regarding to the prediction error, SMLR models reduced the *RMSE* by 26, 34, 31, 26 and 22 % for 1 to 5-day forecasting periods, over the errors in the previous cases. In the ANN models, the *RMSE* indices were 29, 34, 34, 28 and 23 % lower than that of previous models through 1 to 5-day lead times, respectively. For 1-D forecast, ANN reduced the *CV* 32 % whereas SMLR 28 %. From 2 to 5-D forecasts, *CV*s in

Table 5 Performances of selected SMLR Models using upstream data

Lead Time (day)	Input Variables	Calibration		
		R^2	*RMSE* (cm)	*MAPE* (%)
1	ML (H_{t-1}, H_{t-2}), HO (H_{t-1}, H_{t-2} H_{t-3}, H_{t-5}, R_{t-1}, R_{t-3})	0.99	27	2.14
2	ML (H_{t-1}, H_{t-2}, H_{t-3}), HO (H_{t-1}, H_{t-2}, H_{t-5}, R_{t-1}, R_{t-3})	0.97	44	3.88
3	ML (H_{t-1}), HO (H_{t-1}, H_{t-2}, H_{t-4}, R_{t-1}, R_{t-2}, R_{t-3})	0.93	67	6.13
4	ML (H_{t-1}), HO (H_{t-1}, H_{t-2}, H_{t-4}, R_{t-1}, R_{t-2}, R_{t-3})	0.88	91	8.70
5	ML (H_{t-1}), HO (H_{t-1}, H_{t-2}, R_{t-1}, R_{t-2})	0.81	116	11.35

ML Mawlaik (forecasting station), *HO* Homalin (upstream station)

Table 6 Performance of ANN models using upstream data

Lead Time (day)	Structure	Learning Rate	Calibration		
			R^2	*RMSE* (cm)	*MAPE* (%)
1	8-2-1	0.6	0.99	26	2.19
2	8-6-1	0.4	0.97	43	3.70
3	7-3-1	0.7	0.94	64	3.91
4	7-6-1	0.8	0.90	86	8.25
5	5-5-1	0.7	0.83	110	10.47

both models decreased 32, 25, 21 and 18 % relative to the variation of previous models using at-site water level. The results showed that involvement of upstream data could improve the performance of SMLR and ANN models compared to using at-site data alone. Although rainfall data has less influence on the models compared to the water level data, which exhibits strong linear correlation, the upstream rainfall would enhance the model performance and explain the variation of the prediction errors as well. It was found that the first lagged water level of the downstream station and the two past water levels of upstream station are the primary predictors in the river stage forecasting model through 1 to 5-day forecasting. One antecedent rainfall from the upstream station could contribute to the prediction for every lead time.

7.2.1 Performance Comparison

The predicted water levels were compared with observed ones in the validation period for 1 to 5- day lead times, and performance statistics are given in Table 7. It was found that the predicted values by both models agreed well with the observed ones up to 5 days. R^2 of ANN models varied from 0.99 to as low as 0.79 for 1 to 5-day lead time while that of SMLR models was between 0.99 and 0.78. The *RMSE* of ANN models varied from 19 to 109 cm compared to 20 to 110 cm in SMLR models. *MAPE* ranged from 1.62 % for a 1-day forecast to 11.11 % for a 5-day forecast in ANN and 1.81 to 11.27 % in SMLR models. *CV* in the ANN models was lower than that of SMLR models for all forecasts. Figure 8 shows the observed water levels and the predicted ones with 1- to 5-day lead times for the selected flood season. These plots

Table 7 Performance comparison of SMLR and ANN models using upstream data

Models	Lead Time (day)	Validation			
		R^2	*RMSE* (cm)	*MAPE* (%)	*CV* (%)
SMLR	1	0.99	20	1.81	2.38
	2	0.97	39	3.68	4.63
	3	0.93	63	6.29	7.48
	4	0.86	88	8.92	10.45
	5	0.78	110	11.27	13.06
ANN	1	0.99	19	1.62	2.25
	2	0.97	38	3.60	4.51
	3	0.93	62	6.15	7.36
	4	0.86	86	8.72	10.21
	5	0.79	109	11.11	12.90

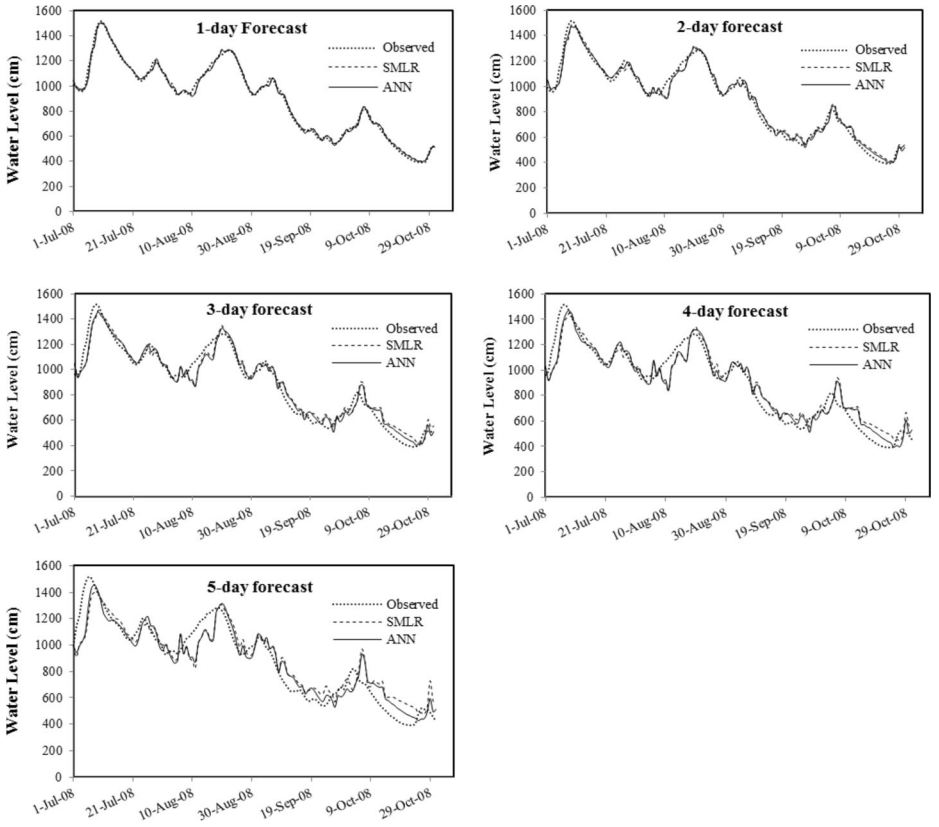

Fig. 8 Observed and predicted water levels for the flood season in 2008

clearly indicate the relative skills of each model across the full range of flood levels. According to the performance indicators, ANN models are superior to the SMLR models in the validation stage, providing lower *RMSE, MAPE* and *CV*, whereas R^2 in both models were almost the same. In the validation stage, the standard deviation of the dependent water level series was 228.3 cm while 227.8 cm for ANN and 227.4 cm for SMLR models, respectively. For the 1-day forecast, the mean value of the observed water level was 842.2 cm and that of the predicted series was 842 cm for ANN and 843.6 cm for SMLR models. It was observed that standard deviations of the modeled values were in close vicinity to that of observed ones, indicating that the models seem to capture the variability of actual phenomenon.

Four extreme flood events during the validation period were compared with the predicted water levels. Figure 9 shows the forecasting performance of the SMLR and the ANN models for 1-day forecast in the extreme flood events. Regarding R^2, ANN models provided a better agreement with the observed floods than SMLR models. For July and August floods in 2008, the relative errors of SMLR forecasts were 1.4 and 1.1 % while ANN models reported 1.1 % in both cases. For the prediction of July and August floods in 2011, ANN models had lower relative errors with 0.7 and 0.8 % compared to the SMLR models with the relative error of 1.5 and 1.4 %. Accuracy of both models was increased by the contribution of upstream data in predicting the high floods. Overall, the ANN models can predict high floods with less than 1 % error for one step ahead forecast. In this particular comparison, ANN models clearly outperformed the conventional regression models.

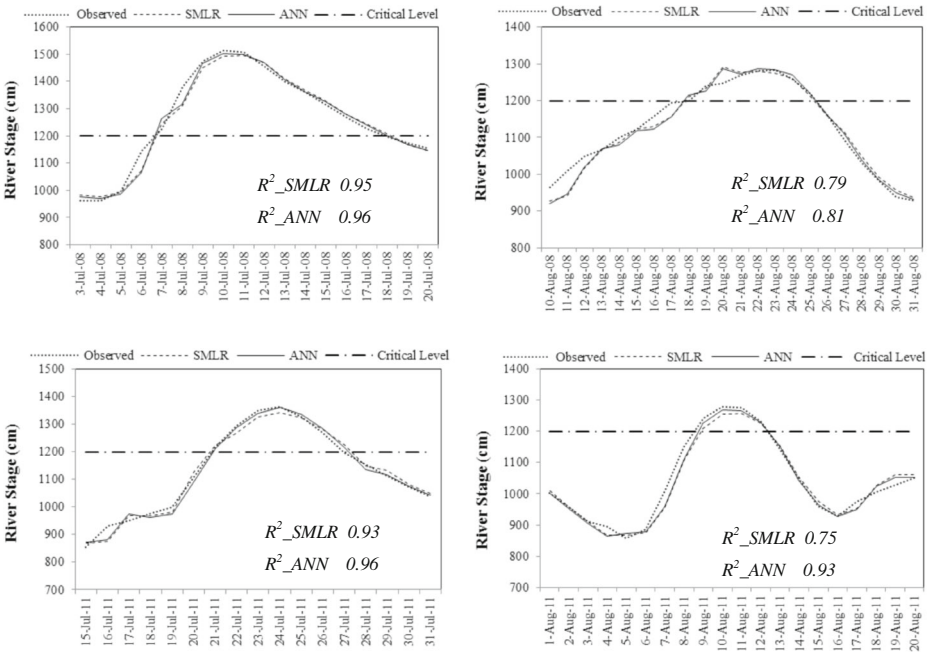

Fig. 9 High Flood forecasting comparison of SMLR and ANN models using upstream data

8 Conclusions

To cope with the situation of data insufficiency, one must develop predictive models that may use one or few of the available hydrometric data to issue a reliable forecast. From the standpoint of avoiding complexity of physical process and providing a reliable forecast, in this study, ANN and SMLR models were developed using past water levels and rainfalls to predict the river stage at a specific location. To suggest the appropriate methodology for the forecasting problem using commonly available data, the performance of the developed models was evaluated under two conditions: (a) using at-site data only and (b) using upstream data. The input vector selection of both models involved auto-, partial- and cross-correlation of the data series. Since the dependent water level series was almost normally distributed and the autoregressive process was dominant, the most recent antecedent data had a greater impact on the regression models.

Overall, the SMLR and ANN models provided satisfactory results in forecasting water level up to five days ahead during the monsoon flood season. Station rainfall could not much contribute to the model performance in terms of R^2. Nonetheless, involvement of the rainfalls reduced the prediction errors in the ANN models, which have the inherent ability of capturing nonlineariy. It was observed that the upstream data contribution could improve the model performances significantly with a higher R^2 and lower errors. Further, the developed ANN models in this study achieved by no means their best performances via a parallel assessment, while the SMLR models exhibit their best forecasts. Nonetheless, the neural network approach has shown consistently better performances than the conventional MLR technique in both conditions, especially for extreme flood prediction with less prediction error.

The study suggests that conventional MLR is simple to use, and the results are quite reliable as long as the relationship between applied variables shows a strong linearity. However, real

world situations never guarantee such conditions and ANN would be a promising alternative tool in case of noisy data. The study recommends that the inclusion of other prediction variables such as areal rainfall and temperature would enhance the model performances. Although using more information is challenging for linear regression models, ANN models, on the other hand, can incorporate different predictors and would provide better forecasts.

The results reveal that ANN models, once trained correctly, yield the reliable results from the limited or desired input and output data, which can be either linear or non-linear. This quality is very useful to water resources management with limited resources. With consistent performances under different assessment conditions, there was a conclusive indication of the ANN models being superior to the regression method. The study would be a remedy to the shortcoming due to the unfair comparison between these two approaches. Finally, as this study and others have shown, there is a convincing basis for the application of ANN flood prediction models in real-time contexts. With this knowledge, estimating future floods of a river system is possible by using past water levels and station rainfalls, without any comprehensive data requirements. Further investigations should be conducted to identify other significant predictors that are commonly available in the region, and build more accurate forecasting models using various relevant methods.

Acknowledgments The study was funded by the Deutscher Akademischer Austausch Dienst (German Academic Exchange Service). The hydro-metric data used in this analysis was provided by the Department of Meteorology and Hydrology, Myanmar.

References

Abudu S, Cui C, King JP, Abudukadeer K (2010) Comparison of performance of statistical models in forecasting monthly streamflow of Kizil River, China. Water Sci Eng 3(3):269–281. doi:10.3882/j.issn.1674-2370.2010.03.003

Asati SR, Rathore SS (2012) Comparative study of stream flow prediction models. Int J Life Sci Biotechnol Pharm Res 1(2):139–151

ASCE Task Committee on application of artificial neural networks in Hydrology (2000a) Artificial neural networks in hydrology. I: Preliminary concepts. J Hydrol Eng 5(2):115–123

ASCE Task Committee on application of artificial neural networks in Hydrology (2000b) Artificial neural networks in hydrology. II: Hydrologic applications. J Hydrol Eng 5(2):124–137

ASE ASEAN Disaster Risk Management Initiative (2010) Synthesis report on ten ASEAN countries disaster risks assessment. World Bank, Association of Southeast Asian Nations (ASEAN), United Nations Office for Disaster Risk Reduction - Regional Office for Asia and Pacific (UNISDR AP), Global Facility for Disaster Reduction and Recovery, the (GFDRR). http://www.unisdr.org/files/18872_asean.pdf. Accessed 27 Jan 2013

Berz G (2000) Flood disasters: lessons from the past—worries for the future. Proceeding of the ICE. Water Marit Eng 142(1):3–8

Bisht DCS, Raju MM, Joshi MC (2010) ANN based river stage-discharge modeling for Godavari River, India. Comput Model New Technol 14(3):48–62

Chang F, Chiang Y, Chang L (2007) Multi-step-ahead neural networks for flood forecasting. Hydrol Sci 52(1):114–130

Cigizoglu HK (2003) Estimation, forecasting and extrapolation of river flows by artificial neural networks. Hydrol Sci 48(3):349–361

Corani G, Guariso G (2005) An Application of pruning in the design of neural networks for real time Flood Forecasting. Neural Comput Appl 14:66–77

Daud S, Shahzada K, Tufail M, Fahad M (2011) Stream flow modeling of River Swat using regressions and artificial neural networks (ANNs) techniques. Adv Mater Res 225–260:679–683. doi:10.4028/www.scientific.net/AMR.255-260.679

Dawson CW, Wilby RL (1999) A comparison of artificial neural networks used for river flow forecasting. Hydrol Earth Syst Sci 3(4):529–540

Dawson CW, Wilby RL (2001) Hydrological modelling using artificial neural networks. Prog Phys Geogr 25(1): 80–108
Dawson CW, Harpham C, Wilby RL, Chen Y (2002) Evaluation of artificial neural network techniques for flow forecasting in the River Yangtze, China. Hydrol Earth Syst Sci 6(4):619–626
Dutta D, Herath S (2004) Trends of floods in Asia and flood risk management with integrated river basin approach. Proc Second Int Conf Asian-Pac Hydrol Water Resour Assoc Singap 1:55–63
Ghasemi A, Zahediasl S (2012) Normality tests for statistical analysis: a guide for Non-statisticians. Int J Endocrinol Metab 10(2):486–489
Had Haddad OB, Sharifi F, Alimohammadi S (2005) ANN in river flow forecasting. Proceedings of the 6th WSEAS Int. Conf. on Evolutionary Computing. Lisbon, Portugal: 316–324
Haykin S (1994) Neural networks a comprehensive foundation. Macmillan College Publishing, New York
Hels Helsel DR, Hirsch RM (2002) Statistical Methods in Water Resources. Techniques of Water- Resources Investigations of the U. S Geological Survey Book 4, Hydrologic Analysis and Interpretation, Chapter A3
Islam AS (2010) Improving flood forecasting in Bangladesh using an artificial neural network. IWA J Hydroinformatics 12(3):351–364
Kisi Ö (2007) Streamflow forecasting using different artificial neural network algorithms. J Hydrol Eng 12(5): 532–539
Kleinbaum DG, Kupper LL, Muller KE, Nizan A (1998) Applied regression analysis and other multivariable methods, 3rd edn. Duxbury Press, Pacific Grove
Magar RB, Jothiprakash V (2011) Intermittent reservoir daily-inflow prediction using lumped and distributed data multi-liner regression models. J Earth Syst Sci 120(6):1067–1084
Minns AW, Hall MJ (1996) Artificial neural networks as rainfall-runoff models. Hydrol Sci 41(3):399–417
Othman F, Naseri M (2011) Reservoir inflow forecasting using artificial neural work. Int J Phys Sci 6(3):434–440
Rajurkar MP, Kothyari UC, Chaube UC (2002) Artificial neural networks for daily rainfall-runoff modeling. Hydrol Sci 47(6):865–877
Rezaeianzadeh M et al (2013) Flood flow forecasting using ANN. ANFIS and regression models. Neural Comput Appl. doi:10.1007/s00521-013-1443-6
Rumelhart DE, Hinton GE, Williams RJ (1986) Learning internal representations by error propagation. In: Parallel distributed processing, vol 1. MIT Press, Cambridge, pp 318–362
Sajikumar N, Thandaveswara BS (1999) A non-linear rainfall-runoff model using an artificial neural network. J Hydrol 216:32–55
Sanyal J, Lu XX (2004) Application of remote sensing in flood management with special reference to monsoon Asia: a review. Nat Hazards 33:283–301
Sattari NT, Apaydin H, Ozturk F (2012) Flow estimations for the Sohu stream using artificial neural networks. Environ Earth Sci 66(7):2031–2045
Sentu D, Regulwar DG (2011) Inflow prediction by different neural network architectures: a case study. Int J Earth Sci Eng 4(6):225–230
Shamseldin AY (2010) Artificial neural network model for river flow forecasting in a developing country. IWA J Hydroinformatics 12(1):22–34
Tareghian R, Kashefipour SM (2007) Application of fuzzy systems and artificial neural networks for flood forecasting. J Appl Sci 7(22):3451–3459
Thirumalaiah K, Deo MC (1998) Real-time flood forecasting using neural networks. Comput Aided Civil Infrastruct Eng 13:101–111
Wang W (2006) Stochasticity, nonlinearity and forecasting of streamflow processes. Ios Press, Amsterdam
Wu CL, Chau KW, Li YS (2008) River stage prediction based on a distributed support vector regression. J Hydrol 358:96–111

Article III

Application of Feedforward Artificial Neural Network in Muskingum Routing: A Black-box forecasting approach for a natural river system

Zaw Zaw Latt

(submitted manuscript)

Title Page

Application of Feedforward Artificial Neural Network in Muskingum Flood Routing: A Black-box Forecasting Approach for a natural River System

Zaw Zaw Latt

Faculty of Sustainability, Institute of Ecology, Leuphana University of Lueneburg, Scharnhorststr. 1, C13.112, Lueneburg 21335, Germany

Corresponding author: **Zaw Zaw Latt**

Tel.: + 49(0)4131- 6772817

Fax: + 49(0)4131- 6771548

Email: zawzawlatt@khalsa.com

Abstract

Due to limited data sources, practical situations in most developing countries favor black-box models for real time flood forecasting. The Muskingum routing model, despite its limitations, is a widely used technique, and produces flood values and the time of the flood peak. This method has been extensively researched to find an ideal parameter estimation of its nonlinear forms, which require more parameters, and are not often adequate for flood routing in natural rivers with multiple peaks. This study examines the application of artificial neural network (ANN) approach based on the Muskingum equation, and compares the feedforward multilayer perceptron (FMLP) models to other reported methods that have tackled the parameter estimation of the nonlinear Muskingum model for benchmark data with a single-peak hydrograph. Using such statistics as the sum of squared deviation, coefficient of efficiency, error of peak discharge and error of time to peak, the FMLP model showed a clear-cut superiority over other methods in flood routing of well-known benchmark data. Further, the FMLP routing model was also proven a promising model for routing real flood hydrographs with multiple peaks of the Chindwin River in northern Myanmar. Unlike other parameter estimation methods, the ANN models directly captured the routing relationship, based on the Muskingum equation and performed well in dealing with complex systems. Because ANN models avoid the complexity of physical processes, the study's results can contribute to the real time flood forecasting in developing countries, where catchment data are scarce.

Keywords: artificial neural network; flood routing; multilayer perceptron; multiple-peaked hydrograph; Muskingum method; nonlinear model

Main Text

1 Introduction

As floods are the most costly and damaging natural disasters in the world (Berz 2000), the determination of streamflow (stage or discharge) at a river station plays an important role in environmental and water resources management. Flood routing, a basis for flood forecasting, is the process of progressively determining the timing and shape of a flood wave at successive points along a river reach. Among two main approaches for flood routing, hydrologic routing (conceptual or system approach) is based on the storage concept, and conversely, hydraulic channel routing (process approach) is based on the principles of mass and momentum conservation. In predicting a particular hydrograph through a river reach, any flood modeling will involve a number of assumptions and simplifications. While high demands on the quantity and quality of input data, as well as on computer resources, restrict the efficiency of hydraulic models in practical applications, approximate models provide satisfactory results in a considerably less expense with a limitation in their generality and accuracy depending on the detailed features of the model (Weinmann 1977). Therefore, simplified approaches that are reasonably accurate, but do not need extensive information on channel reach have been employed in order to compute discharge of relevant sites (Reddy and Wilamowski 2000; Tayfur et al. 2007).

When implementing a flood forecasting system in a developing country, special attention should be paid to the sustainability of its operation (Shamseldin 2010). Channel routing for flood prone river reaches, which only needs the observation of streamflows, is one of the practical solutions for flood forecasting systems in developing countries, where the catchments are not fully monitored, and research on hydrodynamic models is extremely limited. The Muskingum model (McCarthy 1938) is a popular flood routing method in which storage is assumed to be represented by a linear relation of inflow and outflow. In the context of Muskingum routing, flood attenuation properties, which are determined by using a set of observed inflow-outflow hydrographs from a

river reach remain invariant, and are used for routing of future inflow hydrographs in the same reach (Das 2009). Due to its wide applicability in many situations of river flood routing, this method has been extensively researched, with an emphasis on estimating its parameters for linear and nonlinear forms. In most natural rivers where the nonlinear variations in flows or storage between upstream and downstream are predominant, it is desirable to have a model to simulate the nonlinear flood processes.

Several studies on parameter estimation of the Muskingum method have been executed, enabling the account for nonlinear characteristics of the flood wave. To solve the nonlinear forms of the Muskingum approach, mathematical techniques include segmented least squares method (S-LSM) (Gill, 1978), nonlinear least squares (NL-LS) (Yoon and Padmanabhan 1993), Lagrange multiplier (LM) (Das 2004), and the Broyden-Fletcher-Goldfarb-Shanno method (BFGS) (Geem 2006). Barati (2013) demonstrated the use of the Excel solver in which the generalized reduced gradient (GRG) and evolutionary methods are applied for parameter estimation of a nonlinear model. On the other hand, there are more direct methods of deriving the routing coefficients, namely by using a linear programming from a known pair of inflow-outflow hydrographs, without first deriving routing parameters (Stephenson 1979). Moreover, various heuristic algorithms such as genetic algorithm (Mohan 1997; Sivapragasam et al. 2008), simulated annealing and shuffled frog leaping algorithms (Orouji et al. 2013), harmony search (HS) (Kim et al. 2001), particle swarm optimization (PSO) (Chu and Chang 2009), immune clonal selection algorithm (ICSA) (Luo and Xie 2010), and Nelder-Mead Simplex (NMS) algorithm (Barati 2011) have been developed in order to search optimum parameters in nonlinear models.

In the light of improving parameter estimation for nonlinear models, several approaches have been successfully demonstrated, but only for the well-known benchmark data by Wilson (1974). However, three-parameter nonlinear models may not be appropriate for every flood case. As a

result, a Muskingum model with more parameters or a novel black box model is required to achieve a close match between observed and routed flows (Geem 2013). Easa (2013) proposed an improved four-parameter nonlinear Muskingum model, which is superior to any three-parameter nonlinear models, and its applicability has been proven in real flood cases with a double-peaked hydrograph. However, even the four-parameter nonlinear Muskingum model may not be sufficient for flood forecasting in the case of natural rivers with multiple peaks.

A natural monsoon river has high external influences on the relationship between storages and inflow-outflow patterns that could not be fully explained by conventional flood routing procedures. Therefore, the complexity and nonlinear problems in predicting a flood hydrograph of natural river systems motivated the author to try artificial intelligence (AI) approaches, which have the inherent ability of capturing nonlinearity. Due to its success in dealing with complex problems, artificial neural networks (ANN) have been applied to a wide range of hydrological problems such as rainfall-runoff relationships (Minns and Hall 1996; Sattari et al. 2012), stream flow forecasting (Thirumalaiah and Deo 1998; Latt and Wittenberg 2014a), and reservoir inflow prediction (Othman and Naseri 2011). There have, however, been relatively few applications of ANNs to flood routing. For example, Mohan (1997) demonstrated the objective approach of genetic algorithm, without demanding any initial estimate of parameters, is efficient in searching Muskingum routing parameters. Yang and Chang (2001) also applied a multilayer neural network and sensitivity analysis for direct estimation of routing coefficients, using the same inputs as the Muskingum formula. Additionally, Chu (2009) has proven the superiority of a network-based Fuzzy Inference System (FIS), which was designed according to the Muskingum formula for direct mapping of outflows and inflows, over conventional methods for the benchmark data. However, as stated by Geem (2013), researchers have so far only tackled the benchmark data in the parameter estimation optimization of the nonlinear Muskingum model. In earlier studies, the

applicability of different methods was not tested in real flood cases. Even in the study by Easa (2013), only one complete single set of real flood data was used in the model development, and the validity of the model using independent flood data was not reported.

Over time, researchers have searched for better solutions in order to minimize the observed and predicted outflows for the said benchmark data (Geem 2013); however, no conclusive comparison could be discerned because there are mixed fortunes of performances of the reported methods in terms of well-known performance indices. This paper presents a novel black-box approach based on the feedforward ANN network in Muskingum flood routing, in order to further minimize the discrepancy between observed and routed flows for benchmark data as well as for developing a predictive flood model for a natural river in Myanmar dominated by monsoons. The objectives of this study are (1) to investigate the application of ANN in Muskingum flow routing; (2) to compare the performance of ANN with the previously documented methods, which have been used in the parameterization of nonlinear Muskingum routing for the benchmark data; and (3) to assess the applicability of ANN-based Muskingum model for real flood cases of a natural river. Assessment of the robustness of the ANN based Muskingum approach in routing of real flood events with a successful validation would be a remedy to the shortcoming of previous studies.

2 Muskingum Routing

The Muskingum flood routing method, first developed in connection with the design of flood protection schemes in the Muskingum River basin, performs satisfactorily when linearity is not unduly violated. It is the most widely used hydrologic routing method in a lumped system for handling a discharge-storage relationship, based on the continuity equation as

$$I - O = \frac{dS}{dt} \tag{1}$$

Where I = inflow to the reach, O = outflow from the reach, and $\frac{dS}{dt}$ = rate of change in channel storage with respect to time. To derive the Muskingum routing equation, the continuity equation becomes

$$\frac{I_1 + I_2}{2} - \frac{O_1 + O_2}{2} = \frac{S_1 + S_2}{\Delta t} \quad (2)$$

where, Δt is the routing period. While *I*>*O*, the flood wave is advancing and a wedge of storage is produced in the reach. During the recession, *O* exceeds *I* resulting in negative wedge storage. Considering wedge and prism storages, a linear storage function of the Muskingum method is expressed as a function of both inflow and outflow in the form of

$$S = K\,[xI + (1\text{-}x)O] \quad (3)$$

In which *S* = storage volume; *K* = storage coefficient; and *x* = a dimensionless weighting factor. *K* accounts for the translation (or concentration) portion of the routing, as being interpreted as the travel time of the flood wave from the upstream end to the downstream end of the channel reach. The parameter *x* accounts for the storage portion of the routing. To get meaningful results from this approach, it needs to reasonably specify initial conditions and its parameters that reflect the physical realism (Singh and McCANN 1980). *x* is generally restricted in the range from 0 to 0.5. With *K*=Δt and *x* =0.5, the outflow hydrograph retains the same shape as the inflow hydrograph. For *x*=0, Muskingum routing reduces to a linear reservoir routing. Values of *x* greater than 0.5 result hydrograph amplification (i.e. negative diffusion). In determining *x*, greater accuracy may not be necessary because the results of the method are relatively insensitive to the value of this parameter (Chow et al. 1988).

From the continuity and the storage equations, the outflow yields in finite difference form

$$O_{t+\Delta t} = C_0 I_{t+\Delta t} + C_1 I_t + C_2 O_t \quad (4)$$

Since $C_0+C_1+C_2 = 1$, the routing coefficients can be interpreted as weighting coefficients. These three coefficients are functions of K, x and Δt and constant throughout the routing procedures. With sufficient streamflow records, variation of routing parameters can be ascertained through the calibration for several flood events to cover a wide range of flood levels. The parameters K and x are conventionally estimated using a graphical method (i.e. trial and error). A tentative value of x is assumed and the historical data are plotted as S vs. $[xI + (1-x)O]$. The data generally plot in the form of a loop (sometimes there are several loops). The value of x, for which the width of the loop is minimized, is taken to be the correct value for the reach. Despite the use of the trial and error method for many decades, it is time consuming and likely to be subjective. In addition, such estimates tend to be approximate (O' Donnell 1985; Chu 2009).The linear model commonly applied to flood routing may be inappropriate when a nonlinear relationship between the flows and channel storage exists, as it does in most natural rivers.

2.1 Nonlinear models

In natural river reaches, it is common to observe the nonlinear storage function and significant errors may arise in downstream flood routing with the use of the conventional linear Muskingum approach (Barati 2013). Frequently quoted nonlinear (NL) forms of the Muskingum model in the literature (Wilson 1974; Gill 1978; Tung 1985; Yoon and Padmanabhan 1993; Papamichail and Georgiou 1994; Mohan 1997; Kim et al. 2001) are

$$S = K[x\,I^n + (1-x)O^n] \quad (NL\text{-}1) \tag{5}$$

$$S = K[x\,I^n + (1-x)O^m] \quad (NL\text{-}2) \tag{6}$$

$$S = K[x\,I + (1-x)O]^m \quad (NL\text{-}3) \tag{7}$$

Following a similar derivation to that of NL-1, Easa (2013) proposed a four-parameter nonlinear Muksingum model as follows:

$$S = K[x\, I^n + (1 - x)O^n]^m \quad \textit{(NL-4)} \tag{8}$$

These non-linear models have an exponential parameter *n* and *m*, which presumably makes the nonlinear relationship between accumulated storage and weighted flow more accurate (Kim et al. 2001). There are relatively few applications of NL-1 and NL-2 in the literature. For example, Gill (1978) stated that NL-1 has seldom been used in flood routing, although the relationship can be fitted to the storage curves from a theoretical point of view. The NL-3 model is most commonly used in flood routing as it increases the accuracy of the routing (Orouji et al. 2013). For NL-3 and NL-4, the parameters *x, K, n,* and *m* cannot be estimated through a simple graphical method, and the calibration procedure becomes more complicated. Unlike in the linear model, *K* does not describe the travel time of the flood wave in the nonlinear model, and *x* does not need to have the same preconditions (Barati 2011; Easa 2013).

2.2 Objective function

Parameter optimization of nonlinear models search the best routing parameters using an optimization algorithm in order to minimize objective functions. The commonly used objective function is the sum of squared deviation (SSQ), which can be calculated via the sum of the squares of differences between observed outflows and the routed outflows. This is minimized in terms of the variables *x, K, n* and *m* by applying different optimization techniques.

$$\text{Min SSQ} = \sum_{t=1}^{n}\left(O_t - \hat{O}_t\right)^2 \tag{9}$$

Where O_t and $\hat{O}_t$ represent the observed outflow and the routed outflow.

Therefore, the optimization model for NL-3 and NL-4 may be expressed in Eqs. (10) and (11) respectively as

$$\text{SSQ} = \sum_{t=1}^{n}\left[O_t - \left\{\left(\frac{1}{1-X}\right)\left(\frac{S_t}{K}\right)^{1/m} - \left(\frac{x}{1-x}\right)I_t\right\}\right]^2 \tag{10}$$

$$\text{SSQ} = \sum_{t=1}^{n}\left[O_t - \left\{\left(\frac{1}{1-X}\right)\left(\frac{S_t}{K}\right)^{1/m} - \left(\frac{x}{1-x}\right){I_t}^{n}\right\}^{1/n}\right]^2 \tag{11}$$

The value of the parameter x may range theoretically from $-\infty$ to 0.5 (Strupczewski and Kundzewicz 1980) while the parameters K, n and m have no specific constraints. As a measure of wedge storage, the negative value of x appears physically unreasonable; nonetheless, negative x is acceptable from the view of mathematical modeling (Dooge 1973).

3 ANN Approach

ANNs have been used as black-box simplified models in several water resources problems. The black-box type flood forecasting models can be considered as pattern mappings for input-output data sets. Multilayer perceptron (MLP) network (Rumelhart et at. 1986) is usually used for pattern mapping problems and consists of an input layer, one or more hidden layers of computational nodes (neurons), and an output layer of computational nodes. In a feedforward structure, data flow only in one direction. A neuron in a particular layer receives all input from the preceding layer and transmits the values to the succeeding layers of processing element. The schematic representation of the feedforward MLP network designed according to the Muskingum equation (Eq. 4) is shown in Fig. 1. It has one input layer, one hidden layer and one output layer. Each node in a layer is connected to all nodes in the successive layer, and the neurons in the same layer are not connected each other. The data transferred from one neuron to another through the connections are controlled

by the weights. The sum of the product of inputs (x) and their weights (w) minus bias (b) leads to a net as follows:

$$\text{net} = \sum x_i \, . w_i - b \tag{12}$$

Then, the output of a neuron, f (net) is decided by an activation function that determines a response of the node to the input signal it receives. In order to generate an output vector, a training (learning) process is used to find optimal weight matrices and bias vectors that minimize a predetermined error function (E) which is the sum of squares error given as follows.

$$E = \sum_{p=1}^{p} \sum_{i=1}^{N} (y_i - t_i)^2 \tag{13}$$

Here, t_i and y_i represent the target (observed outflow, $O_{t+\Delta t}$) and output (predicted outflow, $\hat{O}_{t+\Delta t}$) at the ith node, respectively; N is the number of output nodes; and p denotes the number of training patterns. Three-layered feedforward MLP models with a single hidden layer were trained with error back propagation, which is essentially a gradient-descent algorithm, to look for optimal performance by trial and error. Each input pattern of the training set was passed through the network from the input layer to the output layer. The network output was compared with the desired target. Then, the error was propagated backward through the network to each node, and the weights are optimally adjusted.

Sigmoid and hyperbolic tangent functions, as given in Eqs. (14) and (15) respectively, were applied in the hidden layer. The linear function (identity), given as $f(x) = x$, was used in the output layer, making the network take any values because predicted outputs may be distorted by nonlinear activation functions.

$$f(x) = \frac{1}{1 + e^{-x}} \tag{14}$$

$$f(x) = \tanh(x) = \frac{e^{x} - e^{-x}}{e^{x} + e^{-x}} \quad (15)$$

In order to overcome numerical instabilities during the training process and to improve the generalization ability, the calibration data sets were standardized in a linear scale, subtracting the mean, and were further divided by the standard deviation. Different learning rates were applied from 0.1 to 0.9, and the momentum was changed in the range of 0.5 to 0.9, as these two parameters affect the convergence speed of the algorithm. Using more nodes in the hidden layer may improve the MLP performance, but on the other hand, the model might learn the error, i.e. noise (Stefanon et al. 2001). The number of hidden layer neurons was changed up to 20 through the training process. The appropriate neuron number was selected depending on the minimum standard error. In the training stage, an early stopping method was applied in order to avoid over fitting. By evaluating the objective function at each iteration on training and testing sets, the training process was stopped in correspondence with the minimum validation error.

4 Performance Criteria

In this study, the performances of various methods were evaluated using four performance indices, namely the coefficient of efficiency (*CE*), the mean relative percent error (*MRE*), the error of peak discharge (*EQp*) and the error of time to peak (*ETp*) given, respectively, as

$$CE = 1 - \frac{\sum_{i=1}^{n}(Q_i - \hat{Q}_i)^2}{\sum_{i=1}^{n}(Q_i - \bar{Q})^2} \quad (16)$$

$$MRE = \frac{1}{n}\sum_{i=1}^{n}\frac{|Q_i - \hat{Q}_i|}{Q_i} * 100 \quad (17)$$

$$EQp = \frac{|Q_p - \hat{Q}_p|}{Q_p} \quad (18)$$

$$ETp = \left|T_p - \hat{T}_p\right| \tag{19}$$

Where Q_i, $\hat{Q}_i$ and $\bar{Q}$ represent observed flow, computed flow and the mean of the observed flows respectively. Q_p and $\hat{Q}_p$ are the observed and estimated peak discharge. T_p and $\hat{T}_p$ are the observed time to peak and computed time to peak respectively.

CE provides the strength of the models 'predictive power. *MRE* yields the relative error, providing how the predicted values are close to the observed ones, and it represents a measure of accuracy in a fitted series, expressed in percentages. *EQp* provides a deviation of computed peak with respect to the observed peak. *ETp* implies how the occurrence of flood peaks is closely estimated. A higher *CE* and a lower value of *MRE*, *EQp* and *ETp* imply a good performance. Through these criteria, the ability of each method can be properly understood.

5 Model application in case studies

In this paper, feed forward multilayer perceptron (FMLP) models were developed according to the Muskingum formula for routing benchmark data and real flood cases. Two case studies are considered in this study.

The first case study is based on the well-known Wilson's benchmark data. The data set is reported to present a nonlinear relationship between weighted discharge and storage and has been extensively studied by others for the assessment of various parameter estimation approaches (Gill 1978). In the data set, there is a smooth nonlinear optimization problem. However, the function to the objective is nonconvex and thus only locally optimal solutions in parameterization can often be expected. The performance of this study's proposed FMLP Muskingum model was compared to that of the previously reported methods, which have been used in the parameterization of nonlinear Muskingum routing.

Main Text

The second case study is based on the real flood cases of the Chindwin River in Myanmar, a typical natural monsoon river with high external disturbance, and the data set is expected to present the nonlinearity of the flood wave. As a natural monsoon-dominated river, significant inflows from possible tributaries along the reach considered are likely throughout the entire monsoon season of July to October. The FMLP models were trained without filtering out this effect or considering it in any form of modeling. Therefore, the true merit of the ANN technique on the basis of the Muskingum method could be assessed, upon the flexibility of predictions and model structures. The applicability of the developed model was also validated with independent flood data.

6 The study area

A forecasting model based on Muskingum routing was applied to the flood prone reach of the Chindwin River in northern Myanmar. Fig. 2 shows the location of the Chindwin River basin and the selected reach for flood routing. Myanmar is one of the tropical countries characterized by the monsoon climate and river flooding is a recurrent natural phenomenon (Sanyal and Lu 2004). With an inadequate density of hydrometric stations in most rivers of the country, estimation of floods in poorly gauged basins is a typical issue of water resources management in Myanmar. Among the principal rivers of the country, the Chindwin River has experienced frequent and severe floods in recent years and the flood risk has increased, especially in the last two decades (Latt and Wittenberg 2014b). However, the river receives relatively little attention. The Chindwin, with its major tributaries, is the most convenient way of communication within the basin connecting it with the main economically developed areas of the country. Due to climate conditions, the flood hazard is a challenge to its important role in the country's social economy. Severe floods hit the Chindwin basin every year at one place or another due to high rainfall

intensities during the southwest monsoon. Since 1965, flood occurrences in the Chindwin basin have been the highest in July and August contributing to 72% of the total number of floods in the basin. In this study, reported floods of two hydrometric stations, namely Homalin and Mawlaik, were considered. Flood estimation by routing the reach between these two stations would be valued in the region because these stations have the highest flood risk in terms of probability and temporal trend in mean annual maxima (Latt and Wittenberg 2014b). The length of the reach from upstream (Homalin) to downstream (Mawlaik) is 114km. According to the basin topography, the reach slope is about 0.0003, which is relatively mild. A flood wave is subjected to translation and reservoir actions during its passage through natural rivers and hydrologic methods are properly used in case the reservoir action dominates the translation action for rivers with a mild slope (Das 2009).

7 Result and Discussion

7.1 Study 1: Benchmark Data

The ANN-based Muskingum routing was applied to the Wilson's benchmark data, which many researchers have tackled, in order to minimize the SSQ and the routing results were compared to that of the previously documented methods. According to the Muskingum formula (Eq. 4), the FMLP structure was built to produce the outflow at the next time step, $O_{t+\Delta t}$ as a function of $I_{t+\Delta t}$, I_t and O_t. Therefore, three neurons in the input layer and one neuron in the output layer constitute the structure of the developed FMLP model. The number of neurons in the hidden layer depends on the complexity of input-output relationships to be captured. In the principle of traditional modeling, independent data sets for validation were used, whereas in the earlier studies for Muskingum parameter estimation that's used the single set Wilson data, the complete inflow-

outflow data were used only for calibration (Das 2009). Therefore, with no exception in this study, 100% of the data was used for training the FMLP models. Validation with an independent data set was not favored. After testing the sigmoid and hyperbolic activation functions in the hidden layer, the results suggest that the hyperbolic tangent function was preferable in this case, providing less prediction error and higher performance than sigmoid function. Using the same function in both hidden and output layers could not minimize the errors. Thus, the linear (identity) function was used in the output layer to ensure taking any values without a bounded range. The combination of the hyperbolic tangent in the hidden layer and the identity function in the output layer makes the models achieve the best performance. Table 1 depicts the best-fit FMLP architectures, determined on the basis of the least errors during calibration. Table 2 refers to the associated weights and bias of the best FMLP model (FMLP-1).

As shown in Fig. 3, minimizing SSQ value using various methods in the earlier studies has a significant improvement. The conventional parameter estimation techniques (PSO, NL-LS, S-LSM and LM) have resulted in SSQ values greater than 100 (Gill 1978; Yoon and Padmanabhan 1993; Das 2004; Chu and Chang 2009), and the other approaches provide relatively lower SSQ. In this study, the proposed FMLP model was compared only to the methods that provided SSQ values lower than 50. With a routing interval of six hours, Fig. 4 shows the comparison between the outflow hydrograph of the Wilson data and the routed outflows by different methods. Table 3 lists the computed outflows using HJ+DFP (Tung 1985), GA (Mohan 1997), ICSA (Luo and Xie 2010), HS (Kim et al. 2001), BFGS (Geem 2006), NMS (Barati 2011), the NL-4 model (Easa 2013), the FIS model (Chu 2009), and the FMLP model. Three decimal places were used in calculating the simulated outflows and comparing the performance of the different methods, except the FIS model, whose simulated flows are originally presented by Chu (2009) in one decimal place. However, the routed flows are mentioned in one decimal place in Table 3 due to

the limited space. Although taking different decimal places in performance indices is sensitive to the results of model comparison, the rounding off effect was faded beyond three decimal points for benchmark data (Barati 2011). Table 4 presents the performance indices of the FMLP model compared to recent studies of nonlinear Muskingum routing. It can be seen that routing performances by different optimization approaches for the NL-3 model are not significantly different from one method to another. In a comparison of different optimization methods, different subjects such as number of iterations, convergence time, and algorithm parameters need to be considered (Barati 2011). However, the study does not extensively discuss the collective strengths and weaknesses of different methods, but compares their performances by using evaluation criteria for benchmark data routing. The detailed explanation of the merit of each method can be read in the literature cited. Since the occurrence of the predicted peak flows coincide with that of the observed maximum outflow, *ETp* values become zero for all methods. Although HJ+DFP and GA methods provide a lower *EQp* than other algorithms, their SSQ values are far from the optimum solution. SSQ values of ICSA, HS, BFGS, and NMS methods are very close to one another. Their *MRE* and *EQp* values are around 2.5% and 0.01, while the *CE* values are the same for these four methods. Therefore, no significant improvement in model performances among these four methods can be detected, although they have their own merits and have been proven promising alternatives for the NL-3 routing procedure. The recent development in parameter estimation for the NL-3 model has resulted in a smaller improvement in SSQ, namely less than 1% (Easa 2013) as well as in *CE*. Evidently, none of the parameter estimation methods for NL-3 models showed a clear-cut superiority over the others in terms of all evaluation criteria. The SSQ value of best existing methods for the NL-3 model was 36.77, which was also confirmed using the GRG algorithm in this study, and for the NL-4 model, it is 7.67. The SSQ value of the FIS model, one of the artificial intelligence approaches, by Chu (2009) is 4.83, and *CE* value is 0.9996, which is the

best performance for benchmark data so far. The NL-4 model and the FIS model significantly outperformed the other models in the Muskingum flood routing of the benchmark data. However, there was a mixed fortune of performances for the NL-4 model and the FIS model. The FIS model has a superior performance over the NL-4 model in terms of SSQ, *CE* and *MRE*, whereas the NL-4 model is superior to the FIS model in terms of *EQp*. In this study, the best FMLP model provides the SSQ value of 4.05, which is the smallest value. The *CE*, *MRE* and *EQp* values of the FMLP model are 0.9997, 0.92% and 0.0024. Therefore, it can be shown that FMLP method is a promising alternative in Muskingum flood routing. The approach was found superior to other previously reported methods that have been used in Muskingum routing for the benchmark data, not only in terms of the objective function, but also in terms of all performance criteria.

7.2 Study 2: Real flood cases

Fig. 5 shows the observed inflow (upstream) and outflow (downstream) hydrographs of the Chindwin river reach. In the case of the Chindwin River, the hydrograph really reflects the behavior of a natural river with external influences, leading to higher outflows than inflows. Instead of first deriving the coefficients *x*, *K* and *m* by a linear or nonlinear Muskingum equation, it is possible to directly search the optimal weights and bias in mapping inflow-outflow, using the artificial intelligence approach. With a routing interval of one day, a FMLP structure was designed according to the Muskingum routing equation, since ANN can map any input-output patterns either in linear or nonlinear form. In the model development, several flood events during the monsoon season (July-October) from the period between 2005 and 2009 were simultaneously used for calibration. The calibration data was further randomly divided into a training set to 80% and a

testing set with 20%. After a successful calibration, the developed model was subsequently validated with the flood data during the monsoon seasons of 2010 and 2011.

As suggested by the previous analysis in the study-1, the hyperbolic tangent function was used in the hidden layer and identity function was used in the output layer. The developed FMLP structure in this case is 3-3-1 (three neurons in the input and hidden layers and one neuron in the output layer). The optimal objective function was achieved through the learning rate of 0.5 and momentum by 0.8. Sum of squares error during the training are 2.278. The computed weights and bias of the FMLP model are shown in Table 5. In an objective manner, three popular statistical measures (*CE, MRE* and *EQp*) were used to describe the performances of the models during calibration and validation. For routing real floods in the Chindwin River, the values of *CE*, *MRE* and *EQp* of the FMLP model during calibration were 0.99, 4.82% and 0.05, respectively. With high values of performance indices, Fig.6 shows a good agreement between the predicted outflows by the proposed model and the observed ones in the calibration period. The residuals of the model do not show a definite pattern, as seen in Fig. 7. Therefore, it can be expected that the residuals are independently distributed. As a result, the developed FMLP model is believed to be satisfactory for further prediction.

Validations of the model results are unavoidable in order to ensure the applicability of the proposed methods to this flood prone reach of the Chindwin River. With the optimally adjusted weight and bias achieved via the training, the FMLP model was reproduced to predict the independent flood events during the validation period. The predicted outflows and the observed ones in the validation period were plotted in Fig. 8, which depicts, except for a few flood peaks, the higher predictability of the ANN-based Muskingum model. Therefore, it is expected that the architecture of the trained network is sufficiently effective to generalize as well as to capture the underlying relationships, when validated with the new data. With a *CE* value of 0.98, the model

result is quite satisfactory. The model provides the *MRE* value of 4.38% in predicting the flows through the entire flood season. With the *EQp* value of 0.04, the error in predicting flood peaks is very low. The FMLP model has shown its robustness and predictability in real flood cases. Overall, this study presents a successful attempt to validate the prediction of real flood events with multiple peaks in this natural river throughout the entire monsoon season. It shows that an ANN approach along with sufficient real time data provides a convenient mechanism for routing of river flows.

8 Conclusions

Several studies have focused on improving the performance of the well-known Muskingum routing, with an emphasis on recommendation of optimization approaches for parameter estimation and direct mapping of input-output relationships, for the benchmark data. In chronological order, better solutions were proposed in minimizing the SSQ value. However, one method was not clearly superior to other methods because there are mixed fortunes of performances for each method in terms of the evaluation criteria. Few studies reported the applicability and performance of the proposed method in real flood cases with successful validation. The fact that nonlinear Muskingum models may not be applicable to every flood event is likely because the inflow-outflow relationship in natural rivers depends not only on the storage characteristics, but also on other external influences.

In this study, the FMLP network with error back propagation was applied for Muskingum flood routing, and its performance was assessed for benchmark data in comparison with the previous reported methods as well as for real flood cases of the Chindwin River in northern Myanmar. In both cases, the performance of the FMLP models was found to be quite satisfactory in terms of all

indices. The results have demonstrated that the FMLP model shows the consistency in its performance by means of all performance indices. Due to the ability of capturing nonlinearity and complex systems, the ANN approach can disregard any external disturbances and successfully capture the inflow-outflow relationship of the real flood cases on the basis of the Muskingum formula, which is sensitive to high disturbances by lateral inflows into the system.

This paper is not primarily interested in extensively discussing the strength and weakness of the individual methods for Muskingum routing, but in highlighting the merit of the artificial intelligence approach as a powerful competitive tool in solving complex or not-fully identified hydrologic systems. While solution algorithms have been studied for nonlinear Muskingum methods with more parameters from a mathematical standpoint, the values of fitted parameters are likely to lose physical meaning. Therefore, a novel black box approach, namely an intelligence method, helps the direct mapping of observed outflows and inflows according to the Muskingum formula and minimizes the discrepancy between observed and routed flows, without knowing routing parameters. For the flood routing of the benchmark data, a clear-cut superiority of the FMLP method over other previously documented methods was discerned. With a set of inflow-outflow records for a natural river reach, the proposed approach has been further shown to be a promising tool for routing of real flood events in natural rivers with high nonlinearity.

Acknowledgements

The study was funded by the Deutscher Akademischer Austausch Dienst (DAAD) (German Academic Exchange Service). The Department of Meteorology and Hydrology in Myanmar is also gratefully acknowledged for providing hydrometric data. The author is highly indebted and grateful to Prof. Hartmut Wittenberg for providing academic advices to this research.

References

Barati R (2011) Parameter estimation of nonlinear Muskinugm models using the Nelder-Mead Simplex algorithm. Journal of Hydrologic Engineering 16(11): 946-954

Barati R (2013) Application of Excel solver for parameter estimation of the nonlinear Muskingum models. KSCE Journal of Civil Engineering 17(5):1139-1148

Berz G (2000) Flood disasters: lessons from the past – worries for the future. Proceeding of the ICE. Water and Maritime Engineering 142(1): 3-8

Chow VT, Maidment DR, Mays LW (1988) Applied Hydrology. McGraw Hill, Singapore.

Chu HJ (2009) The Muskingum flood routing model using a Neuro-Fuzzy Approach. KSCE Journal of Civil Engineering 13(5): 371-376

Chu HJ, Chang LC (2009) Applying Particle Swarm Optimization to Parameter Estimation of the Nonlinear Muskingum Model. J. Hydrol. Eng. 14(9):1024–1027

Das A (2004) Parameter Estimation for Muskingum Models. Journal of Irrigation and Drainage Engineering 130(2): 140–147

Das A (2009) Reverse stream flow routing by using Muskingum models. *Sādhanā* 34, Part 3: 483-499

Dooge JCI (1973) Linear theory of hydrologic systems. Agricultural Research Service, USDA, Technical Bulletin No-1468, Washington D.C.

Easa SM (2013) New and improved four-parameter non-linear Muskingum model. Water Management, Institute of Civil Engineers (ICE), DOI:10.1680/wama.12.00113.

Geem ZW (2006) Parameter estimation for the nonlinear Muskingum model using the BFGS techniques. Journal of Irrigation and Drainage Engineering 132(5): 474-478

Geem ZW (2013) Issues in optimal parameter estimation for the nonlinear Muskingum flood routing model. Engineering Optimization. DOI**:**10.1080/0305215X.2013.768242.

References

Gill MA (1978) Flood routing by the Muskingum method. Journal of Hydrology 36: 353-363

Kim JH, Geem ZW, Kim ES (2001) Parameter estimation of the non-linear Muskingum model using harmony search. Journal of the American Water Resources Association 37(5):1131-1138

Latt ZZ, Wittenberg H (2014a) Improving Flood Forecasting in a Developing Country: A Comparative Study of Stepwise Multiple Linear Regression and Artificial Neural Network. Water Resources Management 28(8): 2109–2128. doi: 10.1007/s11269-014-0600-8

Latt ZZ, Wittenberg H (2014b) Hydrology and flood probability of the monsoon-dominated Chindwin River in northern Myanmar. Journal of Water and Climate Change In Press. doi:10.2166/wcc.2014.075

Luo J, Xie J (2010) Parameter estimation for nonlinear Muskingum model based on Immune Clonal Selection algorithm. Journal of Hydrologic Engineering 15(10): 844-851

McCarthy GT (1938) The unit hydrograph and flood routing. Proc., Conference of the North Atlantic Division, U.S Army Corps of Engineers, New London, C.T.

Minns AW, Hall MJ (1996) Artificial neural networks as rainfall-runoff models. Hydrological sciences 41(3): 399-417

Mohan S (1997) Parameter estimation of nonlinear Muskingum models using genetic algorithm. Journal of Hydraulic engineering 123(2): 137-142

O' Donnell T (1985) A direct three-parameter Muskingum procedure incorporating lateral inflow. Hydrological Sciences 30(4): 479-496

Orouji H, Haddad OB, Mehdipour EF, Mariño MA (2013) Estimation of Muskingum parameter by meta-heuristic algorithms. Water Management, Institute of Civil Engineers (ICE) 166(6): 315-324

Othman F, Naseri M (2011) Reservoir inflow forecasting using artificial neural work. International journal of the physical sciences 6(3): 434-440

References

Papamichail D, Georgiou P (1994) Parameter estimation of linear and nonlinear Muskingum models for river flood routing. Transactions on Ecology and the Environment 7: 139-146

Reddy JM, Wilamowski BM (2000) Adaptive neural networks in regulation of river flows. In: Govindaraju RS and Rao AR (eds) Artificial Neural Networks in Hydrology. Kluwer Academic Publishers, the Netherlands: 153-177.

Rumelhart DE, Hinton GE, Williams RJ (1986) Learning internal representations by error propagation. In: Rumelhart DE, McClelland JL, the PDP research group (eds) Parallel Distributed Processing, Vol. 1. Cambridge, MIT press, pp 318–362

Sanyal J, Lu XX (2004) Application of remote sensing in flood management with special reference to Monsoon Asia: A Review. Natural Hazard 33(2): 283-301

Sattari NT, Apaydin H, Ozturk F (2012) Flow estimations for the Sohu stream using artificial neural networks. Environ. Earth Science 66 (7): 2031–2045

Shamseldin AY (2010) Artificial neural network model for river flow forecasting in a developing country. Journal of Hydroinformatics 12(1): 22-34

Singh VP, McCANN RC (1980) Some notes on Muskingum method of flood routing. Journal of Hydrology 48: 343-361

Sivapragasam C, Maheswaran R, Venkatesh V (2008) Genetic programming approach for flood routing in natural channels. Hydrological Processes 22(5): 623-628

Stefanon B, Volpe V, Moscardini S, Gruber L (2001) Using artificial neural network to model the urine excretion of total and purine derivative Nitrogen fraction in cows. Journal of Nutrition 131(12): 3307-3315

Stephenson D (1979) Direct optimization of Muskingum routing coefficients. An Extension to the paper by Gill, M. A. Flood routing by the Muskingum method. Journal of Hydrology 41: 161-165

References

Strupczewski W, Kundzewicz Z (1980) Muskingum method revisited. Journal of Hydrology 48(3-4): 327-342

Tayfur G, Moramarco T, Singh VP (2007) Predicting and forecasting flow discharge at sites receiving significant lateral inflow. Hydrological Processes 21(14): 1848-1859

Thirumalaiah K, Deo MC (1998) Real-Time Flood Forecasting Using Neural Networks. Computer Aided Civil and Infrastructure Engineering 13: 101-111

Tung Y (1985) River flood routing by nonlinear Muskingum method. Journal of Hydraulic Engineering 111(12): 1447-1460

Weinmann PE (1977) Comparison of flood routing methods for natural rivers. Civil Engineering Reports No. 2, Monash University.

Wilson EM (1974) Engineering Hydrology. MacMillan Education Ltd., Hampshire U.K.

Yang CC, Chang LC (2001). Enhanced efficiency of the parameter estimation of Muskingum model using artificial neural network. Journal of Hydroscience and Hydraulic Engineering 19(2): 47-55

Yoon J, Padmanabhan G (1993) Parameter estimation of linear and nonlinear Muskingum models. Journal of Water Resources Planning and Management 199(5): 600-610

Tables

Table **1** The best FMLP models for Muskingum routing of benchmark data

FMLP models	Model structure	Learning rate	Momentum	Sum of squares error
FMLP-1	3-2-1	0.62	0.9	0.004
FMLP-2	3-2-1	0.40	0.7	0.005
FMLP-3	3-2-1	0.10	0.8	0.005

Tables

Table **2** The calculated weight and bias of the best FMLP model (FMLP-1) for routing benchmark data

Predictor	Target Variable, $O_{t+\Delta t}$		
	Hidden layer		Output layer
	Node 1	Node 2	
Input layer (bias)	0.682	-0.078	
$I_{t+\Delta t}$	-0.497	-0.323	
I_t	-0.198	0.491	
O_t	-0.782	-0.833	
Hidden layer (bias)			0.278
Node 1			-0.964
Node 2			-0.886

Tables

Table **3** Comparison of routed outflows by the FMLP with other methods for Wilson's data

	Observed Flows (m^3s^{-1})		Computed Outflow (m^3s^{-1})								
Time (hr)	I	O	HJ+DFP	GA	ICSA	HS	BFGS	NMS	NL-4	FIS	FMLP
0	22	22	22.0	22.0	22.0	22.0	22.0	22.0	22.0	22.0	22.0
6	23	21	22.0	22.0	22.0	22.0	22.0	22.0	22.0	20.9	20.4
12	35	21	22.4	22.4	22.4	22.4	22.4	22.4	22.3	21.0	21.5
18	71	26	26.7	26.4	26.6	26.3	26.6	26.6	25.7	26.0	26.0
24	103	34	34.8	34.2	34.4	34.2	34.5	34.5	33.1	34.0	33.8
30	111	44	44.7	44.2	44.2	44.2	44.2	44.2	43.6	44.0	44.1
36	109	55	56.9	57.0	56.9	56.9	56.9	56.9	55.8	57.1	55.2
42	100	66	67.7	68.2	68.1	68.2	68.1	68.1	66.5	66.2	65.7
48	86	75	76.3	77.2	77.1	77.1	77.1	77.1	75.2	75.0	75.3
54	71	82	82.2	83.3	83.3	83.3	83.3	83.3	81.6	82.0	81.7
60	59	85	84.7	85.7	85.9	85.9	85.9	85.9	84.7	85.4	85.2
66	47	84	83.5	84.2	84.5	84.5	84.5	84.5	83.8	84.0	84.0
72	39	80	79.8	80.2	80.5	80.6	80.6	80.6	80.1	80.0	79.9
78	32	73	73.3	73.3	73.6	73.7	73.7	73.7	73.0	73.0	72.9
84	28	64	65.5	65.1	65.3	65.4	65.4	65.4	64.3	64.0	64.0
90	24	54	56.5	55.8	55.9	56.0	56.0	56.0	54.2	54.0	54.0
96	22	44	47.5	46.7	46.6	46.7	46.7	46.7	44.6	44.0	44.7
102	21	36	38.7	38.0	37.8	37.8	37.7	37.8	35.8	35.9	35.8
108	20	30	31.4	30.9	30.5	30.5	30.5	30.5	29.2	29.9	29.1
114	19	25	25.9	25.7	25.3	25.3	25.2	25.2	24.7	25.3	24.8
120	19	22	22.1	22.2	21.8	21.8	21.7	21.7	21.7	21.7	22.0
126	18	19	20.2	20.3	20.0	20.0	20.0	20.0	20.1	19.1	20.2

Tables

Table **4** Routing parameters and performance statistics of different techniques for the Wilson's data

Method	Routing Parameter				Objective Function	Performance Indices			
	K	*x*	*m*	*n*	SSQ	*CE*	*MRE*	*EQp*	*ETp*
HJ+DFP	0.0764	0.2677	1.8978		45.61	0.9962	2.974	0.0036	0
GA	0.1033	0.2813	1.8282		38.24	0.9969	2.604	0.0084	0
ICSA	0.0884	0.2862	1.8624		36.80	0.9970	2.526	0.0106	0
HS	0.0883	0.2873	1.8630		36.78	0.9970	2.518	0.0108	0
BFGS	0.0863	0.2869	1.8679		36.77	0.9970	2.526	0.0106	0
NMS	0.0862	0.2869	1.8681		36.77	0.9970	2.525	0.0107	0
NL-4	0.8340	0.2960	4.0790	0.4330	7.67	0.9994	1.531	0.0031	0
FIS					4.83	0.9996	0.40	0.0047	0
FMLP					4.05	0.9997	0.92	0.0024	0

Tables

Table **5** The calculated weight and bias of the FMLP model for routing real flood events of the Chindwin River

Predictor	Target Variable, $O_{t+\Delta t}$			
	Hidden layer			Output layer
	Node 1	Node 2	Node 3	
Input layer (bias)	-0.513	1.184	0.473	
$I_{t+\Delta t}$	-0.126	-0.080	-0.509	
I_t	-0.011	-0.075	0.434	
O_t	-0.338	-0.352	0.313	
Hidden layer (bias)				0.599
Node 1				-1.996
Node 2				-1.805
Node 3				-0.071

Figures

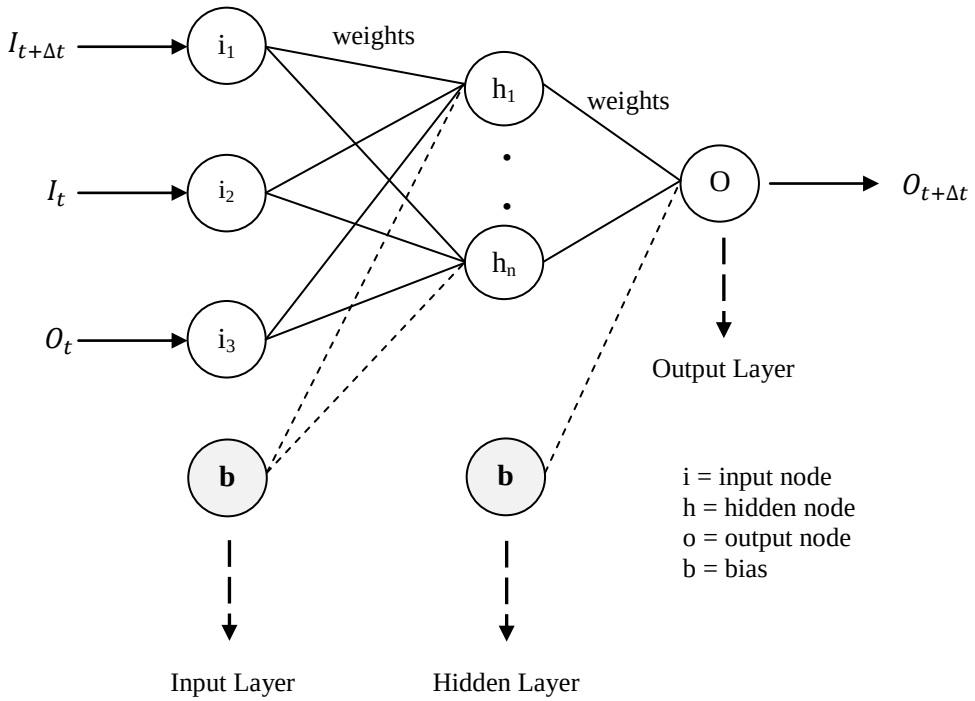

Fig.**1.** Structure of the MLP model for Muskingum routing

Figures

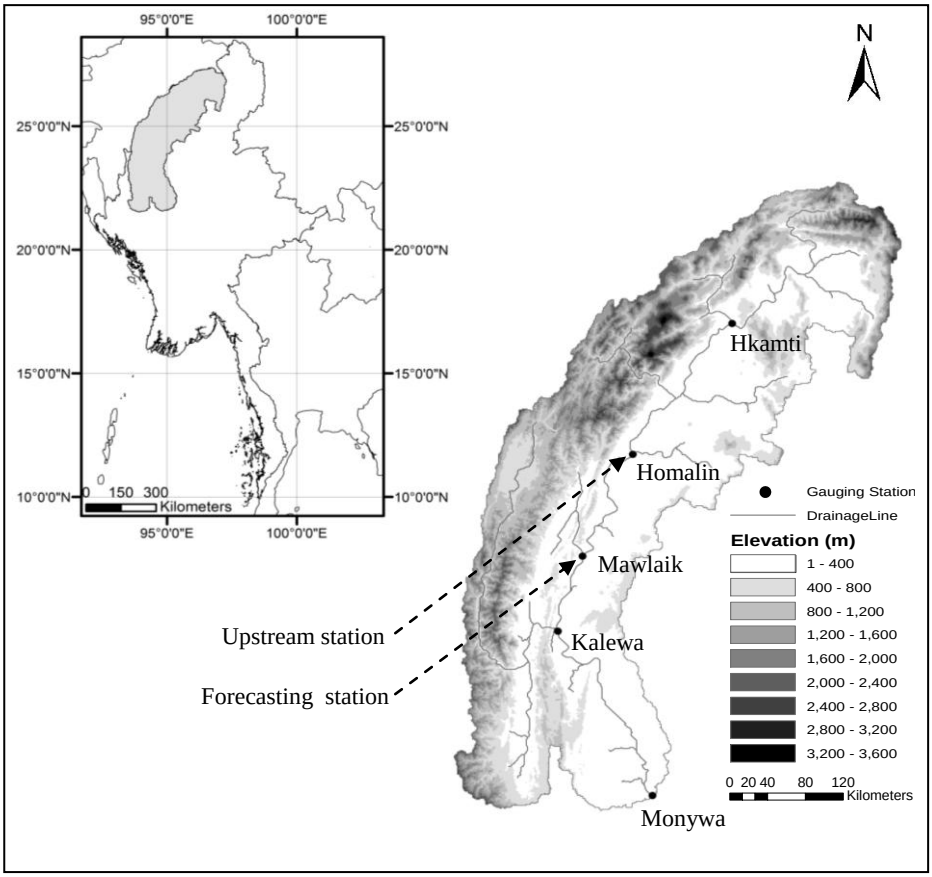

Fig. **2.** Location of the Chindwin river basin

Figures

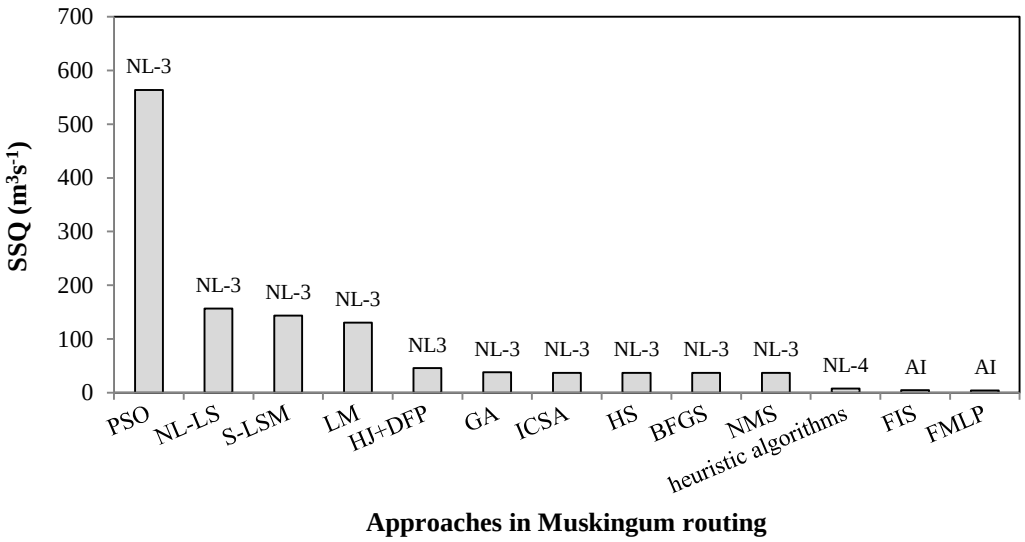

Fig. **3.** Performances of the different approaches in minimizing SSQ for routing the Wilson's benchmark data

Figures

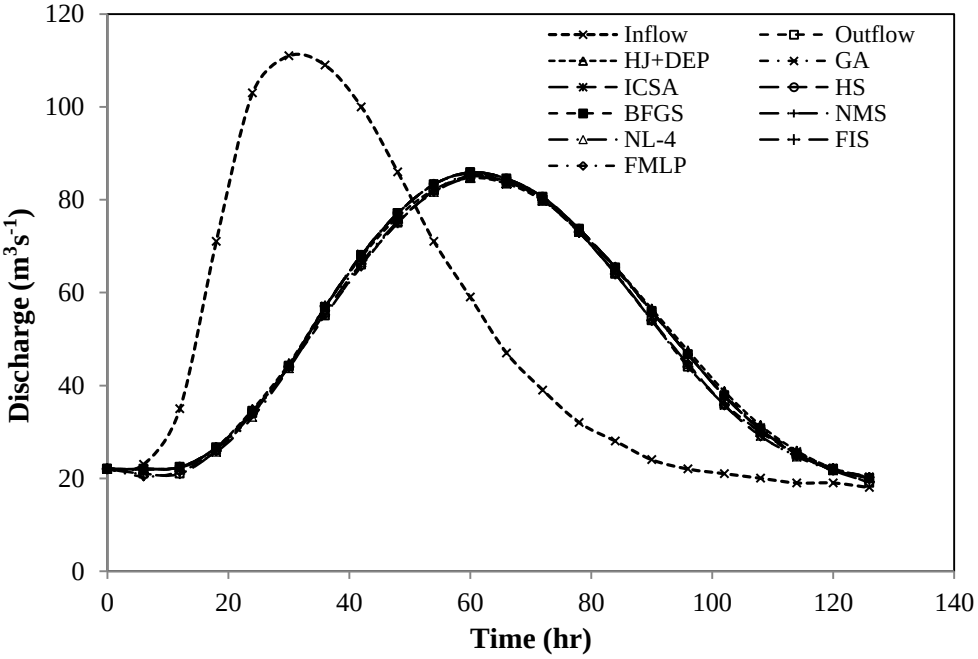

Fig. **4.** Comparison of routed outflows by different methods for Wilson's data

Figures

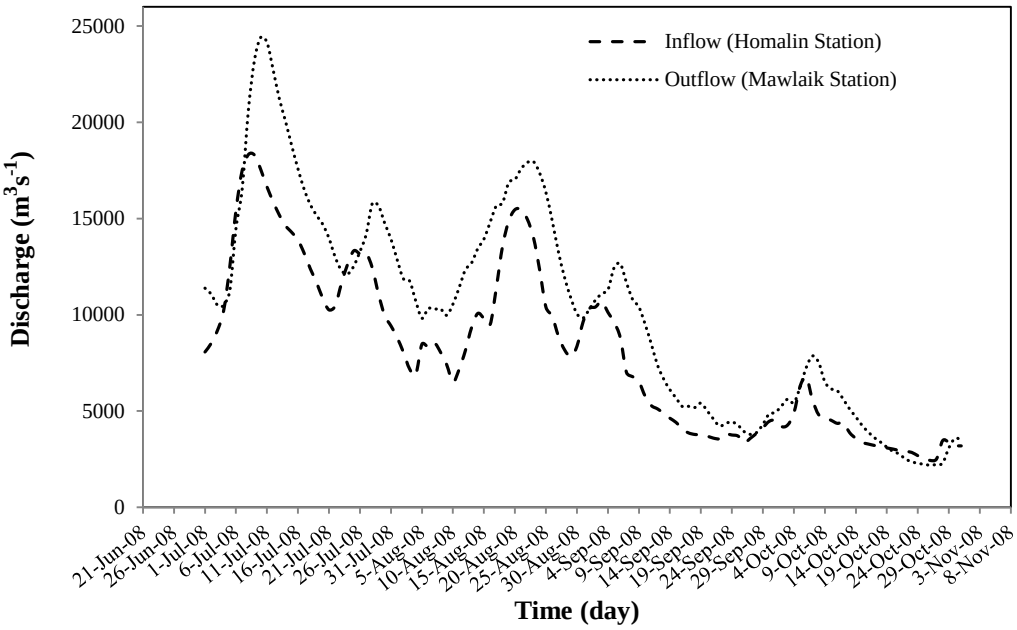

Fig. **5.** Inflow and outflow hydrographs for the Chindwin River reach for the 2008 flood season

Figures

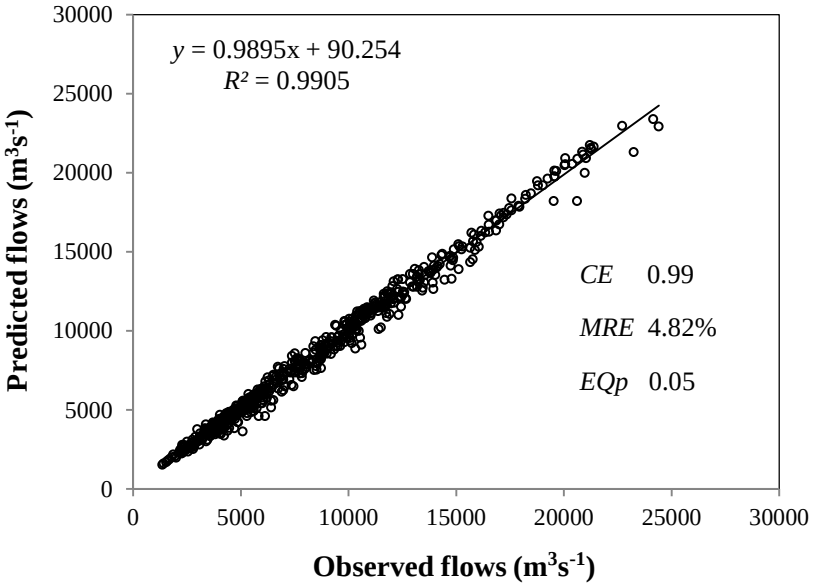

Fig. **6.** Observed and predicted outflows for the Chindwin river reach during calibration

Figures

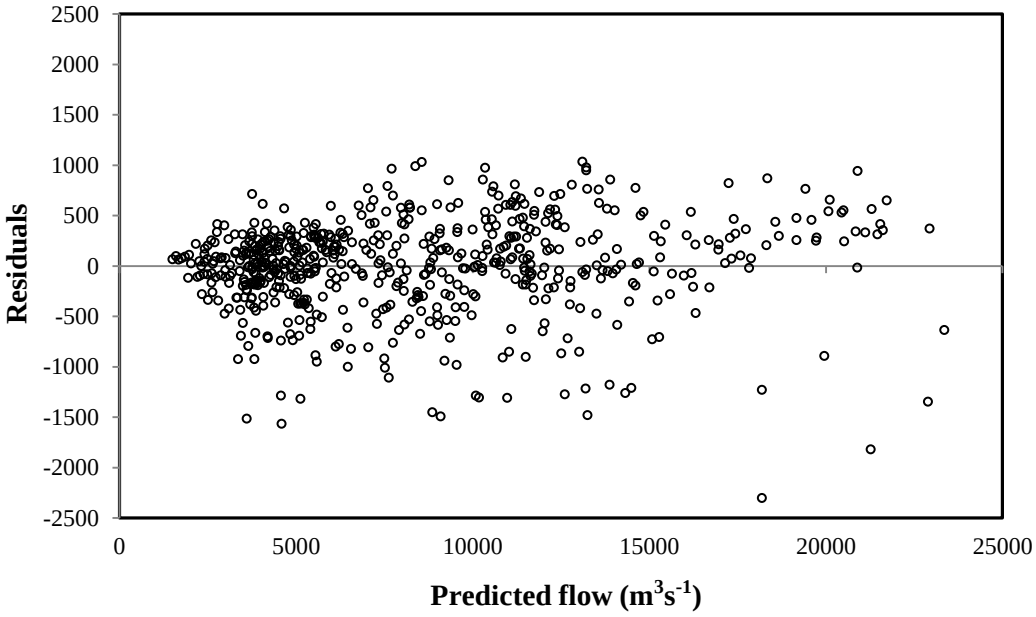

Fig. 7. Residuals vs. predicted plot

Figures

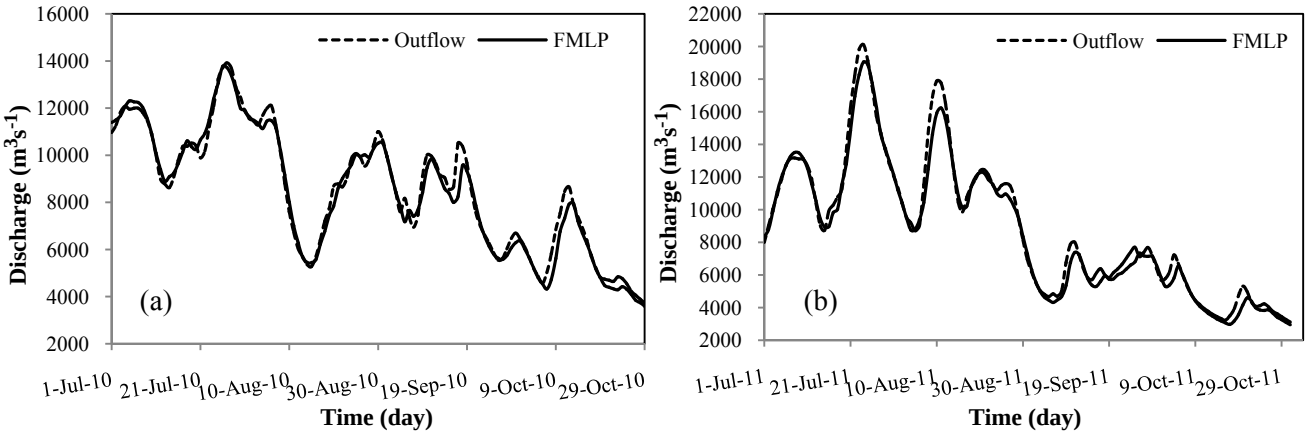

Fig. **8.** Comparison of predicted outflows by the FMLP model and the observed outflows during the validation (a) for 2010 flood season and (b) for 2011 flood season

Supplementary Materials

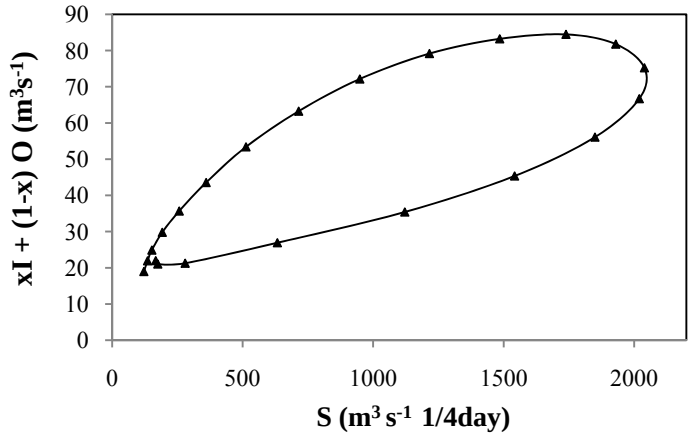

Fig. S1 Non-linear relationship between storage and weighted discharge for the Wilson's benchmark data with single flood peak

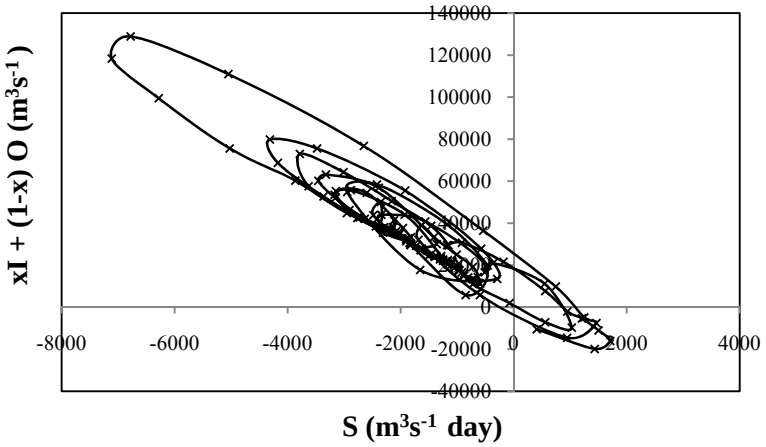

Fig. S2 Non-linear relationship between storage and weighted discharge for the Chindwin River with multiple flood peaks

Article IV

Clustering Hydrological Homogeneous Regions and Neural Network Based Index Flood estimation for Ungauged Catchments: An Example of the Chindwin River in Myanmar

Zaw Zaw Latt, Hartmut Wittenberg, Brigitte Urban

Reprinted from Journal of Water Resources Management 29(3)
doi: 10.1007/s11269-014-0851-4, pages 913-928,

Water Resour Manage (2015) 29:913–928
DOI 10.1007/s11269-014-0851-4

Clustering Hydrological Homogeneous Regions and Neural Network Based Index Flood Estimation for Ungauged Catchments: an Example of the Chindwin River in Myanmar

Zaw Zaw Latt · Hartmut Wittenberg · Brigitte Urban

Received: 20 April 2014 / Accepted: 16 October 2014 /
Published online: 25 October 2014

Abstract A neural network-based regionalization approach using catchment descriptors was proposed for flood management of ungauged catchments in a developing country with low density of the hydrometric network. Through the example of the Chindwin River basin in Myanmar, the study presents the application of principal components and clustering techniques for detecting hydrological homogeneous regions, and the artificial neural network (ANN) approach for regional index flood estimation. Based on catchment physiographic and climatic attributes, the principal component analysis yields three component solutions with 79.2 % cumulative variance. The Ward's method was used to search initial cluster numbers prior to *k*-means clustering, which then objectively classifies the entire catchment into four homogeneous groups. For each homogeneous region clustered by the leading principal components, the regional index flood models are developed via the ANN and regression methods based on the longest flow path, basin elevation, basin slope, soil conservation curve number and mean annual rainfall. The ANN approach captures the nonlinear relationships between the index floods and the catchment descriptors for each cluster, showing its superiority towards the conventional regression method. The results would contribute to national water resources planning and management in Myanmar as well as in other similar regions.

Keywords Artificial neural network · Multivariate clustering · Index flood estimation · Physiographic parameter · Principal component · Ungauged catchment

1 Introduction

Flood is the most costly and damaging natural disaster among other main catastrophes in the world in terms of loss of lives and properties (Berz 2000). During the past 30 years, 40 % of the total number of the flood events in the world occurred in Asia, and Southeast Asia is the second worst flood-affected region of the continent, after South Asia (Dutta and Herath 2004).

Z. Z. Latt (✉) · H. Wittenberg · B. Urban
Faculty of Sustainability, Institute of Ecology, Leuphana University of Lueneburg, Scharnhorststr. 1, C13.112, 21335 Lueneburg, Germany
e-mail: zawzawlatt@khalsa.com

Therefore, understanding flood response characteristics and flood estimates are required not only for design and economic appraisal of hydraulic works, but also for efficient flood management schemes to save human lives and environmental assets. Myanmar, the second biggest country in Southeast Asia, is highly exposed to flood hazards due to its complex topography and high rainfall intensities during the southwest monsoon season. Floods are affected by the spatial distribution of terrestrial and climatic conditions through hydrological processes and therefore, detecting and mapping similar flood response characteristics can assist the water resources practitioners in management decision. As flood mitigation measures are not possible without knowing regional characteristics being an integral part of the flood risk management, special concern is dedicated to the diverse spatial conditions.

To assess flood risk and adopt control measures, one needs to estimate flood magnitude at any watershed location. However, direct flood estimations using past flow data are not always possible due to insufficient flow records, particularly in developing countries like Myanmar. Moreover, with the use of flood statistics, hydrologic regionalization is not possible for sparsely gauged or ungauged basins. Due to the substantial costs involved, the density of hydrometric monitoring stations in Myanmar is 12,000 km^2 per station, which is beyond the minimum adequacy of 1,500 km^2 per station recommended by the World Meteorological Organization (2008). Under these circumstances, regionalization using climatic and catchment physiographic characteristics is an appropriate solution for flood estimation at ungauged basins in Myanmar. Identification of hydrological homogeneous regions and the application of a regional estimation method in identified homogeneous regions plays a major role in any regional flood frequency analysis (RFFA) (Chokmani and Ouarda 2004; Abdolhay et al. 2012).

Watershed classification is generally based on physiographic characteristics of watersheds or their flood behaviors or a combination of both (Razavi and Coulibaly 2013). However, there do not seem to be any specific objective guidelines for identifying homogeneous regions due to the inadequate understanding flood generating mechanisms (Gingras and Adamowski 1993). The choice of variables for clustering and regional flood models depends on data availability and influences on flood generation (GREHYS 1996). However, using geographical proximity alone as surrogate for hydrological similarity might not be satisfactory since the regionalized areas may be hydrologically heterogeneous (Smith and Ward 1998). Moreover, classifying homogeneous regions using geographical properties alone is not completely satisfactory and terrestrial information is needed to be included in the cluster analysis (Hosking and Wallis 1997; Mishra et al. 2009). In the context of watershed classification, recent studies have focused on multivariate statistical analysis, such as principal component (PCA) and cluster analysis (Razavi and Coulibaly 2013). Cluster analysis has been used in numerous areas of water resources and environmental management (Shaban et al. 2010; Goyal and Gupta 2014). For example, Abdolhay et al. (2012) applied factor analysis together with different clustering techniques such as Ward, Fuzzy and Kohonen to identify the homogeneous regions. Similarly Razavi and Coulibaly (2013) have applied PCA to watershed attributes and streamflow series prior to k-means clustering of watershed classification.

In flood regionalization, index flood (IF) is a primary variable to extrapolate flood exceedance probabilities via RFFA. Regression techniques are widely used to estimate IF based on catchment descriptors at ungauged sites (Kohnová and Szolgay 2003; Dawson et al. 2006; Cutore et al. 2007). While this approach is the most consistent and reliable procedure, the log-transformed solution of the conventional power form (regression based) model for the parameter estimation may be biased in a real domain (Pandey and Nguyen 1999; Eng et al. 2007). Logarithmic transformation is not possible to linearize the power form model with the additive error (GREHYS 1996). Moreover, deciding an appropriate model structure in

mapping relations between flood quantiles and catchment attributes is a complex issue in flood regionalization. Despite several non-linear optimization techniques for directly estimating the power form model parameters in real domain, the model structure is fixed (Pandey and Nguyen 1999). On the other hand, a nonlinear technique such as artificial neural networks (ANN) can be used to estimate parameters of such models in a real flood domain as ANNs identify any complex system during training process. Neural solutions have been applied to a wide range of hydrological problems such as rainfall-runoff relationships (Sattari et al. 2012), flood forecasting (Sahay and Srivastava 2014), and groundwater level forecasting (Nayak et al. 2006). In addition, ANNs have been considered as a competitive alternative to conventional statistical methods in streamflow prediction (Cigizoglu 2003; Latt and Wittenberg 2014a). However, there have been relatively few applications of ANNs to regional flood models (Dawson et al. 2006). For example, Aziz et al. (2013) have developed ANN-based regional flood frequency models for Australian catchments. In addition, Besaw et al. (2010) have trained recurrent ANNs on climate-flow data from one basin for streamflow forecasting at ungauged basin with different climate inputs. To correct the transformation bias in the regression technique, neural network approaches would be a robust technique in estimating IF at ungauged sites via catchment descriptors, while conventional regression method has a limitation in use.

To the knowledge of the authors, in contrast to the demanding flood hazards, no specific study on flood regionalization for ungauged catchments has been reported in the context of Myanmar rivers and particularly the Chindwin catchment has received relatively little attention. Therefore, one of the main goals of this paper is to identify homogeneous regions with similar flood response characteristics using PCA and clustering techniques. Secondly, as a measure to overcome the performance inconsistency of the regression technique in a real domain, this paper proposes the ANN technique to establish regional IF models for predefined homogeneous regions, and its performances are then compared to that of the conventional power form model. The flood generating variables and the hydrological homogeneous regions are derived and visualized by using GIS for quick referencing and decision making in national water resources management of Myanmar.

2 The Chindwin River basin

The Chindwin River is located between Latitude 22°06′–26°00′ North and Longitude 94°18′–95°42′ East and covers a catchment area of 113,800 km^2 (Fig. 1). With a length of 985 km, it is the third largest river and one of the principal water resources of Myanmar. With its tributaries, the Chindwin is a major transport artery, and it also connects the basin with the main economically developed areas of the country. In the Chindwin catchment, there are key biodiversity areas such as the Hukaung Valley and the Htamanthi wildlife sanctuaries, as well as major conservation areas such as the Upper Chindwin Catchment Corridor and the Lower Chindwin Forest Corridor which are endowed with an important population of critically endangered animals (NCEA 2009). Overall, the basin is economically and ecologically important for the development of the country.

With an inadequate density of 20,000 km^2 per station, the Chindwin River is experiencing frequent flood hazards, the challenging natural factor relating to its important role in national social-economy. According to the Department of Meteorology and Hydrology (DMH), Myanmar, since 1965 flood occurrences in the Chindwin basin are the highest in July and August, contributing 72 % of the total number of floods in the basin. Due to high rainfall intensities during the southwest monsoon, severe floods hit the Chindwin basin every year at one place or another, and threaten property, assets, human lives and ecological biodiversity in the region. Although the

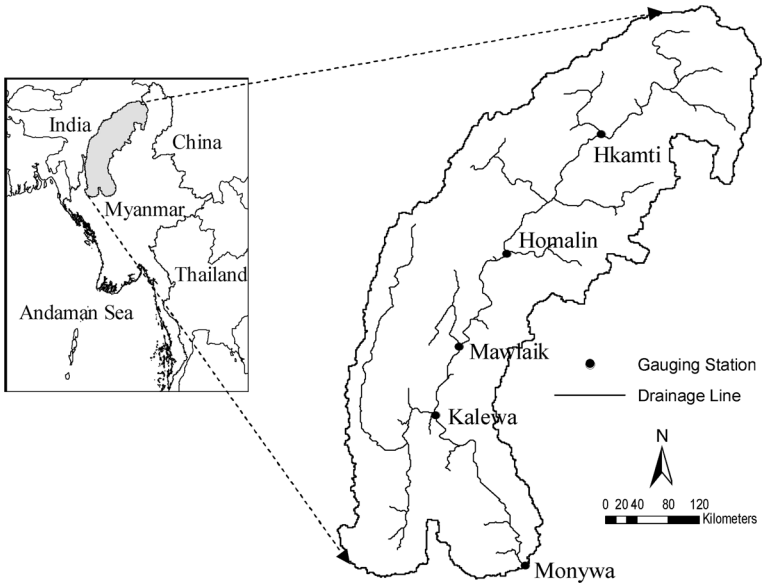

Fig. 1 Location of the Chindwin River basin

stream flows of other tributaries across the entire catchment cannot be monitored, the flood risks in the ungauged regions of the catchment are critical issues threatening the entire community.

3 Materials and Method

The hydrometric data analyzed in this paper mainly consist of daily flows and rainfalls (1965 to 2011) at five gauging stations along the Chindwin River, which were obtained from DMH. Digital elevation model (DEM) data with 1 km resolution were available from the USGS Hydro 1K database (https://lta.cr.usgs.gov/HYDRO1K). Contour maps were provided by the Myanmar Survey Department. Soil and land use information were obtained from the Myanmar Land Use Department as well as from the FAO GeoNetwork (http://www.fao.org/geonetwork/srv/en/main.home). Based on the availability and influences on hydrological responses, five physiographic properties (area, elevation, slope, length, shape factor), two response variables (time of concentration and Soil Conservation Curve Number), and one climatic variable (mean annual rainfall) were considered for pooling homogeneous regions using multivariate statistical analysis (see Table 1).

The analysis presented in this paper comprises three major steps. First, selected clustering variables were determined using GIS and statistical methods. Secondly, principal component and clustering analyses were applied to the derived watershed physiographic and the climatic attributes in order to detect homogeneous regions. Afterwards regional IF models were developed for each clustered region using regression and ANN techniques.

3.1 Deriving Catchment Physiographic and Climatic Parameters

Raw DEM data were first corrected to create a depressionless DEM (Fig. 2a) by filling the sinks. Based on the corrected DEM, ArcHydrol Tools in ArcGIS 10 was used in order to

Table 1 Descriptive statistics for selected flood generating factors

Variables	Definition	Units	Min.	Max.	Mean	S.D	Skewness	Kurtosis
A	Basin Area	km^2	3	11,762	1,990	1,761	3.3	16.4
E	Mean basin elevation	m	69	1,802	792	519	0.5	−0.9
S	Basin slope	%	0.7	16.4	6.7	3.6	0.7	0.1
L	Basin length	km	2	397	90	55	3	16.3
SF	Shape factor	–	1.3	13.4	4.6	2.3	1.8	3.9
CN	Soil conservation curve number	–	65	93	81	8	−0.1	−1.1
T_C	Time of concentration	minute	9	1,138	260	174	2.8	11.8
R	Mean annual rainfall	mm	820	3,710	2,234	733	0.5	−0.5

S.D Standard deviation

derive physiographic and climatic attributes for each subbasin. *E* was calculated as the average ground elevation above mean sea level from all cells (1×1 km) in the basin. *S* was calculated as the ratio of change in rise by change in run. *L* was defined as the longest flow path from the outlet to the farthest basin divide. *SF* was calculated by dividing the squared length by the area (L^2A^{-1}).

T_C influences on the shape and peak of the runoff hydrograph and therefore can be considered a significant factor in runoff generation. T_C for the main stream was determined using the Kirpich (1940) formula given as

$$T_C = 0.0078\left(\frac{L}{\sqrt{S_0}}\right)^{0.77} \quad (1)$$

where, *Tc* is in hours, *L* is the maximum length of the main watercourse (km) and S_0 is its average channel slope. Based on the flow direction, *L* and S_0 were extracted from the flow slope and flow length maps (Fig. 2b and c) using a GIS process to calculate the *Tc* for all subbasins.

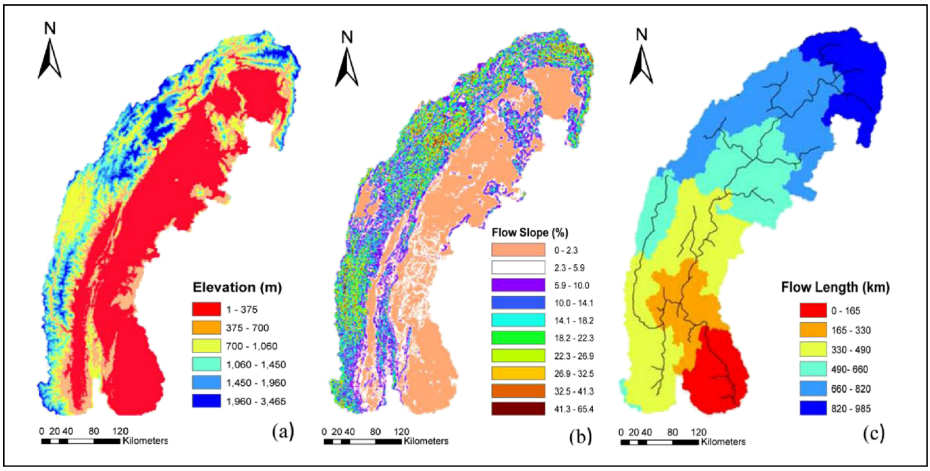

Fig. 2 Digital elevation model (**a**), Flow slope (**b**) and Flow length (**c**) of the Chindwin catchment

Impacts of terrestrial condition such as land cover and soil type were considered in term of *CN*, which characterizes the runoff potential of a basin. *CN* values range from 1 to 100. A higher *CN* represents a higher runoff. Through the GIS process, *CN* for every grid cell in the basin was determined using land use and soil raster data. In this study, collected soil maps were based on the FAO soil units (IUSS Working Group WRB 2006). Therefore, the entire catchment needs to be categorized into hydrologic soil groups (A, B, C and D), according to the USDA (1986) classification. The Chindwin catchment was classified into four major land use types: water, urban land, forest and agriculture. The treated hydrologic soil groups and the reclassed land use data were then homogenized. Afterwards the combined data were linked to the *CN* lookup table, which is based on the normal condition of the antecedent moisture content. Finally, an average *CN* for each subbasin was calculated by intersecting the *CN* and basin area layers.

The rainfall isohyetal map was prepared by using mean annual rainfall (MAR) data at 34 locations to cover the entire catchment; 11 of these are observed stations. Rainfall data for the remaining stations were available from the WorldClim-Global Climate Data (http://www.worldclim.org). An ordinary Kriging method with GIS was applied for spatial interpolation to produce MAR value at each grid cell in the entire catchment. The Kriging uses weights from surrounding measured values for predicting values at unmeasured locations and is expressed as follows:

$$F = \sum_{i=1}^{n} W_i f_i \tag{2}$$

Where F is the prediction of the continuous variable of interest (f), n the number of scatter points, f_i the observed value at the point i, and W is the weighting coefficient to each scattered point. From the gridded MAR map of the entire catchment, MAR values at the respective cells of any boundary i.e. subbasin can be extracted and areal weighted value for each subbasin was calculated.

3.2 Principal Component and Cluster Analysis

The main function of PCA is to reduce the dimensionality of a data set that consists of a large set of interrelated variables, while retaining most of the variation in the data set (Jolliffe 2004). This is achieved by transforming variables into a smaller set of variables (principal components) which are not correlated, and organized so that the first few components retain as much as possible the variation in the original variables. For deriving the significant components to be used in pooling homogeneous regions, seven watershed attributes and one climatic variable (*A, E, S, SF, L, CN,* T_C and *R)* are incorporated into the PCA. To check the appropriateness of PCA, Kaiser-Meyer-Olkin (KMO) statistic is used. KMO is a measure of sampling adequacy, both overall and for each variable (Cerny and Kaiser 1977). The value of the KMO measure varies from 0 to 1, and the value below 0.5 is unacceptable for factor analysis. The factors (components) whose eigenvalues were greater than 1 and whose cumulative variance was greater than 75 % were selected for subsequent clustering processes using leading principal components.

The most commonly used measure in clustering is the Euclidean distance defined as

$$D_{ij} = \left[\sum_{k=1}^{n} \left(x_{ki} - x_{kj} \right)^2 \right]^{1/2} \tag{3}$$

where, x_{ki} is the value of variable x_k in case i and x_{kj} is the value of variable x_k for case j. D_{ij} is the distance between case i and j. Here, a number of cases represented the number of basins. The variables within Eq. (3) were factor scores of the extracted principal components for each

basin. For classifying the basins into homogeneous groups, the hierarchical Ward's method was first applied to get a possible number of clusters using a screet test. Then, non-hierarchical *k*-means clustering (MacQueen 1967) was run with the predefined optimum number in which all cases were placed. *k* refers to the number of clusters. The algorithm starts by choosing the initial *k* cluster centers and classifying cases based on their distance to the centers. At each iteration, the centers are repositioned for a better repetition of data and distances actualized. This procedure is repeated until cluster means do not change much between successive steps. Finally, this algorithm aims at minimizing an objective function, defined as

$$J = \sum_{j=1}^{k} \sum_{i=1}^{n} D_{ij}{}^{2} \tag{4}$$

Where D_{ij} is the Euclidean distance between a data point x_i and the cluster center x_j, n is the number of data points in ith cluster.

3.3 Regional Index Flood Models

From the daily streamflow series of the gauged sites, mean annual maxima were calculated. The IF referred in this study is the mean annual maximum floods (Q_m). Several researchers reported that IF at any location of watershed is mostly governed by corresponding catchment area (Hosking and Wallis 1997; Kohnová and Szolgay 2003; Aziz et al. 2013). The commonly used relationship between the IF and catchment area of the gauged sites is as follows:

$$Q_m = C_0 A^{C_1} \tag{5}$$

Due to the deficiency in flood data in this study, as an indirect method, the computed coefficients (C_0, C_1) from the above relation were used for estimating IF at ungauged sites with respect to their catchment areas. Chokmani and Ouarda (2004) suggest that knowing flow quantiles at neighboring gauged sites, one can estimate flow quantiles at an ungauged site by using an appropriate technique. Flood estimation at a river site should not only take into account a problem-oriented perspective but also data availability, although IF estimation may be constrained by the data availability for a particular application (Bocchiola et al. 2003). Furthermore, in our previous study on the Chindwin catchment, coefficient of variation of flood series is changing with increasing catchment, and annual maxima series of all gauged sites are fitted by the same frequency distribution i.e. Log-Pearson Type 3 (Latt and Wittenberg 2014b). This situation makes the transfer of IF from gauged to ungauged sites plausible and the precondition of IF regionalization is somewhat satisfied, despite limited flood data.

To determine the relations between IF and catchment descriptors for each homogeneous region using regression and ANN techniques, the input vector selection was first decided. While considering several catchment parameters, one variable may have a strong inter-correlation with other attributes. Therefore, the independent variables influencing on the dependent variable can be determined using Pearson correlation coefficient, as a measure of dependencies between variables (Kohnová and Szolgay 2003). Table 2 shows multi-collinearity among the predictors. In building the regional IF models, *L*, *S*, *E*, *CN* and *R* were selected as independent variables on the basis of inter-correlations lower than 0.5.

3.3.1 Regression Based Regional Models

The most commonly used relation between flood statistics (here IF) and a set of climatic and catchment characteristics within a region is the power form model (Thomas and Benson 1970; Cunnane 1988). In this study, the relationship becomes

Table 2 Correlation matrix for independent variables

Variables	A (km^2)	E (m)	S (%)	L (km)	SF	CN	Tc (min)	R (mm)
A (km^2)	1.000	0.334	0.158	0.944	0.475	0.094	0.84	0.027
E (m)	0.334	1.000	0.321	0.259	0.001	0.086	0.108	0.322
S (%)	0.158	0.321	1.000	0.126	0.025	−0.346	−0.148	0.498
L (km)	0.944	0.259	0.126	1.000	0.714	0.083	0.864	−0.018
SF	0.475	0.001	0.025	0.714	1.000	0.052	0.561	−0.113
CN	0.094	0.086	−0.346	0.083	0.052	1.000	0.192	0.002
Tc (min)	0.840	0.108	−0.148	0.864	0.561	0.192	1.000	−0.235
R (mm)	0.027	0.322	0.498	−0.018	−0.113	0.002	−0.235	1.000

$$Q_m = a_0 L^{a_1} S^{a_2} E^{a_s} CN^{a_4} R^{a_5} \varepsilon \tag{6}$$

where Q_m represents IF of each ungauged site in a clustered region, estimated via Eq. (5), in $m^3 s^{-1}$. α_0, α_1, α_2, α_3, α_4 and α_5 are the regression coefficients. ε is the multiplicative error term. By a logarithmic transformation, the above equation can be linearized, and the ordinary least square method was used to find the best fitting regression parameters by minimizing the sum of squared residuals.

3.3.2 ANN Based Regional Models

A feedforward MLP (Rumelhart et al. 1986) is useful for pattern mapping problems for input-output data sets and consists of the input layer, one or more hidden layers of neurons, and an output layer of neurons. To perform a comparison with conventional power form models, ANN structure is based on the Eq. (6) (Fig. 3). The sum of the product of inputs (x) and their weights (w) minus bias (b) constitutes a *net* as follows:

$$net = \sum x_i \cdot w_i - b \tag{7}$$

Then the output of a neuron, f (net) is decided by an activation function that determines a response of the node to the input signal it receives. In order to generate an output vector $Y = (Q_{m1}, Q_{m2}, \ldots\ldots, Q_{mn})$, a training (learning) process was used to find optimal weight matrices and bias vectors that minimize a predetermined error function given as follows.

$$E = \sum_{p=1}^{p} \sum_{i=1}^{N} (y_i - t_i)^2 \tag{8}$$

Here, t_i represent the target (IF from the regionalization) and y_i is the output (predicted IF by ANN) at the i^{th} node respectively; N is the number of output nodes and p denotes the number of training patterns. Three-layered feedforward MLP models with one hidden layer were trained with error back propagation, which is essentially a gradient-descent algorithm, to look for optimal performance by trial and error.

In the model development, the data set, which consists of IF magnitudes and catchment descriptors, representing 80 % of the number of subbasins in each clustered region were used for calibration and 20 % were used for validation. In order to overcome numerical instabilities, such as slow convergence and getting stuck in local minima, during the training process and to improve the generalization ability, the calibration data sets were standardized in a linear scale subtracting the mean and divided by the standard deviation. The data set for training and testing of

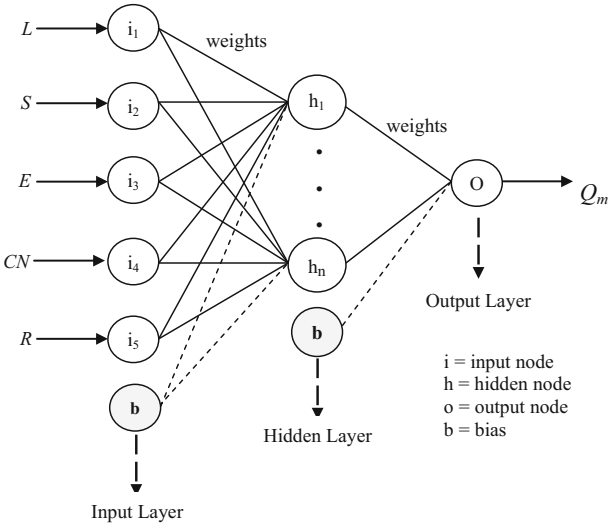

Fig. 3 Configuration of the feedforward ANN (MLP) network

ANN models were the same as the calibration and validation data of the power form models to enable a parallel comparison. Different learning rates were applied while the momentum was set at 0.9. The number of hidden layer neurons was changed up to 20 through the training process. The appropriate neuron number was selected depending on the minimum standard error. By evaluating the objective function at each iteration on training and testing sets, the training process was stopped in correspondence with the minimum validation error. Sigmoid and hyperbolic tangent functions were applied in the hidden layer. The linear function (identity), given as $f(x) = x$, was used in the output layer, making the network take any values without a bounded range.

3.3.3 Performance Evaluation

The best candidate models of ANN and regression methods were determined based on R^2 and sum of square errors in the calibration. The developed regional ANN models and regression models were validated and their performances were compared using the Nash-Sutcliffe coefficient of efficiency (*CE*), root mean-square error (*RMSE*), and mean relative error (*MRE*) given as

$$CE = 1 - \frac{\sum_{i=1}^{n} \left(y_i - \hat{y}\right)^2}{\sum_{i=1}^{n} \left(y_i - \overline{y}\right)^2} \tag{9}$$

$$RMSE = \sqrt{\frac{1}{n} \sum_{i=1}^{n} \left(y_i - \hat{y}_i\right)^2} \tag{10}$$

$$MRE = \frac{1}{n} \sum_{i=1}^{n} \frac{\left|y_i - \hat{y}_i\right|}{y_i} * 100 \tag{11}$$

Where y_i represents the IF from the regionalization, $\hat{y}$ the modeled IF, $\overline{y}$ the average IF, and n the number of observations.

4 Results and Discussion

4.1 Determination of Physiographic and Climatic Parameters

The Chindwin catchment was divided into 57 subbasins (Fig. 4a). The sizes of the basins ranged from 3 to 11,762 km^2. The minimum elevation of the basins was 69 m above mean sea level in the central flat plain, whereas the maximum elevation was close to 1,800 m in the mountainous regions. Average slopes of the basins varied from 0.7 to 16.4 %, while the basin lengths were between 2 and 397 km. Shape factors range from 1.3 to 13.4 as different-sized basins constitute the entire catchment. With a narrow and elongated shape, basin 24 has the biggest shape factor and area because it represents the catchment area of the largest tributary of the Chindwin River. *Tc* values varied from 9 to 1,138 min, according to the orientation of the basins.

In the *CN* calculation, only three hydrologic soil groups (B, C and D) were found in the Chindwin catchment. As a result, the parent geological material of the watershed may have a range of water transmission rates between 0 and 8 mm/h according to USDA (1986). Although the infiltration rate of the soil depends on the depth of impermeable layers, it can be generally said that the catchment has low to moderate infiltration rates. Group A soil, which mostly consists of excessively drained sand or gravel, was not found in the catchment. As shown in Fig. 4b, the *CN* values ranged from 58 (lower runoff) to 100 (higher runoff) across the catchment. The results show that the Chindwin territory has three distinct divisions. The areas with lower *CN* values (55–65) were found in the upper and northeastern parts of the catchment. The middle and southwestern parts have moderate *CN* values (65–80) while the lowest region shows higher *CN* (80–100). Area-weighted average *CN* for each subbasin varied from 65 to 93. Overall, the Chindwin catchment has a moderate to higher runoff potential.

From the MAR map (Fig. 4c), high variation of rainfall over the catchment was due to the regional climate pattern and the topography. The rainfall distribution over the Chindwin basin mostly depends on the disposition of mountainous ridges stretched in the meridian direction and they are forming a natural barrier to the southwest monsoon. Therefore, the slopes exposed to the West receive much more rainfall than the eastern and northeastern slopes. Generally, the rainfall pattern leads to a differentiation of the Chindwin basin into three regions. The upper

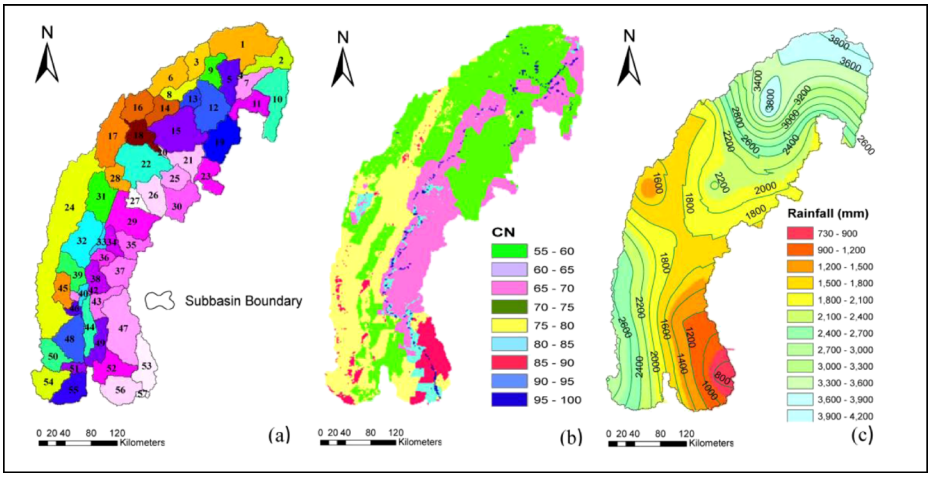

Fig. 4 Delinetaed subbasins (**a**), *CN* (**b**) and mean annual rainfall (**c**) of the Chindwin catchment

and southwestern parts have high annual rainfalls between 2,400 and 3,800 mm. The middle part has been hit by annual rainfall of 1,500 to 2,400 mm, while the lowest regions (south-eastern part) receive the smallest rainfall magnitude per year between 750 and 1,500 mm. Overall, the Chindwin catchment has different physio-climatic features that influence flood generating. Such evidence suggests that there might be broad regional differences in either flood processes or flood types. Therefore, it may be possible to generalize the effects of climatic and catchment attributes on floods within the defined regions.

4.2 Detecting Hydrological Homogeneous Regions

Prior to clustering, PCA was first applied in order to reduce the dimensionality of the data set. Based on the selected flood generating variables (*A, E, S, SF, L, CN, Tc* and *R*) of each basin out of 57 total, the case-variable ratio is 7.1, meaning that the sample size requirement is satisfied. The KMO measure of sampling adequacy of the set of variable is 0.58. Overall, the data set was suitable for data reduction using PCA. As shown in Table 3, the first three components meet the required criteria (the cumulative variance greater than 75 % and eigenvalues greater than 1). The first three PCs explain 41.5, 23.5 and 14.2 %, respectively, and their cumulative variance accounts for 79.2 % of the total variance of the data set. *L*, *Tc* and *A* have a higher correlation with the first principal component while *R* with the second principal component. The *CN* is strongly related to the third principal component. Therefore, classification is expected to be more affected by these attributes. The first PC provides a contrast between physical characteristics of the catchment (with positive coefficients) and mean annual rainfalls (negative coefficients). The main contrast for the second component is between the mean annual rainfall and the shape factor. The third PC is a trade-off between the basin slope and the *CN*.

Using the scores of the first three PCs, the Ward's method initially suggested four clusters, since the scree test i.e. the plot of the number of steps against the coefficients of 3PC solutions showed the distinctive break (elbow) started at step 53 out of 57 steps. The number of clusters obtained by the Ward method was adjusted using the *k*-means algorithm which then classified the entire basin into four homogeneous groups (Fig. 5). Cluster 1 has only basin 24 that is more significant in size and shape factor than other basins. Due

Table 3 Rotated factor loading matrix and variances of principal components

Original variables	Principal components (factor)		
	1	2	3
L	0.980	0.111	−0.220
T_C	0.911	−0.132	0.155
A	0.903	0.217	0.038
SF	0.770	−0.155	−0.137
R	−0.175	0.813	−0.035
E	0.159	0.756	0.215
S	0.062	0.660	−0.554
CN	0.013	0.096	0.927
Eigenvalues	3.317	1.884	1.135
Variance (%)	41.47	23.55	14.19
Cumulative Variance (%)	41.47	65.02	79.21

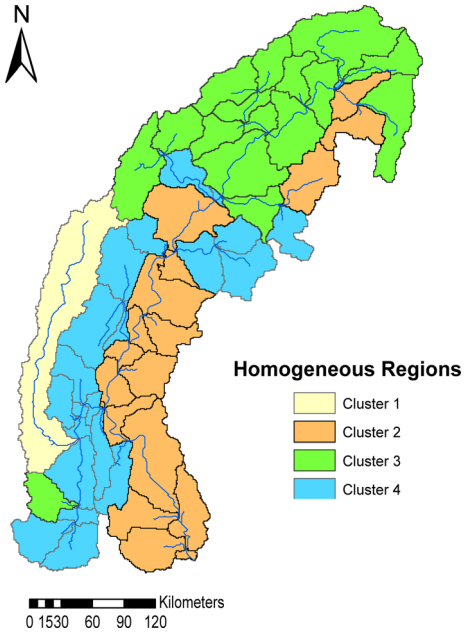

Fig. 5 Hydrological homogeneous regions of the Chindwin catchment

to its highest heterogeneity, the basin 24 cannot be grouped within other regions. Cluster 2, 3 and 4 consisted of 17, 16 and 23 basins, respectively. The areas of Cluster 1, 2, 3 and 4 are 11,762, 33,611, 37,264 and 30,780 km^2, respectively. Cluster 4 shows a greater dissimilarity to Cluster 1, and equal similarity to cluster 2 and 3. With lower mean square errors and higher F statistics, the second PC which is strongly related to mean annual rainfall, was found to be the most influential factor in pooling similar hydrologic regions. In general, the physio-climatic condition of the Chindwin catchment can be understood according to the original flood response characteristics with reference to their location as follows:

With the higher terrain in some parts, Cluster 1 has a moderate rainfall magnitude of 2,000 mm and a moderate runoff potential with average basin *CN* of 76. The highest shape factor of the region may influence the flood hydrograph shape. With higher T_C, this narrow and elongated region can generate a flatter peak flow for longer duration.

Cluster 2 is mainly characterized by a flood plain region with lower basin elevations and comprises a few basins in the northeastern part. The most parts of the region experience lower annual rainfall of 1,700 mm. With the basin *CN* values ranging 84 to 93, the region has a higher runoff potential. Flood hazards may be relatively low in this region due to the low rainfall. However, the extreme climatic effects from its upstream part may superimpose on flooding in it.

In Cluster 3, the mountainous regions are dominant with higher mean basin elevation of 1,344 m accompanied by higher basin slopes (3.4 to 16.4 %). The region, which mainly covers the most upstream parts of the Chindwin catchment to 85 km downstream Hkamti station, receives the highest mean annual rainfall of 3,000 mm, and can generate moderate to higher runoff with mean basin *CN* of 81. Therefore, the region can be regarded as the highest flood potential zone compared to the other clusters.

Table 4 Calibration of regional regression models and performance indices

Region	Regional regression models	Log domain		Real domain
		R^2	Standard Error	R^2
Cluster 2	$Q_m=78 \quad L^{0.48}S^{-0.01}E^{-0.026}CN^{0.47}R^{0.023}$	0.97	0.031	0.96
Cluster 3	$Q_m=959 \quad L^{0.36}S^{-0.04}E^{-0.004}CN^{0.39}R^{-0.18}$	0.90	0.026	0.89
Cluster 4	$Q_m=2588 \quad L^{0.42}S^{-0.04}E^{-0.06}CN^{-0.59}R^{0.027}$	0.97	0.045	0.94

With a mean basin elevation of 470 m, the highland region on the right side of the Chindwin mainstream constitutes the majority of Cluster 4. The region is characterized by a moderate annual precipitation of 2,000 mm and has a moderate runoff potential with *CN* of 74.

4.3 Index Flood Models for Clustered Regions

In regressing IF with basin areas for gauged sites, the empirical power relation ($Q_m = 924\,A^{0.269}$) was found to be the best fit, providing $R^2 = 0.94$. From this relation, IF magnitudes at ungauged sites in each homogeneous region were estimated with respect to the area. For cluster 2, 3 and 4, the relationships between Q_m and catchment physiographic properties were derived. Regional IF model cannot be derived for cluster 1, because sufficient flood and catchment data were not available.

According to Eq. (6), the simultaneous (Enter) regression technique was applied to find the relationship between Q_m and the independent variables because the involvement of all predictors could decrease the standard error of the estimate of the dependent variable. The independence of the predictor variables was evident because small degree of inter-correlation between them suggests they convey little information about each other (see Table 2). The regression based regional IF models for each homogeneous region are shown in Table 4. *L* was found to be the most influencing attribute for all clustered regions since it could explain the most variation of the floods. The coefficients of the power form models in real domain were derived from the log transformed equations. It should be noted that the R^2 values have slightly decreased in the real domain, compared to R^2 in the log domain while calibrating. For each clustered region, feedforward ANN models were also trained using the same input vectors in the regression models. After testing different activation functions, the combination of a hyperbolic tangent in the hidden layer and an identity function in the output layer provides the best performance in this case. The performance statistics of the selected ANN models are shown in Table 5. With higher R^2 for each pooling group, the ANN models can capture a complex relationship between a range of catchment descriptors and associated IF magnitudes.

To get the true merits of ANN techniques, the ANN model results were compared with those of the regression models in the real domain (Table 6). The results of the ANN models for each region explore more consistency in all performance indices than regression models. For cluster 2, the ANN model shows the highest performance in both calibration and validation

Table 5 The structure of regional ANN models in calibration

Region	Structure	Learning rate	R^2	Sum of squares error
Cluster 2	5-6-1	0.7	0.99	0.07
Cluster 3	5-2-1	0.1	0.99	0.02
Cluster 4	5-2-1	0.2	0.96	0.32

Table 6 Comparison between the ANN and regression based regional models in real domain

Region	Calibration						Validation					
	ANN Models			Regression Models			ANN Models			Regression Models		
	CE	RMSE	MRE	CE	RMSE	MRE	CE	RMSE	MRE	CE	RMSE	MRE
Cluster 2	0.99	108	1.3	0.96	243	2.8	0.99	99.5	1.1	0.32	1,071	12.2
Cluster 3	0.99	88	0.8	0.88	288	3.1	0.98	141	1.7	0.74	638	7.8
Cluster 4	0.95	361	6.2	0.94	439	8.4	0.98	217	3.6	0.77	667	13.5

with highest *CE* and least error, whereas the regression model has the least efficiency in validation, with a *CE* value of 0.32 although it has a higher performance with a *CE* value of 0.96 in calibrating. In cluster 3, the regression model shows its highest performance in validation with higher *CE* and least relative error, but, the ANN model still outperforms it. In calibrating, relative percent errors of both ANN and regression models are highest for cluster 4 with 6.2 and 8.4 %, respectively. However, the ANN model can reduce the forecast error in validation, while the regression one could not. In the validation stage, performances of the ANN models are very satisfactory with respect to the *CE* statistics above 0.98 whereas that of the regression models are just satisfactory to cluster 3 and 4 with *CE* values of 0.74 and 0.77, respectively and very poor to cluster 2. Undoubtedly, the ANN models have outperformed the regression models for IF estimation using catchment descriptors. While ANNs are not sensitive to the limited data in this study, a larger data set would be needed to enhance the accuracy of the power form model as Myanmar river basins are characterized by a highly variable flood regime.

5 Conclusions

With the diverse physiographic and climatic conditions, understanding the regional characteristics that reflect hydrological responses play a vital role in water resources management in Myanmar. The study presented the application of clustering techniques in conjunction with PCA for detecting hydrologic homogeneous regions, and the ANN approach for developing regional IF models in ungauged regions. Different climatic and physiographic attributes across the Chindwin catchment suggested that it is possible to generalize the effects of climatic and catchment attributes on floods within the defined regions.

Despite the precise understanding of the underlying mechanisms of flood generation, PCA contributes well to define the significant factors, as clustering variables, which explained 79.2 % of the total variance of the original data set. In clustering with *k*-means algorithm, the second principal component, which is mainly affected by mean annual rainfall, basin elevation and basin slope, has the greatest contribution to classifying the hydrological similarities of the Chindwin watershed. Cluster 3 represents the highest flood potential area in terms of all response variables, whereas the lower part of the cluster 2 is the least flood prone region with lowest annual rainfall. Overall the entire catchment is likely to have moderate to high flood potential, and flood control management at any location in this watershed is of great importance to prevent human lives and environment.

In establishing relationships between IF and catchment attributes, the conventional power form models did not show reliable results in the validation stage although the calibration result was quite satisfactory. In a comparison using real data, the performance of the power form

models is slightly lower than that of the linearized models via log transformation. Therefore, consistency in performances of the regression models could not be expected in every case. The neural network approach, with the inherent ability of capturing nonlinearity, has shown better results than conventional regression techniques in IF regionalization. The performances of the ANN models are very satisfactory to all clusters in both calibration and validation. Since, real world conditions never guarantee a linear relationship between flood magnitudes and catchment properties, ANN approach would be a promising alternative tool for IF estimation from limited input and output data alone, which can be either linear or nonlinear. This quality is very useful for water resources management with limited data type and observation.

In regionalization processes, spatial flood data must have a sufficient density to cover the entire catchment. Therefore, modifications of the regional IF models are required from time to time using more available flood data and catchment attributes. Even if the observed flood data will not be expected in the near future, it is recommended that synthetic annual maximum discharge series of ungauged basins would be generated using available climatic data. As a result, better understanding of similar flood response areas and knowing IF for the entire Chindwin river basin would ease the flood management in Myanmar. Further, the methodology presented in this study provides a useful tool for water resources planning and design of hydraulic structures in developing countries where hydrometric data scarce.

Acknowledgments The study was funded by the Deutscher Akademischer Austausch Dienst (DAAD) (German Academic Exchange Service). The Department of Meteorology and Hydrology, the Survey Department and the Land Use Department in Myanmar are gratefully acknowledged for providing data.

References

Abdolhay A, Saghafian B, Soom MAM, Ghazali AHB (2012) Identification of homogenous regions in Gorganrood basin (Iran) for the purpose of regionalization. Nat Hazards 61:1427–1442

Aziz K, Rahman A, Fang G, Shrestha S (2013) Application of artificial neural networks in regional flood frequency analysis: a case study for Australia. Stoch Env Res Risk A. doi:10.1007/s00477-013-0771-5

Berz G (2000) Flood disasters: lessons from the past – worries for the future. Proceeding of the ICE. Water Marit Eng 142(1):3–8

Besaw LE, Rizzo DM, Bierman PA, Hackett WR (2010) Advances in ungauged streamflow prediction using artificial neural networks. J Hydrol 386:27–37

Bocchiola D, Michele SD, Rosso R (2003) Review of recent advances in index flood estimation. Hydrol Earth Syst Sci 7(3):283–296

Cerny CA, Kaiser HF (1977) A study of a measure of sampling adequacy for factor-analytic correlation matrices. Multivar Behav Res 12(1):43–47

Chokmani K, Ouarda TBMJ (2004) Physiographical space-based kriging for regional flood frequency estimation at ungauged sites. Water Resour Res 40, W12514. doi:10.1029/2003WR002983

Cigizoglu HK (2003) Estimation, forecasting and extrapolation of river flows by artificial neural networks. Hydrol Sci 48(3):349–361

Cunnane C (1988) Methods and merits of regional flood frequency analysis. J Hydrol 100:269–290

Cutore P, Cristaudo G, Campisano A et al (2007) Regional models for the estimation of streamflow series in ungauged basins. Water Resour Manag 21(5):789–800. doi:10.1007/s11269-006-9110-7

Dawson CW, Abrahart RJ, Shamseldin AY, Wilby RL (2006) Flood estimation at ungauged sites using artificial neural networks. J Hydrol 319:391–409

Dutta D, Herath S (2004) Trends of Floods in Asia and Flood Risk Management with Integrated River Basin Approach. Proceedings of the Second International Conference of Asian-Pacific Hydrology and Water Resources Association, Singapore. Vol.1: 55–63

Eng K, Milly PCD, Tasker GD (2007) Flood regionalization: a hybrid geographic and predictor-variable region-of-influence regression method. ASCE J Hydrol Eng 12:585–591

Gingras D, Adamowski K (1993) Homogeneous region delineation based on annual flood generation mechanisms. Hydrol Sci 38(2):103–121

Goyal MK, Gupta V (2014) Identification of homogeneous rainfall regimes in Northeast Region of India using fuzzy cluster analysis. Water Resour Manag. doi:10.1007/s11269-014-0699-7

GREHYS (1996) Presentation and review of some methods for regional flood frequency analysis. J Hydrol 186: 63–84

Hosking JRM, Wallis JR (1997) Regional frequency analysis. Cambridge University Press, UK

IUSS Working Group WRB (2006) World reference base for soil resources 2006. World Soil Resources Reports No. 103. FAO, Rome

Jolliffe IT (2004) Principal component analysis, 2nd edn. Springer Series in Statistics, USA

Kirpich ZP (1940) Time of concentration of small agricultural watersheds. Civ Eng 10(6):362

Kohnová S, Szolgay J (2003) Regional estimation of the index flood and the standard deviation of the summer floods in the Tatry mountains. J Hydrol Hydromech 51(4):241–255

Latt ZZ, Wittenberg H (2014a) Improving flood forecasting in a developing country: a comparative study of stepwise multiple linear regression and artificial neural network. Water Resour Manag 28(8):2109–2128. doi:10.1007/s11269-014-0600-8

Latt ZZ, Wittenberg H (2014b) Hydrology and flood probability of the monsoon-dominated Chindwin River in northern Myanmar. J Water Clim Chang. doi:10.2166/wcc.2014.075

MacQueen J (1967) Some methods for classification and analysis of multivariate observations, proceedings of 5th Berkeley symposium on mathematical statistics and probability, vol 1. University of California Press, Berkeley, pp 281–297

Mishra BK, Takara K, Yamashiki Y, Tachikawa Y (2009) Estimation of index flood in hydrologic regions with limited flood data availability. Ann J Hydraul Eng JSCE 53:55–60

National Commission for Environmental Affairs (NCEA) (2009) Fourth national report to the United Nations Convention on biological diversity. Ministry of Forestry, Myanmar. http://www.cbd.int/doc/world/mm/mm-nr-04-en.pdf. Accessed 11 Jan 2014

Nayak PC, Satyajirao YR, Sudheer KP (2006) Groundwater level forecasting in a shallow aquifer using artificial neural network approach. Water Resour Manag 20:77–90. doi:10.1007/s11269-006-4007-z

Pandey GR, Nguyen V-T-V (1999) A comparative study of regression based methods in regional flood frequency analysis. J Hydrol 225:92–101

Razavi T, Coulibaly P (2013) Classification of Ontario watersheds based on physical attributes and streamflow series. J Hydrol 493:81–94

Rumelhart DE, Hinton GE, Williams RJ (1986) Learning internal representations by error propagation. In: Rumelhart DE, McClelland JL, PDP research group (eds) Parallel distributed processing, vol 1. MIT Press, Cambridge, pp 318–362

Sahay RR, Srivastava A (2014) Predicting monsoon floods in rivers embedding wavelet transform, genetic algorithm and neural network. Water Resour Manag 28:301–317. doi:10.1007/s11269-013-0446-5

Sattari NT, Apaydin H, Ozturk F (2012) Flow estimations for the Sohu stream using artificial neural networks. Environ Earth Sci 66(7):2031–2045

Shaban M, Urban B, El Saadi A, Faisal M (2010) Detection and mapping of water pollution variation in the Nile Delta using multivariate clustering and GIS techniques. J Environ Manag 91:1785–1793

Smith K, Ward R (1998) Floods. Physical process and human impacts. Wiley, England

Thomas DM, Benson MA (1970) Generalization of streamflow characteristics from drainage-basin characteristics. United States Geological Survey, Water-Supply Paper 1975

United States Department of Agriculture (USDA) (1986) Urban Hydrology for small watershed. Technical Release 55

World Meteorological Organization (2008) Guide to Hydrological Practices. Volume 1 Hydrology- From Measurements to Hydrological Information. WMO-No. 168. 6th ed. Geneva